Journal of Medicinal Chemistry

Article

Discovery of N-arylsulfonyl-indole-2-carboxamide Derivatives as Potent, Selective, and Orally Bioavailable Fructose-1,6-Bisphosphatase Inhibitors# Design, Synthesis, In Vivo Glucose Lowering Effects, and X-ray Crystal Complex Analysis

Jie Zhou, Jianbo Bie, Xiaoyu Wang, Quan Liu, Rongcui Li, Hualong Chen, Jinping Hu, Hui Cao, Wenming Ji, Yan Li, Shuainan Liu, Zhu-fang Shen, and Bailing Xu

J. Med. Chem., **Just Accepted Manuscript** • DOI: 10.1021/acs.jmedchem.0c00726 • Publication Date (Web): 21 Aug 2020

is published by the American Chemical Society. 1155 Sixteenth Street N.W., Washington, DC 20036

Discovery of *N*-arylsulfonyl-indole-2-carboxamide Derivatives as Potent, Selective, and Orally Bioavailable Fructose-1,6-Bisphosphatase Inhibitors—Design, Synthesis, In Vivo Glucose Lowering Effects, and X-ray Crystal Complex Analysis

Jie Zhou[†,I], Jianbo Bie[†,I], Xiaoyu Wang[†,I], Quan Liu[‡], Rongcui Li[‡], Hualong Chen[†], Jinping Hu[§], Hui Cao[‡], Wenming Ji[‡], Yan Li[§], Shuainan Liu[‡,*], Zhufang Shen[‡,*], Bailing Xu[†,*]

[†]Beijing Key Laboratory of Active Substances Discovery and Druggability Evaluation, [‡]department of pharmacology, and [§]Beijing Key Laboratory of Non-Clinical Drug Metabolism and PK/PD Study, Institute of Materia Medica, Chinese Academy of Medical Sciences and Peking Union Medical College, Beijing 100050, China

ABSTRACT: Liver fructose-1,6-bisphosphatase (FBPase) is a key enzyme in the gluconeogenesis pathway. Inhibiting FBPase activity represents a potential treatment for type 2 diabetes mellitus. A series of novel *N*-arylsulfonyl-4-arylamino-indole-2-carboxamide derivatives have been disclosed as FBPase inhibitors. Through extensive structure-activity relationship investigations, a promising candidate molecule **Cpd118** (sodium (7-chloro-4-((3-methoxyphenyl)amino)-1-methyl-1*H*-indole-2-carbonyl)((4-methoxyphenyl)sulfonyl)amide) has been identified with high inhibitory activity against human

liver FBPase (IC_{50}, 0.029±0.006 μM) and high selectivity relative to the other six AMP-binding enzymes. Importantly, **Cpd11**8 produced significant glucose-lowering effects on both type 2 diabetic KKAy mice and ZDF rats as demonstrated by substantial reductions in the fasting and postprandial blood glucose levels, as well as the HbA1c level. Furthermore, **Cpd118** elicited a favorable pharmacokinetic profile with the oral bioavailability of 99.1%. Moreover, the X-ray crystal structure of the **Cpd118**-FBPase complex was resolved, which revealed a unique binding mode and provided a structural basis for its high potency and selectivity.

■ INTRODUCTION

Diabetes mellitus is one of the most prevalent chronic diseases worldwide. According to the ninth edition report released by IDF in 2019, approximately 463 million adults (about 9.3% of the population) are suffering from diabetes globally, and this figure is predicted to increase up to 578 million (about 10.2%) by the year of 2030. [1] Diabetes is a metabolic disorder diagnosed by high blood glucose levels (hyperglycemia) in both fasting and postprandial state of patients. The main clinical forms of diabetes include type 1 diabetes mellitus (T1DM), type 2 diabetes mellitus (T2DM), as well as gestational diabetes mellitus, with T2DM accounting for the majority (around 90%) of diagnosed diabetes worldwide. It has been demonstrated that long-term hyperglycemia has been more likely to lead to various debilitating microvascular and macrovascular complications,[2] such as retinopathy and cataract,[3] nephropathy,[4] neuropathy[5] and cardiovascular diseases.[6] Therefore, the control of glucose level is

the primary choice for the treatment of diabetes and its associate complications.

The endogenous glucose production (EGP) in liver plays a key role in regulation of blood glucose level and is positively correlated with fasting blood glucose level.[7] In the fasting state, glucose is solely produced by EGP processes including glycogenolysis and gluconeogenesis. Inhibiting EGP represents a promising strategy for glycemic control. However, no anti-diabetic drugs directly targeting on EGP process are currently available.

Gluconeogenesis is a primary EGP process for liver to produce endogenous glucose, which involves biochemical transformations of a number of non-carbohydrate precursors such as glycerol, alanine and lactate into glucose with the catalysis of several key enzymes including phosphoenopyruvate carboxykinase (PEPCK), fructose-1,6-bisphosphatase (FBPase) and glucose-6-phosphatase (G-6-Pase).[8] During long periods of fasting or starvation, gluconeogenesis contributes to more than 50% glucose production, and this contribution is even more significant in T2DM patients.[9,10] Therefore, targeting on the gluconeogenesis pathway is an appealing approach for the management of T2DM.

FBPase catalyzes the conversion of fructose-1,6-bisphosphate into fructose-6-phosphate and inorganic phosphate. [11] It comprises two isoforms in mammals, namely liver FBPase (encoded by *FBP1* gene, referred to as FBPase or

FBPase1) and muscle FBPase (encoded by *FBP2* gene, referred to as FBPase2). Liver FBPase, mainly expressed in liver and kidney, is a rate-limiting enzyme in hepatic gluconeogenesis pathway, and plays a key role in the regulation of glucose levels. Muscle FBPase is widely expressed in mammal cells including muscle tissue, neurons and liver, functioning as a multifaceted regulator in cells.[12-14] Additionally, it has been observed that liver FBPase is elevated in insulin-resistant and insulin-deficient animal models of diabetes.[15] Therefore, FBPase inhibitors have been intensively explored as anti-diabetic agents for the direct regulation of EGP.

Human liver FBPase is a homotetramer with each monomer consisting of 337 amino acid residues. Three distinct binding sites exist within the tetramer of FBPase: a fructose-1,6-biphosphate binding site and an AMP binding site within each monomer, and a binding pocket situated at the interface between the upper dimer and lower dimer.[16] Among these binding sites, the AMP binding pocket has received more attention because it is presumably a more druggable site compared with the other two sites. The AMP binding allosteric site is 28Å away from the substrate site. Upon binding the AMP to the allosteric site, the quaternary conformation of FBPase could change from the active R state to the inactive T state, inhibiting the catalytic activity of FBPase.[13,17]

Up to date, a number of FBPase inhibitors bearing distinct scaffolds have been identified via either high-throughput screening of compound libraries or

structure-guided design of AMP mimetics.[18-31] Presently, only two phosphonic acid-containing thiazole derivatives were advanced into clinical trials (**Figure 1**). [32] The clinical trial of the first candidate CS-917 was terminated in 2008 due to the toxicity of its metabolite, and the second candidate MB07803 is now in phase II clinical trial.[33,34] Also, these two candidates bearing the phosphonic acid group were developed as phosphonic diamide prodrugs to achieve the oral bioavailability. Evidently, it is challengeing to develop potent and orally bioavailable FBPase inhibitors without a phosphonic acid group.

The indole derivative MDL-29951 was found to be a potent FBPase inhibitor by a high throughput screening in Pfizer.[18] To search for drug-like FBPase inhibitors without a phosphonate or phosphate group, MDL-29951 was chosen as our starting point, and the investigations on structure-activity relationships (SARs) led to a new hit compound **A** (**Figure 2**). [35] Taking advantage of *N*-acyl sulfonamide moiety as the bioisosteric replacement of the carboxyl group, compound **B** (**Figure 2**) was designed, and **Cpd118** was discovered as a potent and orally bioavailable FBPase inhibitor. Herein, the design, synthesis and extensive SAR investigations of *N*-arylsulfonyl-indole-2-carboxamide derivatives were presented. The *in vivo* glucose lowering efficacy in diabetic type 2 animal models and the pharmacokinetic properties of **Cpd118** were disclosed. Furthermore, the cocrystal structure of **Cpd118** bound to FBPase was solved and a distinct binding mode was revealed.

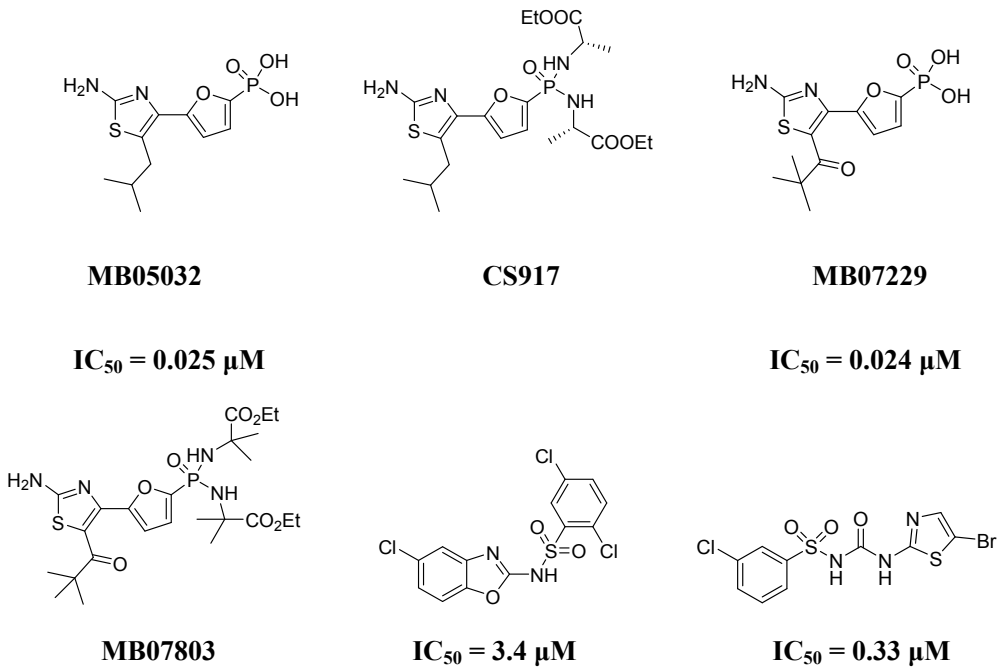

Figure 1. Several reported FBPase inhibitors

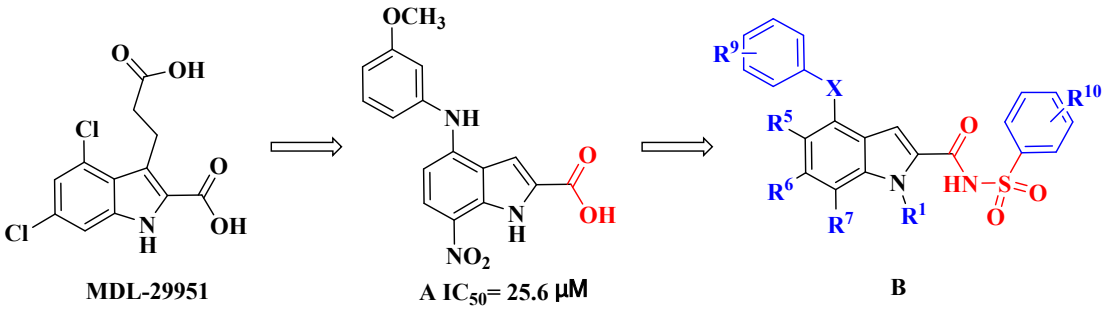

Figure 2. The design and optimization of *N*-arylsulfonyl-indole-2-carboxamides as FBPase inhibitors

■ RESULTS AND DISCUSSION

Molecular Design. The AMP binding allosteric site of FBPase consists of two featured sub-pockets. One is an adenine binding hydrophobic pocket lined with Val17, Ala24, Leu30, and Met177, and the other is a phosphate binding pocket where the phosphate formed a hydrogen binding network with key amino acids including Thr27, Gly28, Glu29, Lys112 and Tyr113 (**Figure 3B-3D**).[36] The phosphate group significantly contributes to the binding affinity; however, the inhibitors bearing a

phosphate moiety confer a poor membrane permeability, which leads to low bioavailability.[37-39] Therefore, we focused on the exploration of inhibitors bearing other acidic groups. As a result, indole-2-carboxylic acid derivatives were identified as FBPase inhibitors.[35] Among them, compound **A** was selected tentatively as the hit structure for further optimization since its structure was quite distinct from known inhibitors. At this point, we utilized the bioisosteric group *N*-acyl sulfonamide in substitution for the carboxylic acid, constructing the *N*-sulfonyl-indole-2-carboxamide derivatives (compound **B**). Delightfully, this bioisosteric replacement worked quite effectively and resulted in the highly potent *N*-phenylsulfonyl-indole-2-carboxamide derivative (compound **32**), with inhibitory potency being improved by 182-fold than that of hit compound **A**. Subsequently, the extensive structural modifications were carried out around the *N*-arylsulfonyl-indole-2-carboxamide scaffold, furnishing the candidate molecule **Cpd118**. Particularly, the X-ray cocrystal structure of **Cpd118** bound to FBPase demonstrated that this class of inhibitors displayed a distinct binding mode, which was presumably different from the hit compound A.

Chemistry. The chemical structures of target compounds (**30-118**) were shown in **Tables 1-7,** and their preparations were illustrated in **Schemes 1-3**. The key intermediate indole-2-carboxylic acid derivatives were synthesized by using the Fischer indole synthesis and Hemetsberger indole synthesis, and their further condensations with various aryl sulfonamides delivered the desired target compounds. The preparation of 7-nitro substituted indole molecules involving Fischer indole

synthesis was outlined in **Scheme 1**. Upon treatment with $NaNO_2$/HCl, followed by $SnCl_2$/HCl, 4-substituted-5-chloro-2-nitroanilines **1a-1d** afforded hydrazine hydrochlorides **2a-2d.** The condensation between **2a-2d** and ethyl pyruvate generated hydrazone derivatives **3a-3d,** which then transformed into the key indole intermediates **4a-4d** in 13-38% yields at 80 ℃ in PPA. Under the catalysis of $Pd_2(dba)_3$/DavePhos, the coupling reaction of compounds **4a-4d** with respectively $ArNH_2$, aliphatic amines, benzylboronic acid pinacol ester, ArOH, or ArSH, yielded **5a1-5a33** and **5b-5d** (53-98%). The NaOH-catalyzed hydrolysis of **5a1-5a33**, **5b-5d** produced 1*H*-indole-2-carboxylic acid derivatives (**6a1-6a33**, **6b-6d**) in 37-99% yields. The construction of target compounds (**30–53, 55-78**) was realized in acceptable yields via the condensation of acid intermediates (**6a1-6a33**, **6b-6d**) with various sulfonamide compounds. Hydrolysis of compound **4a** yielded **7a** and subsequently condensed with benzenesulfonamide, producing a 4-chloro-substituted compound **54.** Moreover, starting from compound **4a**, N_1-substituted indole-2-carboxylic acid derivatives **10a1-10a9** were obtained after three steps of consecutive chemical transformations: alkylation with alkyl halides, Buchwald-Hartwig coupling reaction and hydrolysis reaction. Finally, the condensation between indole-2-carboxylic acid derivatives **10a1-10a9** and 4-methoxybenzenesulfonamide gave rise to target compounds **87-95** in 16-91% yields.

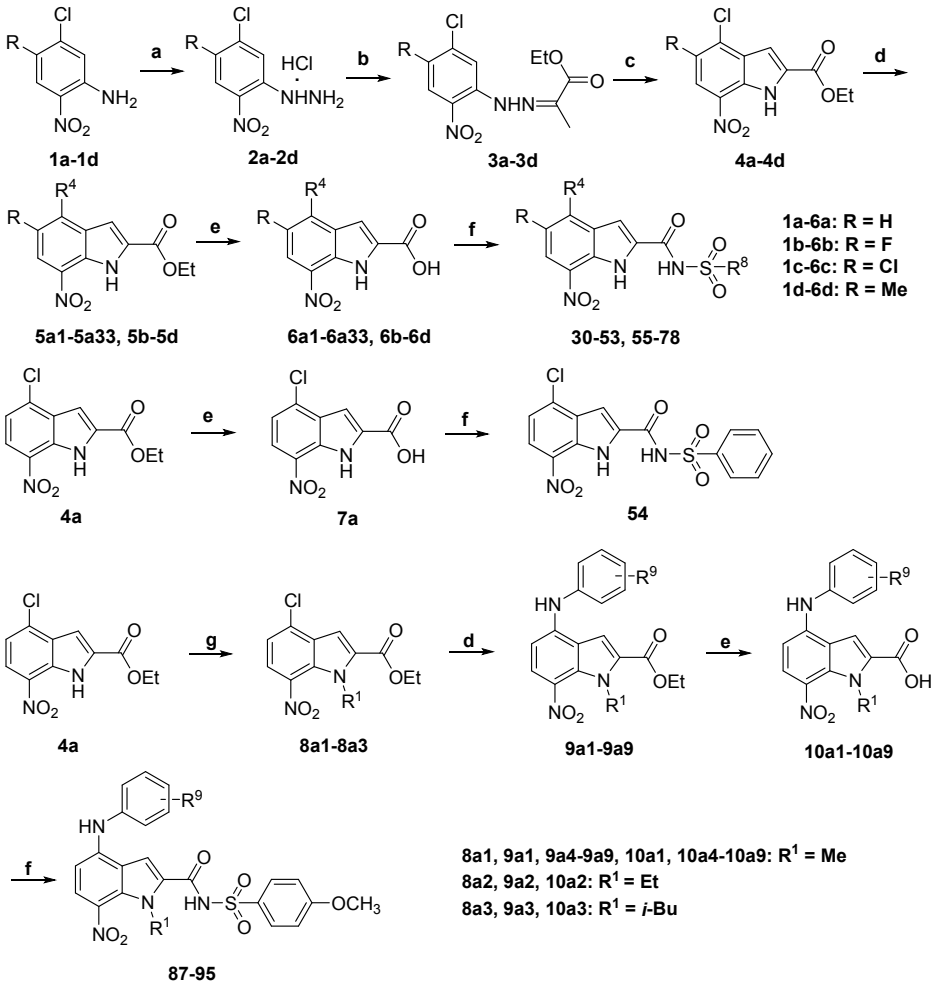

Scheme 1. Reagents and conditions: (a) (i) $NaNO_2$, HCl, 10 ℃, (ii) $SnCl_2$, HCl, 30 ℃;(b) ethyl pyruvate, EtOH, rt; (c) PPA, 80 ℃; (d) $ArNH_2$ or aliphatic amines, $Pd_2(dba)_3$, DavePhos, K_3PO_4(aq), toluene, 100℃; benzylboronic acid pinacol ester, $Pd(dppf)Cl_2$, K_3PO_4, CsF, 1,4-dioxane, H_2O, MW, 100 ℃; ArOH or ArSH, CuI, K_2CO_3, DME, MW, 130℃; (e) NaOH, THF, EtOH and H_2O, r.t.; (f) $R^8SO_2NH_2$, HATU, DMAP, Et_3N, DCM, r.t.; (g) R^1X, Cs_2CO_3, DMF, r.t.

In order to explore the SARs, except for the nitro group on the 7-position of indole ring, other substituents including F, Cl, CN, CF_3 and CH_3 were placed on either the 6-position or 7-position of the indole ring. As depicted in **Scheme 2**, Hemetsberger

indole synthesis was applied to the synthesis of these derivatives. Upon the treatment of ethyl 2-azidoacetate with substituted 2-bromobenzaldehyde (**11a-11g**) in the presence of sodium ethoxide, 2-azido-acrylate derivatives (**12a–12g**) were produced in 12-27% yields and later refluxed in xylene or 1,2-dichlorobenzene, forming the key indole intermediates (**13a–13g**) in 30-93% yields. The coupling reaction of **13a–13g** with 3-methoxyaniline gave esters **14a–14g,** which were then hydrolyzed into indole-2-carboxylic acid derivatives (**15a–15g**). Subseqeuntly, they condensed with 4-methoxybenzenesulfonamide to access target molecules **80-86.** The key intermediate (**18e**) was produced in three steps in high yields, and its condensation with various arylsulfonamides provided the *N*-methyl-7-chloro-substituted target compounds **96-113**. The 4-chloro-substituted target molecules **114** and **115** were synthesized by using indole compound **13h** as the starting material, and target compound **79** was prepared starting from commercially available indole derivative **13i**. Compound **96** was converted into its sodium salt (compound **118, Cpd118**) in the presence of NaOH in a quantitative yield.

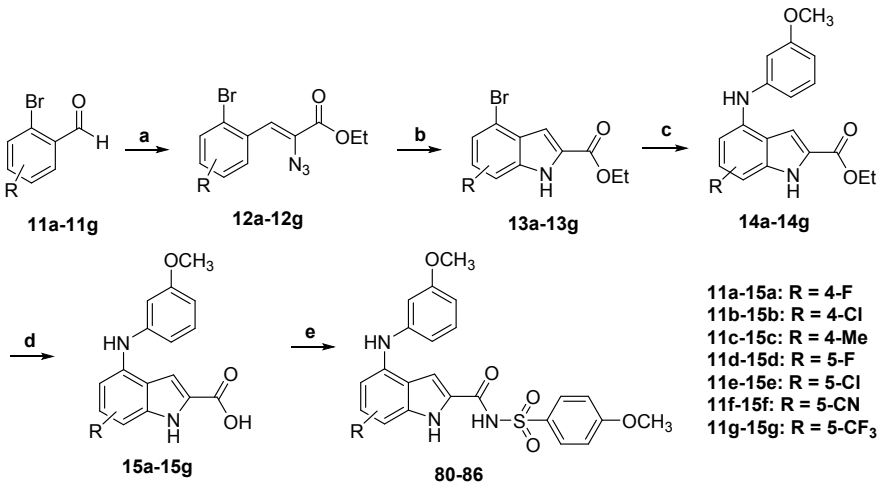

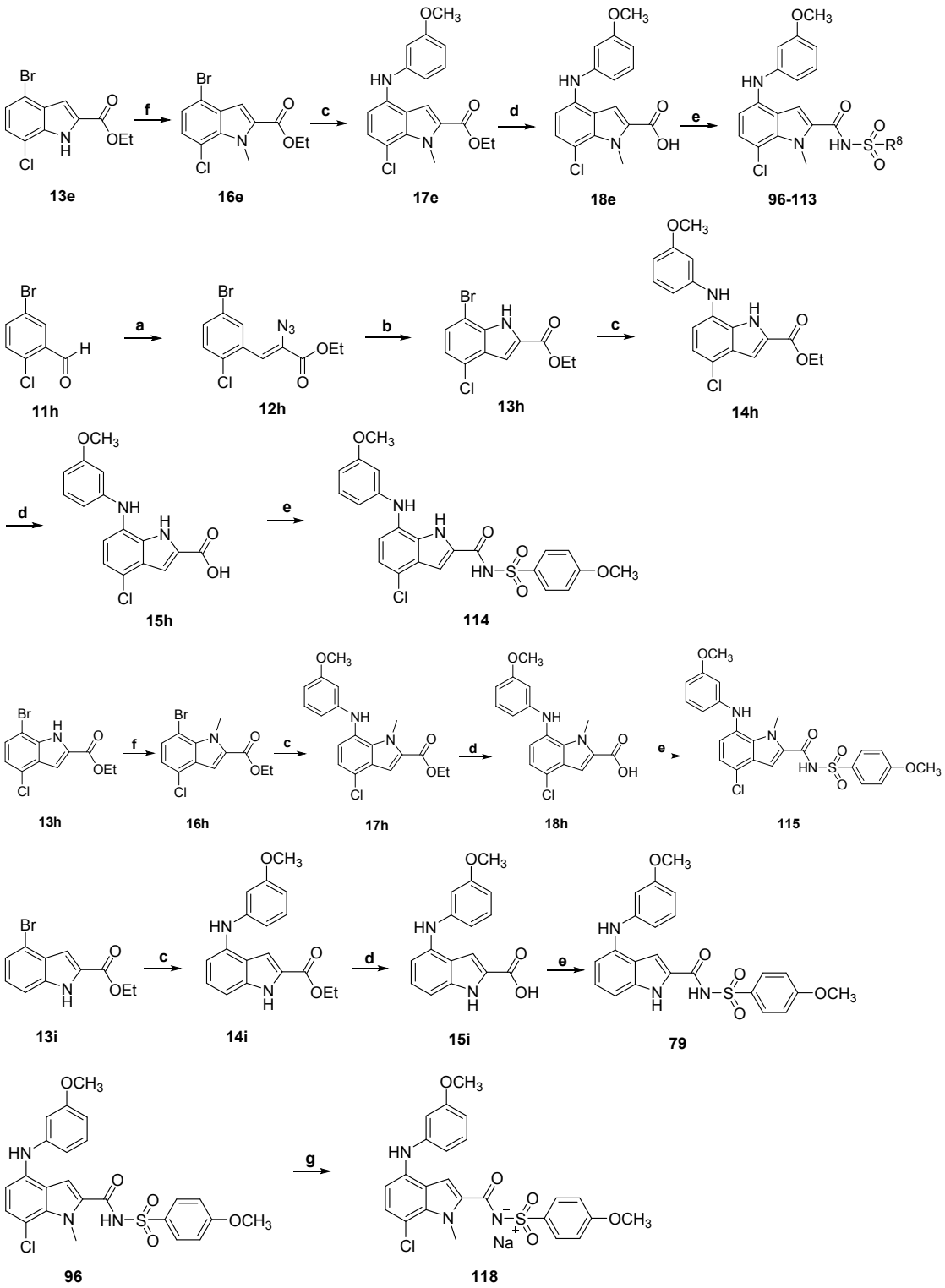

Scheme 2. Reagents and conditions: (a) NaOEt, ethyl azidoacetate, EtOH; (b) xylene or 1,2-dichlorobenzene, reflux; (c) 3-methoxyaniline, $Pd_2(dba)_3$, Xantphos, Na_2CO_3, toluene, H_2O, reflux; (d) NaOH, THF, EtOH and H_2O, r.t.; (e) $R^8SO_2NH_2$, HATU, DMAP, Et_3N, DCM, r.t.; (f)

MeI, Cs_2CO_3, DMF, r.t.; (g) NaOH, H_2O, 80 ℃.

Compounds **116** and **117** bearing benzo[*d*]imidazole and azaindole scaffold respectively, were also designed and synthesized as shown in **Scheme 3**. The benzo[*d*]imidazole derivative **24** was built in a 5-step process starting from 3-nitrobenzene-1,2-diamine in 31% total yield. Then, starting from the key intermediates **24** and **27** (commercially available), target molecules **116** and **117** were constructed by undergoing palladium catalyzed coupling, base catalyzed hydrolysis and condensation reaction.

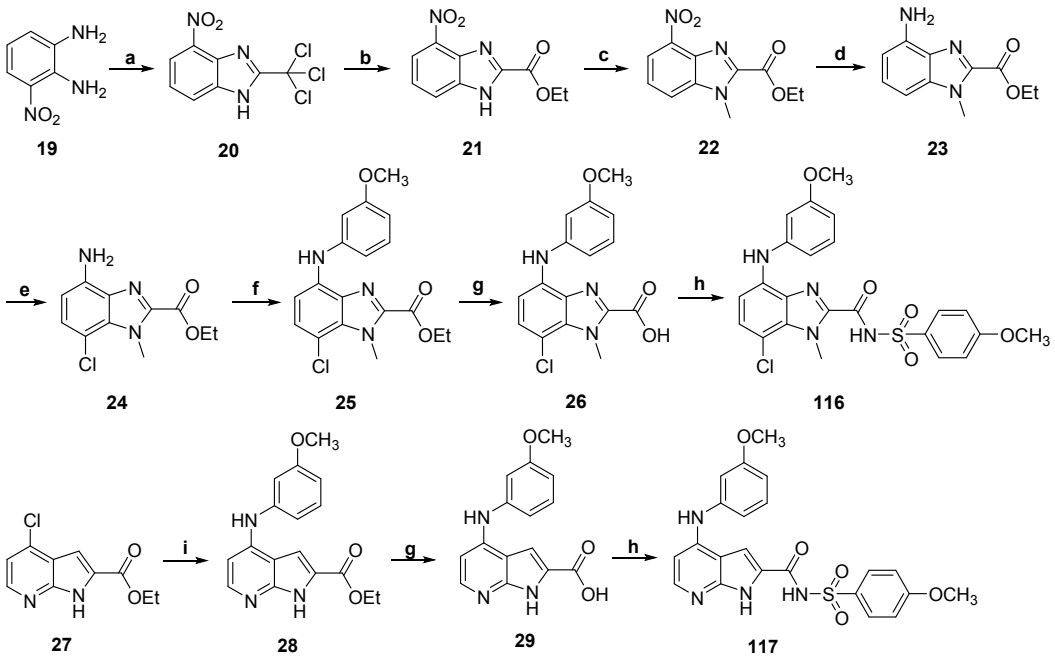

Scheme 3. Reagents and conditions: (a) ethyl 2,2,2-trichloroacetimidate, TFA, ethyl ether/DCM; (b) Cs_2CO_3, EtOH, reflux; (c) MeI, Cs_2CO_3, DMF, r.t.; (d) 10% Pd/C, H_2, EtOH, 1atm, r.t.; (e) NCS, DMF, r.t. (f) 3-bromoanisole, $Pd_2(dba)_3$, DavePhos, K_3PO_4(aq), toluene, 100 ℃; (g) NaOH, THF, EtOH and H_2O, r.t.; (h) 4-methoxybenzenesulfonamide, HATU, DMAP, Et_3N, DCM, 40 ℃; (i) 3-methoxyaniline, $Pd_2(dba)_3$, Xantphos, Na_2CO_3, toluene, H_2O, reflux.

Investigations on the SAR. Recombinant human FBPase activity was evaluated by employing the coupling enzymes phosphoglucose isomerase and glucose-6-phosphate dehydrogenase. The concomitant reduction of $NADP^+$ to NADPH was monitored spectrophotometrically.[40] All target compounds (**30-118)** were tested for their inhibitory activities against human liver FBPase. The corresponding results were summarized in **Tables 1-7**. AMP and MB05032 were used as reference molecules.

Initially, a number of *N*-sulfonyl indole-2-carboxamide derivatives with different R^8 substituents were tentatively designed and tested. As shown in **Table 1**, the simple methylsulfonamide **30** showed no inhibition against FBPase, while the cyclopropylsulfonamide **31** had moderate inhibition (IC_{50} = 2.90 μM). In contrast, the benzenesulfonamide **32** exhibited a much stronger potency with an IC_{50} value of 0.14 μM, which was 182-fold more potent than the hit compound **A** (IC_{50} = 25.6 μM). On the basis of this result, several other representative aromatic sulfonamides (**33-42**) were further evaluated. In fact, all of these aromatic sulfonamides including methoxyl, fluoro, nitro-substituted benzene sulfonamides, thiophene sulfonamide, and naphthalene sulfonamide exhibited high potency, with the IC_{50} values ranging from 0.10 μM to 0.32 μM. Therefore, the above results evidently demonstrated that the *N*-acyl arylsulfonamide was a critical structural feature of this series of inhibitors for producing strong inhibition against FBPase. It was thus speculated that the *N*-acyl sulfonamide moiety could form a hydrogen binding network with the key amino acids of FBPase.

Table 1. The SAR of various *N*-acyl sulfonamide derivatives (30-42) against FBPase[a]

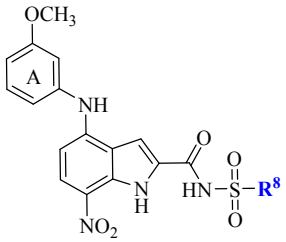

Compd	R^8	IC_{50} (μM)	Compd	R^8	IC_{50} (μM)
30	Me	>50	37	4-fluorophenyl	0.16±0.01
31	cPr	2.90±0.80	38	3-nitrophenyl	0.10±0.01
32	Ph	0.14±0.01	39	4-nitrophenyl	0.21±0.03
33	3-methoxyphenyl	0.15±0.06	40	4-(trifluoromethoxy)phenyl	0.27±0.08
34	4-methoxyphenyl	0.19±0.03	41	thiophen-2-yl	0.32±0.01
35	2-fluorophenyl	0.24±0.09	42	naphthalen-2-yl	0.28±0.02
36	3-fluorophenyl	0.14±0.00			

[a]AMP and MB05032 were used as reference molecules. IC_{50} for AMP was 3.3±0.1 μM. IC_{50} for MB05032 was 0.044±0.012 μM.

As the aromatic sulfonamides were preferred and all of the tested compounds (**32-42**) showed similar potency, we arbitrarily selected the un-substituted benzene and 4-methoxybenzene as the B ring for subsequent SAR investigations on the 4-substituents (R^4) of the indole scaffold (**Table 2**). The replacement of NH in compound **34** with O and S atom produced compounds **43** and **44**, which respectively showed 7.3-fold and 3.7-fold decrease in activity. Furthermore, using the NCH_3 (**45**, IC_{50} > 50 μM) or the carbonyl group to substitute for NH (**46**, IC_{50} > 10 μM) resulted in a loss of activity. Compounds with a two-atom linker were also designed. The

3-methoxybenzylamino-substituted compound **47** and benzamido-substituted compound **48** presented potent inhibition as well. However, the inhibition reduced about 5 times in comparison with compound **34**. Putting together, these data suggested that the NH group between the two aromatic rings was important for inhibition. Presumably, this NH group served as a key H-bond donor in forming a critical hydrogen bond with FBPase.

The alkylamino and cyclohexylamino groups were also incorporated into the 4-position of the indole ring, and the obtained compounds (**49-52**) displayed reduced inhibition with IC_{50} values at a single digit micromolar level. When a morpholino group or a chloro atom was installed onto the 4-position, the resultant compounds **53** (IC_{50}= 35.6 μM) and **54** (IC_{50} = 24.3 μM) displayed an even lower potency. Hence, these data demonstrated that an aromatic amino substituent on the 4-position of the indole ring could strongly bolster the potency. It was conceived that the occurred aromatic hydrophobic interaction and the hydrogen binding interaction have made great contributions for the binding affinity. Therefore, at this stage, the scaffold of 4-arylamino-*N*-arylsulfonyl-1*H*-indole-2-carboxamide was determined as the template structure, which was subjected to further extensive SAR explorations.

Table 2.The SAR of 4-substituted indole derivatives (43-54) against FBPase[a]

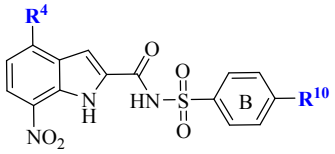

Compd	R^4	R^{10}	IC_{50} (μM)

34	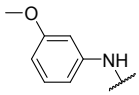	OMe	0.19±0.01
43	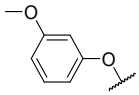	OMe	1.40±0.22
44	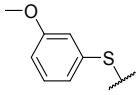	OMe	0.70±0.02
45	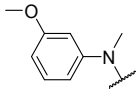	OMe	>50
46	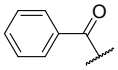	OMe	>10
47	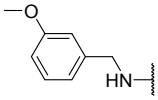	OMe	0.97±0.03
48	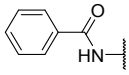	OMe	0.87±0.02
49	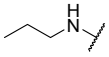	OMe	1.40±0.80
50	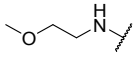	OMe	1.70±0.00
51	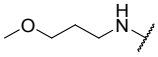	OMe	1.80±0.10
52	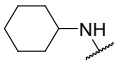	OMe	2.00±0.25
53		H	35.6±5.10
54	Cl	H	24.3±3.20

[a]AMP and MB05032 were used as reference molecules. IC_{50} for AMP was 3.3±0.1 μM. IC_{50} for MB05032 was 0.044±0.012 μM.

The effects of variations on the **A** ring were evaluated and outlined in **Table 3**. The mono-substituted **A** ring with various substituents on different positions was first investigated. Although all of these compounds (**32, 34, 55-69**) were active against FBPase with IC_{50} ranging from 0.12 μM to 3.10 μM, the substituted pattern of substituents had impacts on the inhibition. Introducing a methoxyl group on the

2-position would markedly deteriorate the activity, as compound **55** (IC_{50} = 3.10 μM) was the least potent derivative among compounds **32**, **55** and **56**, and it was 22-fold less potent than compound **32** with a methoxyl group on the 3-position (IC_{50} = 0.14 μM). Furthermore, placing a moiety on the 3-position was usually more favorable than that on the 4-position (**32 vs 56, 62 vs 63, 68 vs 69**). Also, a variety of moieties were tolerated on the 3-position and most of them strongly inhibit the FBPase activity with IC_{50} values ranging from 0.12 μM to 1.01 μM. Particularly, compounds with 3-substituents such as OMe, OEt, OCF_2H, CH_3, $NHCOCH_3$, and NO_2 displayed even stronger inhibition in the series, and their IC_{50} values are of less than 0.16 μM.

Among the di-substituted compounds (**70-74**), 3,4- and 3,5-disubstituted compounds **70**, **73,** and **74** were more active than 2,3- and 2,4-disubstituted compounds **71** and **72**. Hence, it was further supported that substitution on the 2-position of **A** ring was unfavorable for the activity. As for the 3,4,5-trisubstituted derivative, compound **75** (IC_{50} = 0.20 μM) exhibited high potency as well.

Overall, the above-mentioned results suggested that the substitution on the ortho-position of **A** ring was not tolerated. Presumably, the 2-substituent might bring about a steric hindrance or interfere with the hydrogen bond formation of the adjacent NH group. In contrast, the meta- and para-position could accommodate a variety of groups, either electron-donating groups or electron-withdrawing moieties, and that could provide a chance for further improving the structural diversity and drug-like

properties. Given consideration that grafting a substituent on the 3-position of **A** ring significantly enhanced the inhibition and taking synthetic simplicity and drug-like properties into account, we tentatively selected compound **34** as the lead for the next round of optimization.

Table 3.The SAR of substitution on the A ring of 7-nitroindole derivatives (55-75) against FBPase[a]

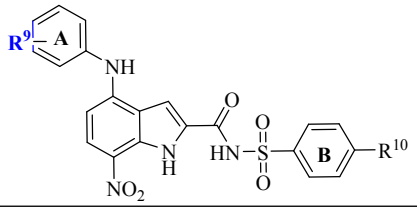

Compd	R^9	R^{10}	IC_{50} (μM)	Compd	R^9	R^{10}	IC_{50} (μM)
32	3-OMe	H	0.14±0.02	65	4-CF_3	OMe	0.91±0.21
34	3-OMe	OMe	0.19±0.01	66	3-NO_2	OMe	0.14±0.03
55	2-OMe	H	3.10±0.31	67	4-NO_2	OMe	0.35±0.02
56	4-OMe	H	1.00±0.20	68	3-morpholino	OMe	0.31±0.01
57	3-OEt	OMe	0.12±0.02	69	4-morpholino	OMe	1.09±0.22
58	3-OCF_2H	OMe	0.13±0.02	70	3,5-dimethoxy	OMe	0.14±0.01
59	3-Me	OMe	0.15±0.11	71	2,3-dimethoxy	OMe	1.46±0.35
60	3-Et	OMe	0.43±0.01	72	2,4-dimethoxy	OMe	1.28±0.11
61	3-acetamido	OMe	0.16±0.02	73	4-Cl-3-OMe	OMe	0.12±0.01
62	3-F	OMe	1.01±0.11	74	4-F-3-OMe	OMe	0.40±0.02
63	4-F	OMe	1.51±0.33	75	3,4,5-trimethoxy	OMe	0.20±0.01
64	3-CF_3	OMe	0.66±0.01				

[a]AMP and MB05032 were used as reference molecules. IC_{50} for AMP was 3.3±0.1 μM. IC_{50} for

MB05032 was 0.044±0.012 μM.

Modifications on the 5-, 6- and 7-positions of the indole ring were subsequently conducted by taking compound **34** as the template structure, and the results were listed in **Table 4**. Introducing an F atom on the 5-position (**76,** IC_{50} = 0.26 μM) produced a comparable activity to compound **34**, while incorporating a Cl or Me group resulted in a 5-fold decrease in activity, suggesting that a bulky substituent was not allowed on the 5-position.

Removing the 7-nitro group led to a drastic decline in inhibition as compound **79** was about 20-fold less active than compound **34**, indicating that the 7-substituent plays a key role in the binding affinity. Therefore, we further prepared other 7-substituted derivatives. Compounds (**83, 85, 86**) with an F, CN or CF_3 group could potently inhibit FBPase, and their IC_{50} values are of 0.57 μM, 0.36 μM and 0.51 μM, respectively. It was noteworthy that compound **84** (IC_{50} = 0.16 μM) with a Cl atom offered a potent and comparable activity to compound **34**. It is well-known that the NO_2 group is not desirable in the drug molecule in terms of drug-like properties, and thus we explored the 7-Cl substituted series of compounds in the later optimization, leading to a candidate molecule **Cpd118**.

The incorporation of an F, Cl or CH_3 group on the 6-position of the indole ring afforded compounds **80-82**, which displayed a reduced inhibition (IC_{50}, 1.1 μM - 3.6 μM), suggesting that the 6-substituent on the indole ring was not boosting the binding

affinity. Therefore, we retained a nitro group or a chloro atom on the 7-position of the indole ring in the following SAR investigation.

Table 4. The SAR of substitution on the 5-, 6- and 7-positions of indole derivatives (76-86) against FBPase[a]

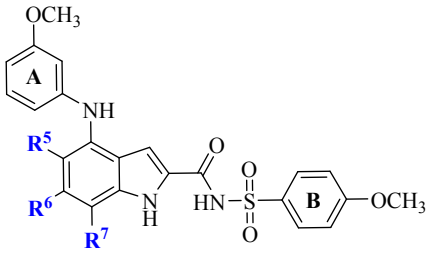

Compd	R^5	R^6	R^7	IC_{50} (μM)	Compd	R^5	R^6	R^7	IC_{50} (μM)
34	H	H	NO_2	0.19±0.02	81	H	Cl	H	1.1±0.01
76	F	H	NO_2	0.26±0.01	82	H	Me	H	3.6±0.62
77	Cl	H	NO_2	0.95±0.01	83	H	H	F	0.57±0.02
78	Me	H	NO_2	0.95±0.02	84	H	H	Cl	0.16±0.02
79	H	H	H	3.7±0.42	85	H	H	CN	0.36±0.01
80	H	F	H	1.2±0.14	86	H	H	CF_3	0.51±0.02

[a]AMP and MB05032 were used as reference molecules. IC_{50} for AMP was 3.3±0.1 μM. IC_{50} for MB05032 was 0.044±0.012 μM.

The effects of alkylation on the indole nitrogen atom of the lead compound **34** were also explored and illustrated in **Table 5**. The methylation on the nitrogen atom produced a remarkable boost on inhibition, compound **87** presented double-digit nanomolar potency with an IC_{50} value of 0.04 μM, which was comparable to the clinical candidate MB05032. In contrast, introducing an ethyl or isobutyl group did not increase the potency, the IC_{50} values of compounds **88** and **89** were 0.21 μM and

0.40 μM, respectively. Clearly, the methyl group was more favorable than the larger alkyl group, suggesting that a small pocket existed around the indole nitrogen. Thus, the methylation was performed on a number of the previously obtained potent derivatives with IC_{50} values of 0.10 μM - 0.20 μM. In fact, the *N*-methylation did not always give rise to an enhancement in potency. Some of the compounds (**90, 92, 93** and **95**) produced an increased activity, and their IC_{50} values (0.059 μM – 0.09 μM) reached the 10^{-8} M level. In contrast, compound **91** (IC_{50} = 0.23 μM) showed comparable activity to its unsubstituted counterpart; and compound **94** (IC_{50} = 1.30 μM) with a trimethoxyl group displayed a 6-fold decrease in potency compared with the corresponding unsubstituted derivative **75**. These facts implicated that the *N*-methylation not only brought about a beneficial hydrophobic interaction, but also might have an impact on the binding of substituted A ring.

Table 5. The SAR of *N*-alkylation of 7-nitroindole derivatives (87-95) against FBPase[a]

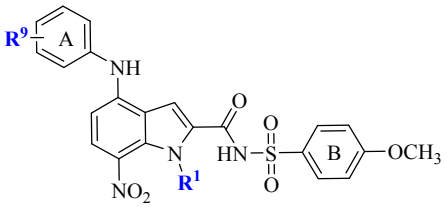

Compd	R^1	R^9	IC_{50} (μM)	Compd	R^1	R^9	IC_{50} (μM)
34	H	3-OMe	0.19±0.01	91	Me	3-EtO	0.23±0.01
87	Me	3-OMe	0.04±0.01	92	Me	3-acetamido	0.059±0.002
88	Et	3-OMe	0.21±0.02	93	Me	3,5-dimethoxy	0.063±0.001
89	iBu	3-OMe	0.40±0.11	94	Me	3,4,5-trimethoxy	1.30±0.22
90	Me	3-Me	0.09±0.01	95	Me	4-Cl-3-OMe	0.063±0.003

[a]AMP and MB05032 were used as reference molecules. IC_{50} for AMP was 3.3±0.1 μM. IC_{50} for

MB05032 was 0.044±0.012 μM.

Since the 7-chloro-substituted indole derivatives were supposed to be more drug-like than the 7-nitro substituted derivatives, we further broadened the SARs based on this template. As shown in **Table 6**, the methylation of compound **84** afforded compound **96**, which exhibited remarkable inhibition with an IC_{50} value of 0.052 μM, and this potency was comparable to that of compound **87** (the 7-nitro substituted analog) and MB05032. The other four compounds (**103, 105-107**) with a methyl, trifluoromethyl or cyano substituent on the *meta*- or *para*-position of benzene ring were also identified with a pronounced potency (IC_{50}, 0.056 μM - 0.085 μM). Of note, compound **104** (IC_{50} = 0.77 μM) with a trifluoromethyl group on the *ortho*-position and compound **108** (IC_{50} = 0.94 μM) with a bulky *iso*-butyl group on the *meta*-position of benzene ring showed moderate inhibition. In addition, the benzo-heterocyclic derivatives (**111-113**) were also examined and none of them showed the desired high potency. To summarize, these results suggested that the binding pocket occupied by the arylsulfonyl moiety was a key binding site and an appropriate modification on this fragment would provide an opportunity for the improvement in potency.

Table 6. The SAR of *N*-acyl arylsulfonamide containing 7-chloroindole derivatives (96-113) against FBPase[a]

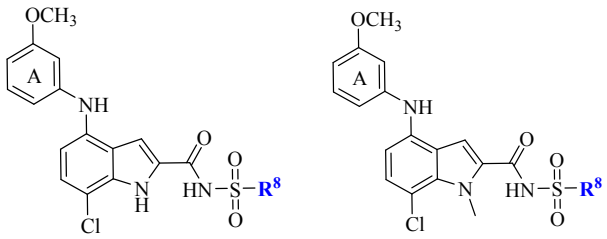

84 **96-113**

Compd	R^8	IC_{50} (μM)	Compd	R^8	IC_{50} (μM)
84	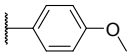	0.16±0.02	105	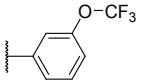	0.085±0.011
96	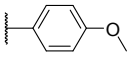	0.052±0.006	106	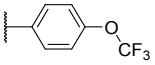	0.07±0.02
97		0.18±0.03	107	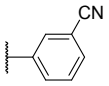	0.056±0.002
98	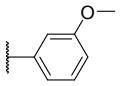	0.15±0.01	108	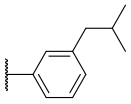	0.94±0.02
99		0.14±0.02	109		0.22±0.08
100		0.23±0.01	110	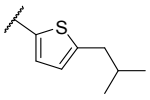	0.13±0.03
101	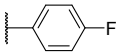	0.47±0.06	111	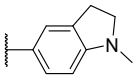	0.59±0.26
102		0.14±0.02	112	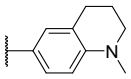	0.54±0.08
103	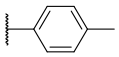	0.071±0.004	113	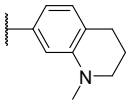	0.67±0.11

104	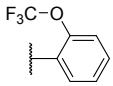	0.77±0.03

[a]AMP and MB05032 were used as reference molecules. IC_{50} for AMP was 3.3±0.1 μM. IC_{50} for MB05032 was 0.044±0.012 μM.

As shown in **Table 7**, we also exchanged the position of the chloro atom and 3-methoxyphenylamino group of compounds **84** and **96** resulted in 4-chloro substituted compounds **114** and **115**. Compound **114** (IC_{50} = 0.10 μM) had similar potency with compound **84**, while the inhibition of the *N*-methyl derivative **115** (IC_{50} > 10 μM) was declined markedly, indicating that the methyl group on this position could severely interfered with the binding due to its steric hindrance, presumably. In comparison with compound **96**, as the close analogs of indole scaffold, the benzo[*d*]imidazole analog **116** (IC_{50} = 0.027 μM) offered a comparable inhibition, and the aza-indole analog **117** showed a 15-fold reduction in potency. The replacement of the indole scaffold would be a choice for obtaining novel FBPase inhibitors with diversified structures.

Table 7. The SAR of various heterocyclic rings containing derivatives (114-118) against FBPase[a]

Compd	structure	IC_{50} (μM)
114	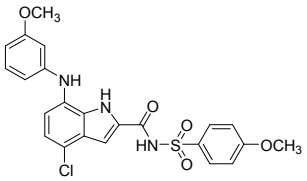	0.10±0.01

115	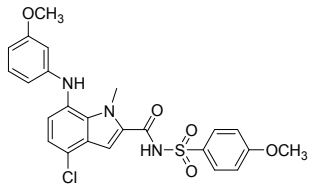	>10
116	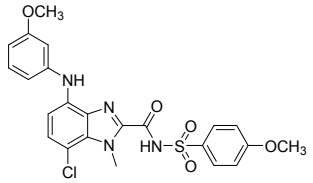	0.027±0.003
117	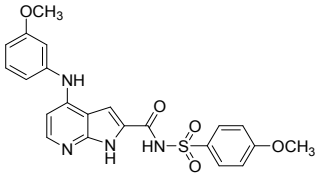	0.71±0.02
118	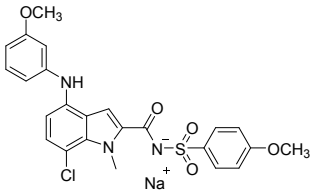	0.029±0.006

[a]AMP and MB05032 were used as reference molecules. IC_{50} for AMP was 3.3±0.1 μM. IC_{50} for MB05032 was 0.044±0.012 μM.

The Analysis of Cocrystal Structure of FBPase Complexed with Cpd118. The X-ray cocrystal structure of **Cpd118** bound to FBPase was solved to a resolution of 2.40 Å (PDB: 6LW2). As shown in **Figure 3**, the tetramer of the protein contained four small molecules, and each molecule occupied two sites, the adenine pocket of AMP binding site and the interface region between two monomers (**Figure 3, A and B**). Obviously, **Cpd118** has a very different binding mode from AMP, which fully occupied both the adenine sub-pocket and the phosphate binding site. As shown in **Figure 3C** and **3D**, **Cpd118** occupied the adenine binding pocket with its 4-methoxybenzenesulfonamide fragment interacting with amino acids Glu20, Ala24,

and Leu30 through hydrophobic interactions, the *N*-acyl sulfonamide linker, which was tentatively used as the bioisostere of the phosphate, was situated above of the phosphate pocket. Noticeably, a water molecule was observed in this phosphate binding site instead, bridging rich hydrogen binding interactions between the O atom of the sulfonyl group and the characteristic amino acids Thr27, Glu29, Lys112, and Tyr113. These binding interactions would certainly boost the binding affinity. Importantly, the *N*-acyl sulfonamide linker itself actually formed an extensive hydrogen bond network with the key amino acids Leu30 and Thr31, which were supposed to contribute to the binding affinity to a great extent. Furthermore, these H-bond interactions facilitated this linker to protrude into the narrow channel formed by Gly26, Thr27, and Gly28 on the front and Leu30 and Thr31 on the back, thus orientating the indole part into the subunit interface region (**Figure 3, C**). Strikingly, at this interface area, the extensive π-π stacking interactions were observed: one is between the two indole rings, and the other is between the two 3-methoxybenzene rings from monomers A (B) and D (C), respectively. These strong aromatic hydrophobic interactions were another critical feature of this series of inhibitors, and played remarkable roles for stabilization of the complex. Moreover, the indole ring interacted with the side chain of Arg22, and the 3-methoxyphenyl fragment interacted with Arg25 through hydrophobic interactions as well. Additionally, one more critical binding feature was also observed. The NH group between the two aromatic moieties formed a hydrogen bond with the C=O group of Gly26. This was consistent with the results of SARs as a replacement of the NH group with NCH_3 would lead to a marked

decrease in potency. It was also observed that both *N*-methyl group and 7-chloro atom on the indole ring situated in a hydrophobic area lined with the side chains of Met18 and Arg22, and the SARs demonstrated that these small hydrophobic groups had pronounced effects on the binding affinity.

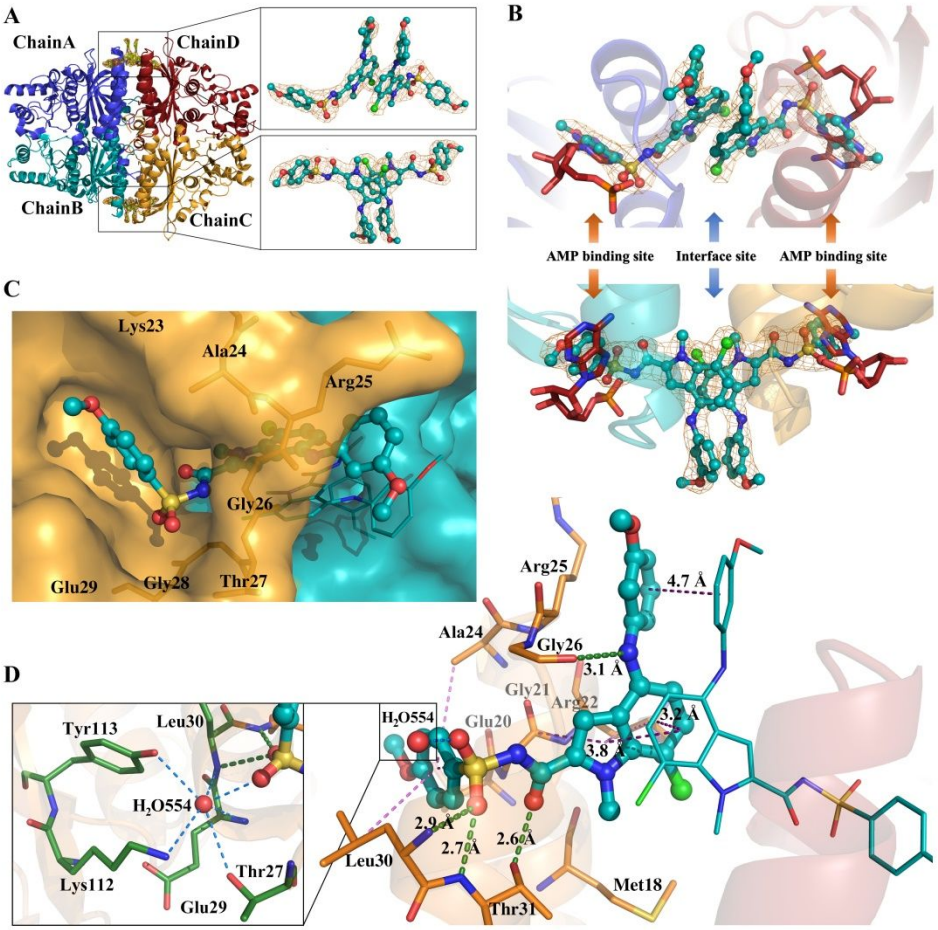

Figure 3. The cocrystal structure of FBPase in complex with Cpd118 (PDB 6LW2) (A) Overview of FBPase comprised of four monomers and a close view of the ligands; (B) The binding pose of Cpd118 which occupied the subunits interface and a part of AMP binding site (the AMP from 1FTA was shown in red);[36] (C) The binding pose of Cpd118 and the tunnel formed by Gly26, Thr27 and Gly 28; (D) Detailed interactions of Cpd118 with key amino acides, green dashes and blue dashes for H-bonds and purple dashes for hydrophobic interactions, the distance for H-bonds and the centroid of aromatic rings were labelled. The

image was created with PyMol software.[41] The $2F_o$-F_c electron density maps of (A) and (B) were contoured at 1σ.

Collectively, **Cpd118** took a distinct binding mode, which simultaneously exploited both the AMP domain and the interface region via three characteristic fragments including the *N*-acyl sulfonamide, 4-methoxybenzene ring, and 4-arylaminoindole moiety. These structural features created a very different binding mode from that of the well-known AMP mimics such as MB05032, which fully made use of the AMP allosteric binding site. Interestingly, we noted that the benzoxazole benzenesulfonamide derivatives (**Figure 1**) and the sulfonyl ureido derivatives (**Figure 1**) were reported to have a similar binding mode to **Cpd118**.[20,21,30,31] They all utilized the adenine pocket of AMP and the hydrogen binding interactions with Leu30 and Thr31 as well. However, at the interface binding region, these two types of molecules did not build up extensive π-π stacking interactions as **Cpd118**. In summary, this series of *N*-acyl arylsulfonamide inhibitors with a unique binding mode provided an opportunity for achieving highly potent and drug-like allosteric dual binding site inhibitors against FBPase.

The Enzymatic Activity and Selectivity of Cpd118. The pyruvate is a substrate of the gluconeogenesis process. The oral administration of pyruvate to fasting animals can result in an enhancement of blood glucose level through the gluconeogenesis process. Therefore, the oral pyruvate tolerance test (OPTT) in normal fasting ICR

mice or alloxan-induced diabetic mice was used to quickly screen the *in vivo* efficacy of the obtained highly potent FBPase inhibitors, which had IC_{50} values at the double digit nanomolar level. As a result, **Cpd118** (the sodium salt of compound **96**) was found to be the most potent compound in the OPTT test by measuring the blood glucose level. Hence, **Cpd118** was selected for further evaluation in terms of its enzymatic activity, selectivity, and *in vivo* glucose lowering efficacy in type 2 diabetic animal models.

As shown in **Table 8, Cpd118** exhibited strong inhibition against FBPase (0.029±0.006 μM), whereas no significant inhibition or activation was observed towards six other key AMP-binding enzymes with their IC_{50} or EC_{50} values of more than 100 μM or 10 μM, respectively. **Cpd118** displayed an excellent selectivity against all six tested enzymes.

Table 8. FBPase inhibitory potency and selectivity of Cpd118

Enzymes	IC_{50} (μM)[a]	EC_{50} (μM)[a]
Human liver FBPase	0.029±0.006	—
AMP deaminase	> 100	—
Adenylate kinase (AK)	> 100	—
Adenosine kinase (ADK)	> 100	—
Glycogen phosphorylase	—	> 100
Phosphofructokinase (PFK)	—	> 100
AMP-activated protein kinase	—	> 10

	(AMPKα1β1γ1)

[a]The inhibition of enzymes is expressed as IC_{50}, while activation of enzymes is expressed as EC_{50}.

The in vivo Glucose-lowering Effects of Cpd118. To assess the potency of **Cpd118** in blood glucose management *in vivo*, long-term glucose-lowering effects of **Cpd118** were evaluated in type 2 diabetic KKAy mice and ZDF rats, respectively. As shown in **Figure 4(A-C)**, after oral administration of **Cpd118** at a dose of 200 mg/kg for 26 days to the diabetic KKAy mice, fasting blood glucose level declined by 35% and postprandial blood glucose decreased by 49%, respectively. As expected, the level of HbA1c was reduced to 5.5% after 30 days of treatment, and the diabetic model (DM) control group was around 6.2%.

Similarly, amelioration of fasting blood glucose and postprandial hyperglycemia were also observed in the diabetic ZDF rats. As shown in **Figure 4(D-F)**, after oral administration of **Cpd118** at a dose of 50 mg/kg for 29 days, the fasting and postprandial blood glucose levels declined by 27% and 24%, respectively. Noticeably, the HbA1c level was significantly lower (4.2%) after 32 days of treatment, while the corresponding level of the DM control group was 6.2%. It is demonstrating that **Cpd118** could constantly and efficiently control the blood glucose level of both diabetic animal models during the long period of treatment.

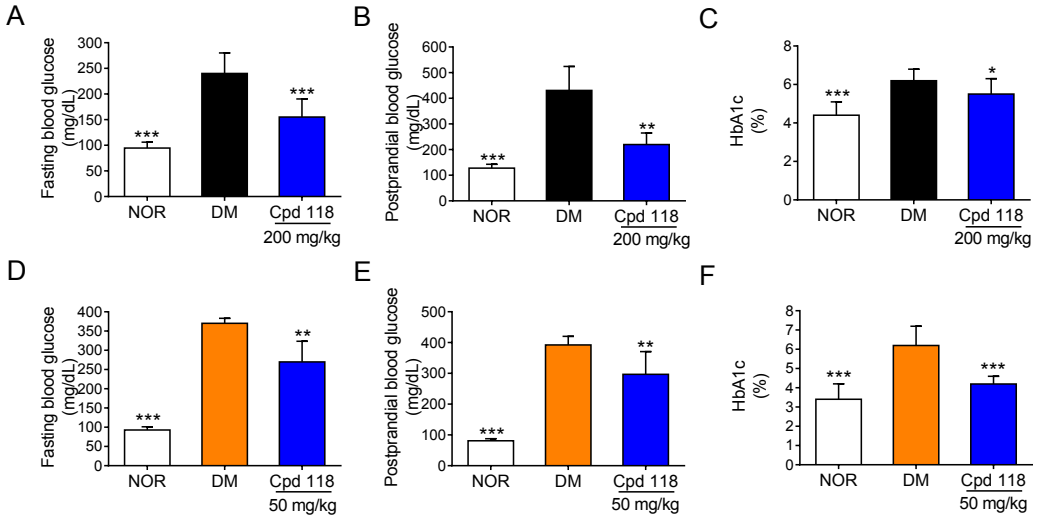

Figure 4. Long-term treatment with Cpd118 ameliorates hyperglycemia in diabetic KKAy mice (200 mg/kg, orally) and diabetic ZDF rats (50 mg/kg, orally). The fasting and postprandial blood glucose levels in diabetic KKAy mice after 26-day treatment (A and B) and in diabetic ZDF rats after 29-day treatment (D and E). Glycated hemoglobin concentration (HbA1c) in diabetic KKAy mice after 30-day treatment (C) and in diabetic ZDF rats after 32-day treatment (F). Values are expressed as mean ± SD, n = 8 in each group, *p < 0.05, **p < 0.01, ***p < 0.001 vs the DM group.

Inhibitory Effects of Cpd118 on Gluconeogenesis. The oral pyruvate tolerance test (OPTT) was conducted in KKAy mice after 34-day treatment and in ZDF rats after 24-day treatment. Both the overnight fasting blood glucose at 0 min (baseline, fasted overnight) and blood glucose at the 30 min after pyruvate loading were decreased in both animal models (**Figure 5A and 5D**). In comparison with the DM control group, the mean increase rate of the blood glucose at 30 min declined drastically by 83.8% and 58.3% (**Figure 5B and 5E**). These results indicated that

Cpd118 possessed a strong capability for inhibiting gluconeogenesis. Furthermore, at the end of treatment, the FBPase activities in the liver of both KKAy mice and ZDF rats were assessed and the reduction of 94.7% and 28% were observed, respectively (**Figure 5C and 5F**).

FBPase catalyzes the reaction converting the substrate fructose-1,6-bisphosphate ($F1,6P_2$) to the product fructose-6-phosphate (F6P). As such, the inhibition of FBPase would reduce the production of F6P. Therefore, we performed a targeted metabolomics study using ultra-high-performance liquid chromatography-tandem mass spectroscopy and gas chromatography-mass spectroscopy to discriminate the targeted energy metabolites profiles in liver samples in the ZDF rats. As anticipated, in comparison with the DM control group, the hepatic F6P levels markedly decreased in the **Cpd118**-treated group (**Figrue 5G**). Taken together, these results demonstrated that **Cpd118** could impede the gluconeogenesis in the liver of diabetic animal models by inhibiting the liver FBPase activity, thereby leading to a substantial decline of blood glucose levels.

Lactate is one of the major gluconeogenic precursors. The lactate elevation is a concern of blocking gluconeogenesis pathway, which impacts the safety potential of FBPase inhibitors. Thus, the hepatic and blood lactate levels were detected. As shown in **Figure 5H** and **5I**， **Cpd118** did not have an impact on the lactate level after 39 days of treatment in ZDF rats, as the lactate level in the treated group was similar to

that of the DM control group, suggesting that **Cpd118** could reduce the blood glucose level with a low risk of hyperlactatemia.

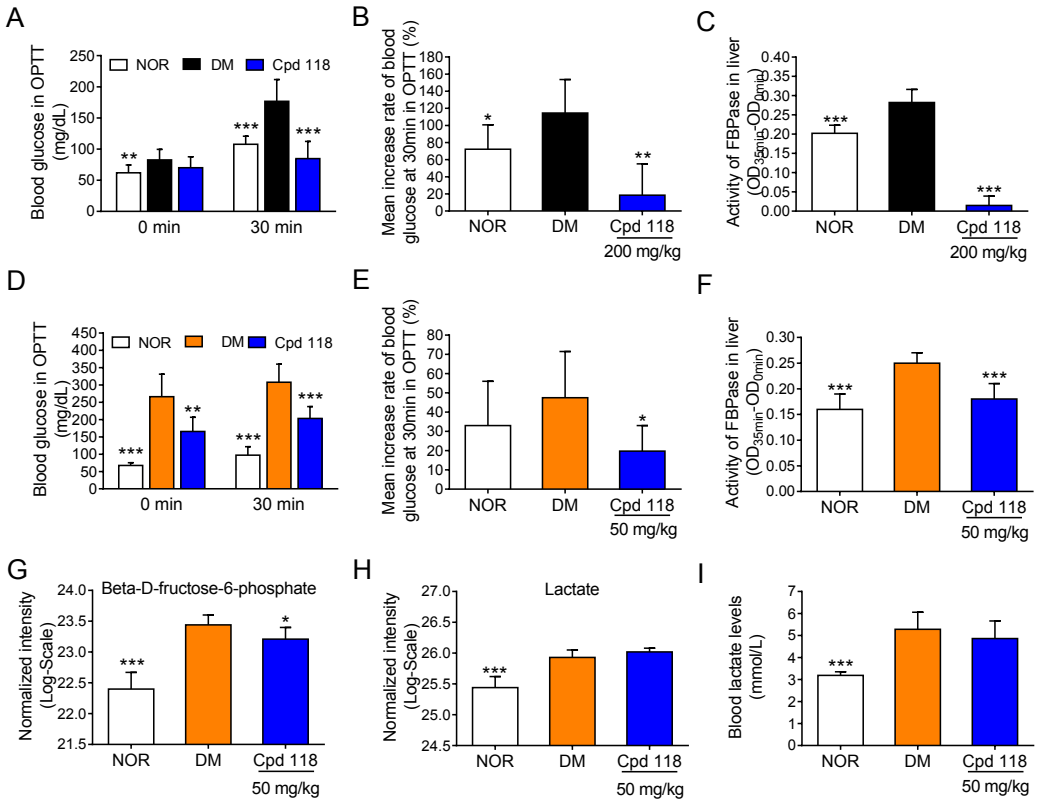

Figure 5. Long-term treatment with Cpd118 inhibits *in vivo* gluconeogenesis in diabetic KKAy mice (200 mg/kg, orally) and diabetic ZDF rats (50 mg/kg, orally). Effects on the overnight-fasted blood glucose (0 min) and 30 min after pyruvate (2 g/kg) loading in the diabetic KKAy mice on the 34th day of treatment (A) and in the ZDF rats on the 24th day of treatment (D). Mean increase rate of blood glucose at 30 min in OPTT of the diabetic KKAy mice (B) and that of the diabetic ZDF rats (E). The activity of FBPase in the liver of KKAy mice at the end of treatment (C) and that in the liver of ZDF rats (F). LC-MS analysis of fructose-6-phosphate (G) and lactate (H) in the liver of ZDF rat at the end of treatment (n = 6-8, mean ± SD). (I) Blood lactate levels in diabetic ZDF rats at the end of treatment. Values are expressed as mean ± SD, n = 8 in each group, *p < 0.05, **p < 0.01, ***p < 0.001 vs the

DM group.

Cpd118 Inhibited Gluconeogenesis via Downregulating the Expression of FBPase Protein levels. To further investigate the molecular mechanism of **Cpd118** on gluconeogenesis, the FBPase expression was measured as well. As shown in **Figure 6A and 6B**, at concentrations of 5 μM and 10 μM, **Cpd118** blocked the glucose production and downregulated the expression level of FBPase in HepG2 cells after 4 h starvation in a dose-dependent manner. We also examined the effect of **Cpd118** on hepatic FBPase expression in the KKAy mice and ZDF rats. As shown in **Figure 6C and 6D**, the downregulation of hepatic FBPase expressions was also observed. Theses results suggested that **Cpd118** could reduce glucose production and gluconeogenesis through both the inhibition of FBPase activity and downregulation of its expression. The detailed mechanism of **Cpd118** on regulating FBPase needs to be further explored.

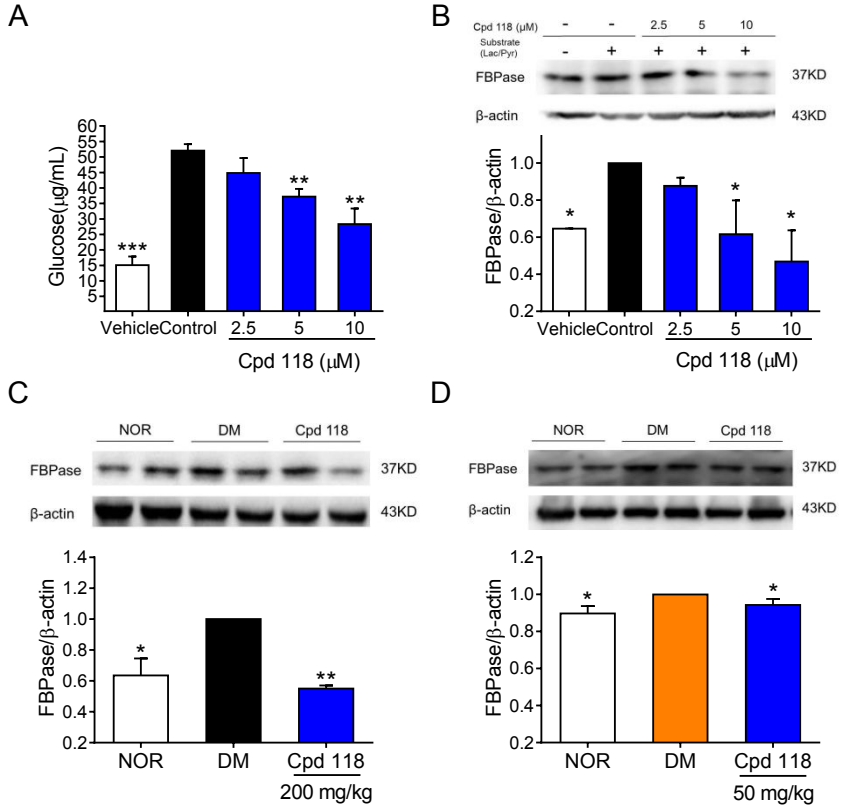

Figure 6. The effects of Cpd118 treatment on FBPase expression (A) Inhibitory effects of Cpd118 on gluconeogenesis substrate conversion to glucose in HepG2 cells. (B) Effects on the FBPase expression in HepG2 cells. Values are expressed as mean ± SD, n = 3 in each condition, *p < 0.05, **p < 0.01, ***p < 0.001 vs Vehicle. (C and D) Effects on the expression level of liver FBPase in the diabetic KKAy mice (C) and ZDF rats (D) at the end of treatment. Data represented the mean of at least three independent experiments. Values are expressed as mean ± SD, n = 6 in each group, *p < 0.05, **p < 0.01, ***p < 0.001 vs the DM group.

The Pharmacokinetic Profile of Cpd118. The pharmacokinetic properties of **Cpd118** were evaluated by intravenous and oral administration. As shown in **Table 9**, **Cpd118** produced a high exposure concentration. The half-life ($t_{1/2}$) was 5.32 h and

the oral bioavailability reached 99.1% at a single dose of 50 mg/kg to SD rats. Therefore, **Cpd118** possessed a desirable and appropriate plasma pharmacokinetic profile for orally delivering.

Table 9. The pharmacokinetic profile of Cpd118

Parameters	Unit	mean±SD (3 mg/kg, i.v.)	mean±SD (50 mg/kg, p.o.)
AUC(0-t)	h*μg/mL	40.17 ±2.02	663.90 ± 114.83
AUC(0-∞)	h*μg/mL	40.21±1.98	663.91 ± 114.83
MRT(0-t)	h	2.54±0.11	7.88 ± 0.89
MRT(0-∞)	h	2.56±0.04	7.88 ± 0.89
t1/2z	h	3.32±0.05	5.32 ± 1.03
Tmax	h	-	5.60 ± 3.85
Cmax	μg /mL	-	53.74 ± 7.32
Vz	mL/kg	357.90 ± 13.37	590.31 ± 160.34
CLz	mL/h/kg	74.72±3.64	77.20 ± 13.73
F			99.1%

■ CONCLUSION

Based on the hit structure **A** bearing a new 4-arylamino-indole-2-carboxylic acid scaffold, a novel class of highly potent FBPase inhibitors with *N*-arylsulfonyl-4-arylamino-indole-2-carboxamide template were achieved by taking advantage of the bioisosteric replacement strategy. The extensive SAR investigations

and the crystal structure of FBPase-**Cpd118** complex demonstrated that three key structural features contributed greatly to the high potency and selectivity. The arylsulfonamide segment bound to the adenine subpocket of AMP binding site via hydrophobic interactions. The *N*-acyl sulfonamide not only formed critical and characteristic hydrogen binding interactions with Leu30 and Thr31, but also constructed an H-bond network with Thr27, Glu29, Lys112, and Tyr113 through a water bridge. The favorable π-π stacking interactions between the two indole rings and two 4-aminoaryl moieties from different monomer were built up. Furthermore, a featured hydrogen bond was observed between the NH group and Gly26. Overall, these hydrogen binding interactions and π-π stacking interactions are unique to this class of FBPase inhibitors, conferring them with high potency and high selectivity.

In this work, **Cpd118** was selected as a candidate compound and its pharmacodymic and pharmacokinetic properties were evaluated. It exhibited profound glucose-lowering effects in both diabetic KKAy mice and ZDF rats after a long-term treatment, and the HbA1c decreased significantly, demonstrating that **Cpd118** was able to provide a persistent and robust glycemic control. Furthermore, **Cpd118** elicited a strong capability of blocking the gluconeogenesis process in the liver of the two type 2 diabetic animal models, as the glucose level was markedly reduced in the OPTT test. Impressively, at the end of long-term treatment with **Cpd118**, the suppression of both enzymatic activity and FBPase expression in the liver tissue of both diabetic animal models were observed. Additionally, the product of FBPase

catalyzed biotransformation, fructose-6-phosphate in the liver was found to be reduced with metabolomics study. These results supported that **Cpd118** could impede the gluconeogenesis pathway via direct inhibiting FBPase activity and expression, resulting in significant reductions in fasting and postprandial blood glucose level.

Interestingly, no hypoglycemia and lactate elevation were observed after long-term treatment of **Cpd118** in diabetic animal models, although these concerns existed by targeting on the glucogenesis pathway. Moreover, the pharmacokinetic profile of **Cpd118** suggested that it had desirable PK properties with the bioavailability of 99.1%.

In conclusion, **Cpd118** was an attractive FBPase inhibitor with a novel scaffold for further development in terms of its preferable *in vivo* efficacy and PK properties. It was expected to be useful for the treatment of type 2 diabetes characterized by both overt fasting and postprandial hyperglycemia. This work demonstrated that highly potent FBPase inhibitors with good oral bioavailability could be achieved without using any prodrug strategies.

■ EXPERIMENTAL SECTION

General Information. Unless otherwise noted, all materials were obtained from commercial suppliers and used without further purification. All reactions involving air- or moisture-sensitive reagents were performed under an argon atmosphere.

Melting points were measured on a Yanaco micro melting point apparatus and are uncorrected. 1H NMR (300 MHz and 400 MHz) on a Varian Mercury spectrometer was recorded in DMSO-d_6 or $CDCl_3$. Chemical shifts are reported in δ (ppm) units relative to the internal standard tetramethylsilane (TMS). High resolution mass spectra (HRMS) were obtained on an Agilent Technologies LC/MSD TOF spectrometer. All chemicals and solvents used were of reagent grade without purified or dried before use. All the reactions were monitored by thin-layer chromatography (TLC) on pre-coated silica gel G plates at 254 nm under a UV lamp. Column chromatography separations were performed with silica gel (200 - 300 mesh).

Synthesis of Compounds. *General procedure for preparation of N-(subtituted-sulfonyl)-indole-2-carboxamide derivatives (**30-118**)*. A mixture of 2-carboxylic acid derivatives (compounds **6, 7, 10, 15, 18, 26, 29**) (1 eq), HATU (1.5 eq), DMAP (0.5 eq) and Et_3N (2 eq) in DCM was stirred and then substituted-sulfonamide (2 eq) was added. The mixture was stirred at room temperature for 20 h and then evaporated. The residue was dissolved in EtOAc, and washed with 1 M dilute hydrochloric acid and water. The crude product obtained after concentration was purified by column chromatography or recrystallization to give title products. Compounds **30-53, 55-117** were prepared with this method. Compound **54** was prepared using EDC instead of HATU as the condensation reagent.

4-((3-Methoxyphenyl)amino)-N-(methylsulfonyl)-7-nitro-1H-indole-2-carboxamide

(30): yellow solid; yield: 75%; mp: >250 °C; ^{1}H-NMR (300 MHz, DMSO-d_6) δ (ppm): 12.67 (brs, 1H), 11.99 (s, 1H), 9.69 (s, 1H), 8.17 (d, J = 9.3 Hz, 1H), 7.98 (s, 1H), 7.36 (t, J = 8.1 Hz, 1H), 6.98 (d, J = 8.1 Hz, 1H), 6.93 (s, 1H), 6.81 (d, J = 9.0 Hz, 2H), 3.79 (s, 3H), 3.43 (s, 3H); ^{13}C-NMR (150 MHz, DMSO-d_6): δ (ppm): 160.12, 158.31, 147.05, 140.39, 131.97, 130.27, 128.83, 127.23, 124.14, 116.79, 114.93, 110.63, 110.48, 108.43, 102.22, 55.17, 41.49; HRMS (ESI): *m/z,* calcd. for $C_{17}H_{17}N_4O_6S$ $[M+H]^+$: 405.0863, found 405.0839.

N-(Cyclopropylsulfonyl)-4-((3-methoxyphenyl)amino)-7-nitro-1H-indole-2-carboxamide **(31):** yellow solid; yield: 83%; mp: 270-272 °C; ^{1}H-NMR (400 MHz, DMSO-d_6) δ (ppm): 12.63 (brs, 1H), 11.95 (s, 1H), 9.69 (s, 1H), 8.17 (d, J = 9.2 Hz, 1H), 7.98 (s, 1H), 7.36 (t, J = 8.0 Hz, 1H), 6.98 (d, J = 8.0 Hz, 1H), 6.94 (s, 1H), 6.81 (d, J = 8.8 Hz, 2H), 3.79 (s, 3H), 3.16-3.18 (m, 1H), 1.16-1.19 (m, 4H); ^{13}C-NMR (150 MHz, DMSO-d_6): δ (ppm): 160.11, 158.00, 147.04, 140.38, 131.99, 130.26, 128.73, 127.21, 124.14, 116.80, 114.92, 110.62, 110.46, 108.41, 102.26, 55.17, 31.04, 5.69; HRMS (ESI): *m/z,* calcd. for $C_{19}H_{19}N_4O_6S$ $[M+H]^+$: 431.1020, found 431.1005.

4-((3-Methoxyphenyl)amino)-7-nitro-N-(phenylsulfonyl)-1H-indole-2-carboxamide **(32):** yellow solid; yield: 79%; mp: >250 °C; ^{1}H-NMR (400 MHz, DMSO-d_6) δ (ppm): 13.10 (brs, 1H), 11.90 (brs, 1H), 9.65 (s, 1H), 8.15 (d, J = 8.8 Hz, 1H), 8.05 (d, J = 7.6 Hz, 2H), 7.86 (s, 1H), 7.75 (t, J = 7.2 Hz, 1H), 7.67 (t, J = 7.6 Hz, 2H), 7.35 (t, J = 8.4 Hz, 1H), 6.95 (d, J = 8.0 Hz, 1H), 6.91 (s, 1H), 6.78 (t, J = 9.6 Hz,

2H), 3.78 (s, 3H); ^{13}C-NMR (150 MHz, DMSO-d_6): δ (ppm): 160.11, 157.36, 147.09, 140.34, 139.29, 133.83, 132.01, 130.27, 129.20, 128.49, 127.69, 127.26, 124.10, 116.72, 114.98, 110.56, 110.51, 108.47, 102.27, 55.16; HRMS (ESI): *m/z,* calcd. for $C_{22}H_{19}N_4O_6S$ $[M+H]^+$: 467.1020, found 467.1005.

4-((3-Methoxyphenyl)amino)-N-((3-methoxyphenyl)sulfonyl)-7-nitro-1H-indole-2-carboxamide **(33):** yellow solid; yield: 88%; mp: 153-154 °C; ^{1}H NMR (400 MHz, DMSO-d_6) δ (ppm): 11.84 (brs, 2H), 9.63 (s, 1H), 8.14 (d, J = 9.2 Hz, 1H), 7.84 (s, 1H), 7.55-7.61 (m, 2H), 7.51 (s, 1H), 7.29-7.36 (m, 2H), 6.94 (d, J = 8.0 Hz, 1H), 6.90 (s, 1H), 6.78 (t, J = 9.2 Hz, 2H), 3.84 (s, 3H), 3.76 (s, 3H); ^{13}C-NMR (150 MHz, DMSO-d_6): δ (ppm): 161.10, 159.15, 157.41, 147.07, 140.55, 140.33, 131.99, 130.49, 130.26, 128.55, 127.23, 124.09, 119.59, 119.45, 116.73, 114.96, 112.79, 110.49, 108.44, 102.27, 55.67, 55.16; HRMS (ESI): *m/z,* calcd. for $C_{23}H_{21}N_4O_7S$ $[M+H]^+$: 497.1131, found 497.1117.

4-((3-Methoxyphenyl)amino)-N-((4-methoxyphenyl)sulfonyl)-7-nitro-1H-indole-2-carboxamide **(34):** yellow solid; yield: 55%; mp: >250 °C; ^{1}H-NMR (400 MHz, DMSO-d_6) δ (ppm): 12.91 (brs, 1H), 11.85 (brs, 1H), 9.62 (brs, 1H), 8.13 (d, J = 9.2 Hz, 1H), 7.96 (d, J = 8.4 Hz, 2H), 7.82 (s, 1H), 7.33 (t, J = 8.0 Hz, 1H), 7.15 (d, J = 8.4 Hz, 2H), 6.94 (d, J = 8.0 Hz, 1H), 6.89 (s, 1H), 6.77 (t, J = 9.6 Hz, 2H), 3.85 (s, 3H), 3.76 (s, 3H); ^{13}C-NMR (100 MHz, DMSO-d_6): δ (ppm): 163.22, 160.10, 157.24, 147.05, 140.34, 131.96, 130.68, 130.25, 130.17, 128.61, 127.17, 124.10, 116.71,

114.98, 114.29, 110.48, 110.39, 108.47, 102.26, 55.78, 55.16. HRMS (ESI): *m/z,* calcd. for $C_{23}H_{21}N_4O_7S$ $[M+H]^+$: 497.1126, found 497.1117.

N-((2-Fluorophenyl)sulfonyl)-4-((3-methoxyphenyl)amino)-7-nitro-1H-indole-2-carbo xamide **(35):** yellow solid; yield: 79%; mp: >250 °C; ^{1}H-NMR (300 MHz, DMSO-d_6) δ (ppm): 11.93 (brs, 1H), 9.65 (s, 1H), 8.16 (d, J = 9.3 Hz, 1H), 8.04 (t, J = 6.9 Hz, 1H), 7.79-7.85 (m, 2H), 7.48 (t, J = 8.4 Hz, 2H), 7.34 (t, J = 8.1 Hz, 1H), 6.94 (d, J = 8.4 Hz, 1H), 6.90 (s, 1H), 6.78 (t, J = 8.4 Hz, 2H), 3.77 (s, 3H); HRMS (ESI): *m/z,* calcd. for $C_{22}H_{18}N_4O_6FS$ $[M+H]^+$: 485.0926, found 485.0897.

N-((3-Fluorophenyl)sulfonyl)-4-((3-methoxyphenyl)amino)-7-nitro-1H-indole-2-carbo xamide **(36):** yellow solid; yield: 54%; mp: >250 °C; ^{1}H NMR (400 MHz, DMSO-d_6) δ (ppm): 11.84 (brs, 1H), 9.66 (s, 1H), 8.15 (d, J = 9.2 Hz, 1H), 7.83-7.91 (m, 3H), 7.74 (dd, J_1 = 13.6 Hz, J_2 = 8.0 Hz, 1H), 7.63 (t, J = 8.0 Hz, 1H), 7.35 (t, J = 8.0 Hz, 1H), 6.95 (d, J = 8.0 Hz, 1H), 6.91 (s, 1H), 6.79 (t, J = 9.2 Hz, 2H), 3.78 (s, 3H); HRMS (ESI): *m/z,* calcd. for $C_{22}H_{18}N_4O_6FS$ $[M+H]^+$: 485.0931, found 485.0918.

N-((4-Fluorophenyl)sulfonyl)-4-((3-methoxyphenyl)amino)-7-nitro-1H-indole-2-carbo xamide **(37):** yellow solid; yield: 74%; mp: >250 °C; ^{1}H-NMR (400 MHz, DMSO-d_6) δ (ppm): 11.88 (brs, 1H), 9.66 (s, 1H), 8.11-8.16 (m, 3H), 7.86 (s, 1H), 7.51 (t, J = 8.8 Hz, 2H), 7.35 (t, J = 8.0 Hz, 1H), 6.95 (d, J = 8.0 Hz, 1H), 6.91 (s, 1H), 6.79 (t, J = 9.6 Hz, 2H), 3.78 (s, 3H); ^{13}C-NMR (150 MHz, DMSO-d_6): δ (ppm): 164.85 (J_{CF} = 251.1 Hz), 160.09, 157.53, 147.09, 140.34, 135.63, 131.98, 131.02 (J_{CF} = 9.6 Hz),

130.25, 128.57, 127.23, 124.06, 116.72, 116.37 (J_{CF} = 24.1 Hz), 114.97, 110.49, 108.47, 102.27, 55.16; HRMS (ESI): *m/z,* calcd. for $C_{22}H_{18}N_4O_6FS$ $[M+H]^+$: 485.0931, found 485.0919.

4-((3-Methoxyphenyl)amino)-7-nitro-N-((3-nitrophenyl)sulfonyl)-1H-indole-2-carbox amide **(38):** orange solid; yield: 79%; mp: 255-256 °C; ^{1}H-NMR (400 MHz, DMSO-d_6) δ (ppm): 11.74 (brs, 1H), 9.64 (s, 1H), 8.75 (s, 1H), 8.56 (d, J = 8.4 Hz, 1H), 8.46 (d, J = 8.0 Hz, 1H), 8.15 (d, J = 9.2 Hz, 1H), 7.97 (t, J = 8.0 Hz, 1H), 7.85 (s, 1H), 7.35 (t, J = 8.4 Hz, 1H), 6.95 (d, J = 8.0 Hz, 1H), 6.91 (s, 1H), 6.79 (d, J = 8.4 Hz, 1H), 6.77 (d, J = 9.2 Hz, 1H), 3.78 (s, 3H); HRMS (ESI): *m/z,* calcd. for $C_{22}H_{18}N_5O_8S$ $[M+H]^+$: 512.0871, found 512.0857.

4-((3-Methoxyphenyl)amino)-7-nitro-N-((4-nitrophenyl)sulfonyl)-1H-indole-2-carbox amide **(39):** orange solid; yield: 86%; mp: 259-261 °C; ^{1}H-NMR (400 MHz, DMSO-d_6) δ (ppm): 11.73 (brs, 1H), 9.67 (s, 1H), 8.45 (d, J = 8.8 Hz, 2H), 8.29 (d, J = 8.8 Hz, 2H), 8.15 (d, J = 9.2 Hz, 1H), 7.84 (s, 1H), 7.35 (t, J = 8.0 Hz, 1H), 6.95 (d, J = 8.4 Hz, 1H), 6.91 (s, 1H), 6.78 (t, J = 9.2 Hz, 2H), 3.78 (s, 3H); ^{13}C-NMR (150 MHz, DMSO-d_6): δ (ppm): 160.09, 158.21, 150.11, 147.12, 145.14, 140.33, 131.90, 130.24, 129.33, 128.97, 127.17, 124.39, 124.02, 116.78, 114.98, 110.49, 110.19, 108.48, 102.28, 55.16; HRMS (ESI): *m/z,* calcd. for $C_{22}H_{18}N_5O_8S$ $[M+H]^+$: 512.0871, found 512.0857.

4-((3-Methoxyphenyl)amino)-7-nitro-N-((4-(trifluoromethoxy)phenyl)sulfonyl)-1H-indole-2-carboxamide **(40):** orange solid; yield: 74%; mp: 263-265 °C; ^{1}H-NMR (400 MHz, DMSO-d_6) δ (ppm): 11.80 (brs, 1H), 9.66 (s, 1H), 8.14-8.19 (m, 3H), 7.85 (s, 1H), 7.65 (d, J = 8.4 Hz, 2H), 7.35 (d, J = 8.0 Hz, 1H), 6.95 (d, J = 8.0 Hz, 1H), 6.91 (s, 1H), 6.79 (t, J = 9.2 Hz, 2H), 3.78 (s, 3H); HRMS (ESI): *m/z,* calcd. for $C_{23}H_{18}N_4O_7F_3S$ $[M+H]^+$: 551.0843, found 551.0821.

4-((3-Methoxyphenyl)amino)-7-nitro-N-(thiophen-2-ylsulfonyl)-1H-indole-2-carboxamide **(41):** orange solid; yield: 81%; mp: 249-250 °C; ^{1}H-NMR (400 MHz, DMSO-d_6) δ (ppm): 11.84 (brs, 1H), 9.67 (s, 1H), 8.15 (d, J = 9.2 Hz, 1H), 8.08 (d, J = 4.8 Hz, 1H), 7.90-7.91 (m, 2H), 7.35 (t, J = 8.4 Hz, 1H), 7.24 (t, J = 4.4 Hz, 1H), 6.96 (d, J = 8.0 Hz, 1H), 6.92 (s, 1H), 6.80 (d, J = 8.0 Hz, 1H), 6.78 (d, J = 9.2 Hz, 1H), 3.78 (s, 3H); ^{13}C-NMR (150 MHz, DMSO-d_6): δ (ppm): 160.10, 157.49, 147.08, 140.35, 139.58, 134.90, 134.44, 131.98, 130.26, 128.63, 127.55, 127.23, 124.08, 116.76, 114.95, 110.48, 108.44, 102.28, 55.16; HRMS (ESI): *m/z,* calcd. for $C_{20}H_{17}N_4O_6S_2$ $[M+H]^+$: 473.0584, found 473.0568.

4-((3-Methoxyphenyl)amino)-N-(naphthalen-2-ylsulfonyl)-7-nitro-1H-indole-2-carboxamide **(42):** orange solid; yield: 84%; mp: 254-255 °C; H-NMR (DMSO-d_6) δ (ppm): 13.16 (brs, 1H), 11.88 (brs, 1H), 9.63 (s, 1H), 8.73 (s, 1H), 8.27 (d, J = 8.0 Hz, 1H), 8.18 (d, J = 8.8 Hz, 1H), 8.15 (d, J = 9.2 Hz, 1H), 8.08 (d, J = 8.0 Hz, 1H), 8.01 (d, J = 8.8 Hz, 1H), 7.82 (s, 1H), 7.69-7.78 (m, 2H), 7.34 (t, J = 8.0 Hz, 1H), 6.93 (d, J = 8.0 Hz, 1H), 6.89 (s, 1H), 6.77 (t, J = 9.2 Hz, 2H), 3.76 (s, 3H); ^{13}C-NMR (150 MHz,

DMSO-d_6): δ (ppm): 160.08, 157.40, 147.07, 140.31, 136.24, 134.70, 132.00, 131.43, 130.24, 129.50, 129.43, 129.40, 129.32, 128.49, 127.86, 127.76, 127.24, 124.07, 122.47, 116.70, 114.97, 110.49, 108.46, 102.25, 55.14; HRMS (ESI): *m/z,* calcd. for $C_{26}H_{21}N_4O_6S$ $[M+H]^+$: 517.1182, found 517.1193.

4-(3-Methoxyphenoxy)-N-((4-methoxyphenyl)sulfonyl)-7-nitro-1H-indole-2-carboxamide **(43):** light yellow solid; yield: 86%; mp: 242-244 °C; ^{1}H-NMR (400 MHz, DMSO-d_6) δ (ppm): 12.90 (brs, 1H), 11.79 (s, 1H), 8.27 (d, J = 9.2 Hz, 1H), 7.97 (d, J = 8.8 Hz, 2H), 7.52 (s, 1H), 7.41 (t, J = 8.4 Hz, 1H), 7.17 (d, J = 8.8 Hz, 2H), 6.92 (d, J = 8.4 Hz, 1H), 6.85 (s, 1H), 6.79 (d, J = 8.0 Hz, 1H), 6.56 (d, J = 8.8 Hz, 1H), 3.86 (s, 3H), 3.77 (s, 3H); HRMS (ESI): *m/z,* calcd. for $C_{23}H_{20}N_3O_8S$ $[M+H]^+$: 498.0971, found 498.0957.

N-((4-Methoxyphenyl)sulfonyl)-4-((3-methoxyphenyl)thio)-7-nitro-1H-indole-2-carboxamide **(44):** light yellow solid; yield: 73%; mp: 200-202 °C; ^{1}H-NMR (300 MHz, DMSO-d_6) δ (ppm): 12.88 (brs, 1H), 11.81 (s, 1H), 8.18 (d, J = 9.0 Hz, 1H), 7.98 (d, J = 9.0 Hz, 2H), 7.59 (s, 1H), 7.45 (t, J = 7.2 Hz, 1H), 7.10-7.19 (m, 5H), 6.75 (d, J = 8.4 Hz, 1H), 3.86 (s, 3H), 3.78 (s, 3H); ^{13}C-NMR (150 MHz, DMSO-d_6): δ (ppm): 163.29, 160.16, 157.40, 142.46, 131.51, 131.13, 130.49, 130.26, 130.00, 128.96, 126.96, 126.19, 123.19, 119.13, 117.57, 115.73, 114.31, 108.00, 55.79, 55.41; HRMS (ESI): *m/z,* calcd. for $C_{23}H_{20}N_3O_7S$ $[M+H]^+$: 514.0737, found 514.0717.

4-((3-Methoxyphenyl)(methyl)amino)-N-((4-methoxyphenyl)sulfonyl)-7-nitro-1H-indo

le-2-carboxamide **(45):** orange solid; yield: 90%; mp: 245-247 °C; ^{1}H-NMR (400 MHz, DMSO-d_6) δ (ppm): 12.82 (brs, 1H), 11.66 (s, 1H), 8.19 (d, J = 9.2 Hz, 1H), 7.90 (d, J = 8.8 Hz, 2H), 7.37 (t, J = 8.0 Hz, 1H), 7.14 (d, J = 8.4 Hz, 2H), 6.96 (d, J = 8.4 Hz, 1H), 6.90 (s, 1H), 6.82 (d, J = 7.6 Hz, 1H), 6.61 (d, J = 9.2 Hz, 1H), 6.37 (s, 1H), 3.85 (s, 3H), 3.75 (s, 3H), 3.55 (s, 3H); ^{13}C-NMR (125 MHz, DMSO-d_6): δ (ppm): 163.21, 160.54, 150.49, 148.33, 132.52, 130.86, 130.21, 126.41, 124.04, 118.24, 116.51, 114.31, 112.78, 111.76, 105.90, 55.79, 55.39, 42.93. HRMS (ESI): *m/z,* calcd. for $C_{24}H_{23}N_4O_7S$ $[M+H]^+$: 511.1287, found 511.1277.

4-Benzoyl-N-((4-methoxyphenyl)sulfonyl)-7-nitro-1H-indole-2-carboxamide **(46):** yellow solid; yield: 38%; mp: 235-237 °C; ^{1}H-NMR (400 MHz, DMSO-d_6) δ (ppm): 12.98 (brs, 1H), 11.94 (s, 1H), 8.39 (d, J = 8.4 Hz, 1H), 7.96 (d, J = 8.8 Hz, 2H), 7.73-7.79 (m, 3H), 7.59 (t, J = 7.6 Hz, 2H), 7.55 (t, J = 8.0 Hz, 2H), 7.16 (d, J = 8.8 Hz, 2H), 3.85 (s, 3H); HRMS (ESI): *m/z*, calcd for $C_{23}H_{18}N_3O_7S$ $[M+H^+]$: 480.0865, found 480.0844.

4-((3-Methoxybenzyl)amino)-N-((4-methoxyphenyl)sulfonyl)-7-nitro-1H-indole-2-carboxamide **(47):** orange solid; yield: 92%; mp: 233-234 °C; ^{1}H-NMR (400 MHz, DMSO-d_6) δ (ppm): 12.86 (brs, 1H), 11.78 (brs, 1H), 8.62 (t, J = 5.6 Hz, 1H), 8.06 (d, J = 9.2 Hz, 1H), 7.96 (d, J = 8.8 Hz, 2H), 7.81 (brs, 1H), 7.24 (t, J = 8.0 Hz, 1H), 7.16 (d, J = 8.4 Hz, 2H), 6.91 (d, J = 7.2 Hz, 2H), 6.82 (d, J = 7.6 Hz, 1H), 6.30 (d, J = 9.2 Hz, 1H), 4.58 (d, J = 6.0 Hz, 2H), 3.86 (s, 3H), 3.71 (s, 3H); ^{13}C-NMR (150 MHz, DMSO-d_6): δ (ppm): 163.15, 159.38, 157.25, 150.38, 140.01, 131.73, 130.77, 130.11,

129.58, 127.72, 127.63, 122.42, 119.08, 115.14, 114.26, 112.84, 112.30, 110.59, 100.39, 55.76, 54.96, 45.65; HRMS (ESI): *m/z,* calcd. for $C_{24}H_{23}N_4O_7S$ $[M+H]^+$: 511.1282, found 511.1262.

4-Benzamido-N-((4-methoxyphenyl)sulfonyl)-7-nitro-1H-indole-2-carboxamide **(48):** orange solid; yield: 75%; mp: 253-255 °C; ^{1}H-NMR (400 MHz, DMSO-d_6) δ (ppm): 12.94 (brs, 1H), 11.84 (s, 1H), 10.75 (s, 1H), 8.36 (d, J = 8.8 Hz, 1H), 7.94-8.02 (m, 6H), 7.66 (t, J = 7.2 Hz, 1H), 7.58 (t, J = 7.2 Hz, 2H), 7.16 (d, J = 8.8 Hz, 2H), 3.85 (s, 3H); ^{13}C-NMR (150 MHz, DMSO-d_6): δ (ppm): 166.62, 163.24, 157.54, 140.32, 134.16, 132.20, 130.79, 130.19, 129.11, 128.39, 128.27, 127.62, 124.43, 121.68, 114.27, 113.96, 111.79, 110.29, 55.79; HRMS (ESI): *m/z,* calcd. for $C_{23}H_{19}N_4O_7S$ $[M+H]^+$: 495.0969, found 495.0959.

N-((4-Methoxyphenyl)sulfonyl)-7-nitro-4-(propylamino)-1H-indole-2-carboxamide **(49):** yellow solid; yield: 81%; mp: 284-286 °C; ^{1}H-NMR (400 MHz, DMSO-d_6) δ (ppm): 12.85 (brs, 1H), 11.75 (s, 1H), 8.10 (d, J = 8.8 Hz, 2H), 7.97 (d, J = 8.8 Hz, 2H), 7.81 (s, 1H), 7.16 (d, J = 8.8 Hz, 2H), 6.36 (d, J = 9.2 Hz, 1H), 3.86 (s, 3H), 3.32 (q, J = 6.0 Hz, 2H), 1.65 (sext, J = 7.2 Hz, 2H), 0.94 (t, J = 7.2 Hz, 3H); HRMS (ESI): *m/z,* calcd. for $C_{19}H_{21}N_4O_6S$ $[M+H]^+$: 433.1176, found 433.1161.

4-((2-Methoxyethyl)amino)-N-((4-methoxyphenyl)sulfonyl)-7-nitro-1H-indole-2-carboxamide **(50):** yellow solid; yield: 58%; mp: 208-210 °C; ^{1}H-NMR (400 MHz,

DMSO-d_6) δ (ppm): 12.83 (brs, 1H), 11.74 (s, 1H), 8.10 (d, J = 9.2 Hz, 1H), 8.05 (s, 1H), 7.95 (d, J = 8.4 Hz, 2H), 7.77 (s, 1H), 7.15 (d, J = 7.6 Hz, 2H), 6.40 (d, J = 9.2 Hz, 1H), 3.85 (s, 3H), 3.56 (s, 4H), 3.27 (s, 3H); ^{13}C-NMR (150 MHz, DMSO-d_6): δ (ppm): 163.06, 157.37, 150.63, 131.78, 130.06, 127.75, 122.10, 114.91, 114.20, 110.47, 100.14, 70.04, 58.10, 55.74, 42.47; HRMS (ESI): *m/z,* calcd. for $C_{19}H_{21}N_4O_7S$ $[M+H]^+$: 449.1131, found 449.1115.

N-((4-Methoxyphenyl)sulfonyl)-4-((3-methoxypropyl)amino)-7-nitro-1H-indole-2-carboxamide **(51):** yellow solid; yield: 69%; mp: 249-250 °C; ^{1}H-NMR (400 MHz, DMSO-d_6) δ (ppm): 12.86 (brs, 1H), 11.77 (s, 1H), 8.12 (d, J = 9.2 Hz, 1H), 8.01 (brs, 1H), 7.97 (d, J = 8.4 Hz, 2H), 7.77 (s, 1H), 7.16 (d, J = 8.8 Hz, 2H), 6.35 (d, J = 9.2 Hz, 1H), 3.86 (s, 3H), 3.41 (t, J = 5.6 Hz, 4H), 3.24 (s, 3H), 1.83-1.89 (m, 2H); HRMS (ESI): *m/z,* calcd. for $C_{20}H_{23}N_4O_7S$ $[M+H]^+$: 463.1282, found 463.1262.

4-(Cyclohexylamino)-N-((4-methoxyphenyl)sulfonyl)-7-nitro-1H-indole-2-carboxamide **(52):** orange solid; yield: 73%; mp: >250 °C; ^{1}H-NMR (400 MHz, DMSO-d_6) δ (ppm): 12.81 (s, 1H), 11.74 (s, 1H), 8.09 (d, J = 8.8 Hz, 1H), 7.96 (d, J = 8.0 Hz, 2H), 7.87 (s, 1H), 7.73 (d, J = 6.8 Hz, 1H), 7.16 (d, J = 8.4 Hz, 2H), 6.40 (d, J = 9.2 Hz, 1H), 3.85 (s, 3H), 3.60 (s, 1H), 1.95-1.99 (m, 2H), 1.75 (brs, 2H), 1.64 (d, J = 11.2 Hz, 1H), 1.35-1.37 (m, 4H), 1.18 (brs, 1H).

4-Morpholino-7-nitro-N-(phenylsulfonyl)-1H-indole-2-carboxamide **(53):** yellow

solid; yield: 67%; mp: 258-259 °C; ^{1}H-NMR (400 MHz, DMSO-d_6) δ (ppm): 10.99 (brs, 1H), 8.11 (d, J = 8.8 Hz, 1H), 7.98 (d, J = 7.2 Hz, 2H), 7.56-7.64 (m, 3H), 7.50 (brs, 1H), 6.65 (d, J = 9.2 Hz, 1H), 3.81 (t, J = 4.0 Hz, 4H), 3.61 (t, J = 4.0 Hz, 4H); ^{13}C-NMR (150 MHz, DMSO-d_6): δ (ppm): 152.73, 132.45, 131.77, 128.59, 127.44, 125.16, 124.58, 117.72, 108.46, 105.88, 65.95, 49.85; HRMS (ESI): *m/z,* calcd. for $C_{19}H_{19}N_4O_6S$ $[M+H]^+$: 431.1020, found 431.1003.

4-Chloro-7-nitro-N-(phenylsulfonyl)-1H-indole-2-carboxamide **(54):** light-yellow solid; yield: 46%; mp: >250 °C; ^{1}H-NMR (400 MHz, DMSO-d_6) δ (ppm): 11.97 (brs, 1H), 8.28 (d, J = 8.8 Hz, 1H), 8.05 (d, J = 7.2 Hz, 2H), 7.75 (t, J = 7.2 Hz, 1H), 7.67 (t, J = 7.2 Hz, 2H), 7.61 (s, 1H), 7.46 (d, J = 8.4 Hz, 1H); HRMS (ESI): *m/z,* calcd. for $C_{15}H_{11}N_3O_5ClS$ $[M+H]^+$: 380.01023, found 380.0092.

4-((2-Methoxyphenyl)amino)-7-nitro-N-(phenylsulfonyl)-1H-indole-2-carboxamide **(55):** orange solid; yield: 92%; mp: 245-246 °C; ^{1}H-NMR (400 MHz, DMSO-d_6) δ (ppm): 13.10 (brs, 1H), 11.83 (brs, 1H), 9.38 (s, 1H), 8.07 (d, J = 9.6 Hz, 1H), 8.04 (d, J = 8.0 Hz, 2H), 7.79 (s, 1H), 7.74 (t, J = 7.2 Hz, 1H), 7.66 (t, J = 7.2 Hz, 2H), 7.30-7.36 (m, 2H), 7.19 (d, J = 8.4 Hz, 1H), 7.04 (t, J = 7.6 Hz, 1H), 6.12 (d, J = 9.2 Hz, 1H), 3.76 (s, 3H); HRMS (ESI): *m/z,* calcd. for $C_{22}H_{19}N_4O_6S$ $[M+H]^+$: 467.1020, found 467.1008.

4-((4-Methoxyphenyl)amino)-7-nitro-N-(phenylsulfonyl)-1H-indole-2-carboxamide **(56):** red-brown solid; yield: 45%; mp: 258-260 °C; ^{1}H-NMR (300 MHz, DMSO-d_6) δ

(ppm): 13.10 (brs, 1H), 11.86 (brs, 1H), 9.61 (s, 1H), 8.10 (d, J = 9.0 Hz, 1H), 8.04 (d, J = 7.5 Hz, 2H), 7.80 (s, 1H), 7.75 (t, J = 7.2 Hz, 1H), 7.67 (t, J = 7.5 Hz, 2H), 7.28 (d, J = 9.0 Hz, 2H), 7.03 (d, J = 9.0 Hz, 2H), 6.46 (d, J = 9.0 Hz, 1H), 3.79 (s, 3H); ^{13}C-NMR (150 MHz, DMSO-d_6): δ (ppm): 157.36, 157.03, 148.54, 139.34, 133.77, 132.14, 131.45, 129.18, 128.19, 127.67, 127.50, 125.76, 123.29, 115.81, 114.75, 110.67, 101.41, 55.31; HRMS (ESI): *m/z,* calcd. for $C_{22}H_{19}N_4O_6S$ $[M+H]^+$: 467.1020, found 467.1004.

4-((3-Ethoxyphenyl)amino)-N-((4-methoxyphenyl)sulfonyl)-7-nitro-1H-indole-2-carboxamide **(57):** yellow solid; yield: 57%; mp: 225-227 °C; ^{1}H-NMR (400 MHz, DMSO-d_6) δ (ppm): 12.98 (brs, 1H), 11.88 (brs, 1H), 9.65 (s, 1H), 8.15 (d, J = 9.2 Hz, 1H), 7.98 (d, J = 8.8 Hz, 2H), 7.84 (s, 1H), 7.33 (t, J = 8.0 Hz, 1H), 7.17 (d, J = 8.8 Hz, 2H), 6.93 (d, J = 8.0 Hz, 1H), 6.89 (s, 1H), 6.78 (d, J = 6.4 Hz, 1H), 6.76 (d, J = 8.8 Hz, 1H), 4.04 (q, J = 6.8 Hz, 2H), 3.86 (s, 3H), 1.33 (t, J = 6.8 Hz, 3H); ^{13}C-NMR (150 MHz, DMSO-d_6): δ (ppm): 163.21, 159.34, 157.25, 147.10, 140.34, 131.97, 130.69, 130.22, 130.16, 128.55, 127.18, 124.04, 116.70, 114.89, 114.29, 111.00, 110.53, 108.86, 102.28, 63.10, 55.78, 14.60; HRMS (ESI): *m/z,* calcd. for $C_{24}H_{23}N_4O_7S$ $[M+H]^+$: 511.1287, found 511.1277.

4-((3-(Difluoromethoxy)phenyl)amino)-N-((4-methoxyphenyl)sulfonyl)-7-nitro-1H-indole-2-carboxamide **(58):** yellow solid; yield: 80%; mp: 259-261 °C; ^{1}H-NMR (400 MHz, DMSO-d_6) δ (ppm): 12.93 (brs, 1H), 11.91 (s, 1H), 9.71 (s, 1H), 8.17 (d, J =

9.2 Hz, 1H), 7.98 (d, *J* = 8.8 Hz, 2H), 7.83 (s, 1H), 7.48 (t, *J* = 8.0 Hz, 1H), 7.28 (t, *J* = 74.0 Hz, 1H), 7.26 (d, *J* = 8.0 Hz, 1H), 7.17 (d, *J* = 8.8 Hz, 2H), 7.15 (s, 1H), 7.00 (d, *J* = 8.4 Hz, 1H), 6.83 (d, *J* = 9.2 Hz, 1H), 3.86 (s, 3H); HRMS (ESI): *m/z,* calcd. for $C_{23}H_{19}N_4O_7F_2S$ $[M+H]^+$: 533.0937, found 533.0926.

N-((4-Methoxyphenyl)sulfonyl)-7-nitro-4-(m-tolylamino)-1H-indole-2-carboxamide **(59):** orange solid; yield: 88%; mp: 265-267 °C; ^{1}H-NMR (400 MHz, DMSO-d_6) δ (ppm): 12.91 (brs, 1H), 11.88 (brs, 1H), 9.63 (s, 1H), 8.13 (d, *J* = 8.8 Hz, 1H), 7.98 (d, *J* = 8.8 Hz, 2H), 7.84 (s, 1H), 7.33 (t, *J* = 8.0 Hz, 1H), 7.15-7.18 (m, 4H), 7.05 (d, *J* = 7.2 Hz, 1H), 6.69 (d, *J* = 9.2 Hz, 1H), 3.86 (s, 3H), 2.34 (s, 3H). ^{13}C-NMR (125 MHz, DMSO-d_6): δ (ppm): 147.42, 139.01, 138.96, 132.01, 130.21, 129.36, 127.32, 125.76, 123.88, 123.71, 120.29, 116.52, 114.33, 101.96, 55.82, 21.01. HRMS (ESI): *m/z,* calcd. for $C_{23}H_{21}N_4O_6S$ $[M+H]^+$: 481.1182, found 481.1171.

4-((3-Ethylphenyl)amino)-N-((4-methoxyphenyl)sulfonyl)-7-nitro-1H-indole-2-carbox amide **(60):** yellow solid; yield: 54%; mp: 231-233 °C; ^{1}H-NMR (400 MHz, DMSO-d_6) δ (ppm): 12.91 (brs, 1H), 11.88 (brs, 1H), 9.65 (s, 1H), 8.14 (d, *J* = 9.2 Hz, 1H), 7.98 (d, *J* = 8.4 Hz, 2H), 7.83 (s, 1H), 7.36 (t, *J* = 7.6 Hz, 1H), 7.13-7.22 (m, 4H), 7.08 (d, *J* = 7.6 Hz, 1H), 6.69 (d, *J* = 8.8 Hz, 1H), 3.86 (s, 3H), 2.63 (q, *J* = 7.2 Hz, 2H), 1.20 (t, *J* = 7.2 Hz, 3H); ^{13}C-NMR (150 MHz, DMSO-d_6): δ (ppm): 163.21, 157.22, 147.40, 145.29, 138.99, 132.01, 130.68, 130.16, 129.36, 128.51, 127.27, 124.53, 123.85, 122.53, 120.46, 116.46, 114.29, 110.47, 101.95, 55.78, 28.03, 15.45;

HRMS (ESI): *m/z,* calcd. for $C_{24}H_{23}N_4O_6S$ $[M+H]^+$: 495.1333, found 495.1313.

4-((3-Acetamidophenyl)amino)-N-((4-methoxyphenyl)sulfonyl)-7-nitro-1H-indole-2-carboxamide **(61):** yellow solid; yield: 42%; mp: 235-237 °C; ^{1}H-NMR (400 MHz, DMSO-d_6) δ (ppm): 12.92 (brs, 1H), 10.04 (s, 1H), 9.64 (s, 1H), 8.09 (s, 1H), 7.93 (s, 2H), 7.75 (s, 2H), 7.33 (s, 2H), 7.11 (s, 2H), 7.03 (s, 1H), 6.73 (d, J = 8.8 Hz, 1H), 3.84 (s, 3H), 2.05 (s, 3H); HRMS (ESI): *m/z,* calcd. for $C_{24}H_{22}N_5O_7S$ $[M+H]^+$: 524.1234, found 524.1222.

4-((3-Fluorophenyl)amino)-N-((4-methoxyphenyl)sulfonyl)-7-nitro-1H-indole-2-carboxamide **(62):** yellow solid; yield: 59%; mp: >250 °C; ^{1}H-NMR (300 MHz, DMSO-d_6) δ (ppm): 12.87 (brs, 1H), 11.92 (s, 1H), 9.70 (s, 1H), 8.18 (d, J = 9.0 Hz, 1H), 7.98 (d, J = 9.0 Hz, 2H), 7.83 (d, J = 2.1 Hz, 1H), 7.43-7.48 (m, 1H), 7.20-7.23 (m, 2H), 7.17 (d, J = 8.7 Hz, 2H), 7.02 (t, J = 9.0 Hz, 1H), 6.84 (d, J = 9.0 Hz, 1H), 3.86 (s, 3H); HRMS (ESI): *m/z,* calcd. for $C_{22}H_{18}N_4O_6FS$ $[M+H]^+$: 485.0926, found 485.0909.

4-((4-Fluorophenyl)amino)-N-((4-methoxyphenyl)sulfonyl)-7-nitro-1H-indole-2-carboxamide **(63):** red solid; yield: 73%; mp: >250 °C; ^{1}H-NMR (300 MHz, DMSO-d_6) δ (ppm): 12.93 (brs, 1H), 11.90 (brs, 1H), 9.66 (s, 1H), 8.13 (d, J = 9.3 Hz, 1H), 7.98 (d, J = 8.7 Hz, 2H), 7.81 (d, J = 2.1 Hz, 1H), 7.38-7.42 (m, 2H), 7.30 (t, J = 8.4 Hz, 2H), 7.18 (d, J = 8.7 Hz, 2H), 6.58 (d, J = 9.0 Hz, 1H), 3.86 (s, 3H); ^{13}C-NMR (150 MHz, DMSO-d_6): δ (ppm): 163.21, 159.34 (J_{CF} = 240.6 Hz), 157.21, 147.65, 135.33

(J_{CF} = 2.3 Hz), 131.96, 130.66, 130.17, 128.57, 127.24, 125.64 (J_{CF} = 8.3 Hz), 123.94, 116.35, 116.27 (J_{CF} = 22.2 Hz), 114.30, 110.36, 101.57, 55.78; HRMS (ESI): *m/z,* calcd. for $C_{22}H_{18}N_4O_6FS$ $[M+H]^+$: 485.0926, found 485.0911.

N-((4-methoxyphenyl)sulfonyl)-7-nitro-4-((3-(trifluoromethyl)phenyl)amino)-1H-indole-2-carboxamide **(64):** yellow solid; yield: 67%; mp: >250 °C; ^{1}H-NMR (400 MHz, DMSO-d_6) δ (ppm): 12.93 (brs, 1H), 11.92 (brs, 1H), 9.78 (s, 1H), 8.19 (d, J = 9.2 Hz, 1H), 7.98 (d, J = 8.8 Hz, 2H), 7.82 (s, 1H), 7.65-7.72 (m, 3H), 7.52 (d, J = 7.6 Hz, 1H), 7.17 (d, J = 8.4 Hz, 2H), 6.84 (d, J = 8.8 Hz, 1H), 3.86 (s, 3H); HRMS (ESI): *m/z,* calcd. for $C_{23}H_{18}N_4O_6F_3S$ $[M+H]^+$: 535.0894, found 535.0872.

N-((4-methoxyphenyl)sulfonyl)-7-nitro-4-((4-(trifluoromethyl)phenyl)amino)-1H-indole-2-carboxamide **(65):** orange-red solid; yield: 76%; mp: 278-280 °C; ^{1}H-NMR (400 MHz, DMSO-d_6) δ (ppm): 12.88 (brs, 1H), 11.92 (brs, 1H), 9.83 (s, 1H), 8.19 (d, J = 8.8 Hz, 1H), 7.98 (d, J = 8.4 Hz, 2H), 7.84 (s, 1H), 7.76 (d, J = 8.0 Hz, 2H), 7.55 (d, J = 8.0 Hz, 2H), 7.17 (d, J = 8.4 Hz, 2H), 6.97 (d, J = 8.8 Hz, 1H), 3.86 (s, 3H); HRMS (ESI): *m/z,* calcd. for $C_{23}H_{18}N_4O_6F_3S$ $[M+H]^+$: 535.0894, found 535.0877.

N-((4-methoxyphenyl)sulfonyl)-7-nitro-4-((3-nitrophenyl)amino)-1H-indole-2-carboxamide **(66):** orange solid; yield: 83%; mp: >250 °C; ^{1}H-NMR (300 MHz, DMSO-d_6) δ (ppm): 12.94 (brs, 1H), 11.93 (s, 1H), 9.89 (s, 1H), 8.20 (d, J = 9.0 Hz, 1H), 8.15 (t, J = 2.1 Hz, 1H), 7.98 (d, J = 8.7 Hz, 3H), 7.82-7.84 (m, 2H), 7.70 (t, J = 7.8 Hz, 1H),

6.17 (d, J = 9.0 Hz, 2H), 6.95 (d, J = 9.3 Hz, 1H), 3.86 (s, 3H); HRMS (ESI): *m/z,* calcd. for $C_{22}H_{18}N_5O_8S$ $[M+H]^+$: 512.0871, found 512.0865.

N-((4-methoxyphenyl)sulfonyl)-7-nitro-4-((4-nitrophenyl)amino)-1H-indole-2-carboxamide **(67):** orange solid; yield: 83%; mp: >250 °C; ^{1}H-NMR (300 MHz, DMSO-d_6) δ (ppm): 12.95 (brs, 1H), 11.94 (brs, 1H), 10.09 (s, 1H), 8.25 (d, J = 9.0 Hz, 3H), 7.98 (d, J = 9.0 Hz, 2H), 7.82 (d, J = 1.8 Hz, 1H), 7.52 (d, J = 9.0 Hz, 2H), 7.16 (t, J = 8.7 Hz, 3H), 3.86 (s, 3H); ^{13}C-NMR (150 MHz, DMSO-d_6): δ (ppm): 163.24, 157.30, 146.97, 143.59, 141.44, 131.52, 130.61, 130.18, 129.65, 126.61, 125.98, 125.53, 119.33, 119.11, 114.29, 109.90, 105.44, 55.79; HRMS (ESI): *m/z,* calcd. for $C_{22}H_{18}N_5O_8S$ $[M+H]^+$: 512.0871, found 512.0856.

N-((4-Methoxyphenyl)sulfonyl)-4-((3-morpholinophenyl)amino)-7-nitro-1H-indole-2-carboxamide **(68):** orange solid; yield: 97%; mp: 188-189 °C; ^{1}H-NMR (300 MHz, DMSO-d_6) δ (ppm): 12.91 (brs, 1H), 11.90 (s, 1H), 9.64 (s, 1H), 8.14 (d, J = 9.3 Hz, 1H), 7.98 (d, J = 8.4 Hz, 2H), 7.84 (s, 1H), 7.31 (t, J = 7.8 Hz, 1H), 7.18 (d, J = 8.7 Hz, 2H), 6.92 (s, 1H), 6.85 (t, J = 7.8 Hz, 2H), 6.72 (d, J = 9.0 Hz, 1H), 3.86 (s, 3H), 3.75 (brs, 4H), 3.15 (brs, 4H); HRMS (ESI): *m/z,* calcd. for $C_{26}H_{26}N_5O_7S$ $[M+H]^+$: 552.1553, found 552.1538.

N-((4-Methoxyphenyl)sulfonyl)-4-((4-morpholinophenyl)amino)-7-nitro-1H-indole-2-carboxamide **(69):** orange solid; yield: 78%; mp: 180-182 °C; ^{1}H-NMR (300 MHz, DMSO-d_6) δ (ppm): 12.92 (brs, 1H), 11.89 (s, 1H), 9.67 (s, 1H), 8.11 (d, J = 9.0 Hz,

1H), 7.98 (d, J = 9.0 Hz, 2H), 7.83 (d, J = 1.8 Hz, 1H), 7.28 (d, J = 9.0 Hz, 2H), 7.18 (d, J = 8.7 Hz, 4H), 6.54 (d, J = 9.0 Hz, 1H), 3.86 (s, 3H), 3.82 (s, 4H), 3.22 (s, 4H); ^{13}C-NMR (150 MHz, DMSO-d_6): δ (ppm): 163.24, 157.17, 151.08, 147.88, 132.07, 130.64, 130.18, 128.33, 127.36, 124.56, 123.60, 120.68, 117.67, 116.17, 114.32, 110.62, 101.77, 65.37, 55.79, 49.91; HRMS (ESI): *m/z,* calcd. for $C_{26}H_{26}N_5O_7S$ $[M+H]^+$: 552.1547, found 552.1529.

4-((3,5-Dimethoxyphenyl)amino)-N-((4-methoxyphenyl)sulfonyl)-7-nitro-1H-indole-2-carboxamide **(70):** orange solid; yield: 80%; mp: 180-182 °C; ^{1}H-NMR (400 MHz, DMSO-d_6) δ (ppm): 12.90 (brs, 1H), 11.89 (brs, 1H), 9.60 (s, 1H), 8.16 (d, J = 8.8 Hz, 1H), 7.98 (d, J = 8.8 Hz, 2H), 7.85 (s, 1H), 7.17 (d, J = 8.8 Hz, 2H), 6.83 (d, J = 9.2 Hz, 1H), 6.52 (d, J = 1.6 Hz, 2H), 6.36 (s, 1H), 3.86 (s, 3H), 3.76 (s, 6H); ^{13}C-NMR (150 MHz, DMSO-d_6): δ (ppm): 163.23, 161.02, 157.22, 146.86, 140.92, 131.93, 130.64, 130.17, 128.61, 127.15, 124.18, 116.84, 114.30, 110.38, 102.65, 100.83, 96.79, 55.78, 55.27; HRMS (ESI): *m/z,* calcd. for $C_{24}H_{23}N_4O_8S$ $[M+H]^+$: 527.1231, found 527.1211.

4-((2,3-Dimethoxyphenyl)amino)-N-((4-methoxyphenyl)sulfonyl)-7-nitro-1H-indole-2-carboxamide **(71):** red solid; yield: 95%; mp: 220-222 °C; ^{1}H-NMR (400 MHz, DMSO-d_6) δ (ppm): 12.90 (brs, 1H), 11.85 (s, 1H), 9.40 (s, 1H), 8.09 (d, J = 9.6 Hz, 1H), 7.97 (d, J = 8.8 Hz, 2H), 7.81 (s, 1H), 7.17 (d, J = 8.8 Hz, 2H), 7.15 (t, J = 8.0 Hz, 1H), 7.04 (d, J = 8.4 Hz, 1H), 6.92 (d, J = 8.0 Hz, 1H), 6.21 (d, J = 9.2 Hz, 1H), 3.86 (s, 3H), 3.85 (s, 3H), 3.60 (s, 3H); HRMS (ESI): *m/z,* calcd. for $C_{24}H_{23}N_4O_8S$

[M+H]$^+$: 527.1231, found 527.1215.

4-((2,4-Dimethoxyphenyl)amino)-N-((4-methoxyphenyl)sulfonyl)-7-nitro-1H-indole-2-carboxamide **(72):** orange solid; yield: 89%; mp: 254-255 °C; ^{1}H-NMR (400 MHz, DMSO-d_6) δ (ppm): 12.89 (brs, 1H), 11.82 (brs, 1H), 9.30 (s, 1H), 8.04 (d, J = 9.2 Hz, 1H), 7.97 (d, J = 8.0 Hz, 2H), 7.75 (s, 1H), 7.16-7.22 (m, 3H), 6.74 (s, 1H), 6.61 (d, J = 8.4 Hz, 1H), 6.02 (d, J = 9.2 Hz, 1H), 3.86 (s, 3H), 3.82 (s, 3H), 3.73 (s, 3H); HRMS (ESI): *m/z,* calcd. for $C_{24}H_{23}N_4O_8S$ [M+H]$^+$: 527.1231, found 527.1211.

4-((4-Chloro-3-methoxyphenyl)amino)-N-((4-methoxyphenyl)sulfonyl)-7-nitro-1H-indole-2-carboxamide **(73):** orange solid; yield: 91%; mp: 275-277 °C; ^{1}H-NMR (400 MHz, DMSO-d_6) δ (ppm): 12.92 (brs, 1H), 11.90 (brs, 1H), 9.70 (s, 1H), 8.15 (d, J = 9.2 Hz, 1H), 7.98 (d, J = 8.8 Hz, 2H), 7.83 (s, 1H), 7.46 (d, J = 8.4 Hz, 1H), 7.17 (d, J = 8.4 Hz, 2H), 7.11 (s, 1H), 6.96 (d, J = 8.4 Hz, 1H), 6.82 (d, J = 9.2 Hz, 1H), 3.86 (s, 6H); ^{13}C-NMR (125 MHz, DMSO-d_6): δ (ppm): 163.26, 155.05, 146.65, 139.47, 131.92, 130.31, 130.23, 127.12, 124.43, 119.00, 116.97, 116.47, 115.27, 114.34, 107.42, 102.52, 56.11, 55.82. HRMS (ESI): *m/z,* calcd. for $C_{23}H_{20}N_4O_7ClS$ [M+H]$^+$: 531.0741, found 531.0732.

4-((4-Fluoro-3-methoxyphenyl)amino)-N-((4-methoxyphenyl)sulfonyl)-7-nitro-1H-indole-2-carboxamide **(74):** orange solid; yield: 65%; mp: >250 °C; ^{1}H-NMR (400 MHz, DMSO-d_6) δ (ppm): 12.92 (brs, 1H), 11.89 (s, 1H), 9.65 (s, 1H), 8.13 (d, J = 9.2 Hz, 1H), 7.98 (d, J = 8.8 Hz, 2H), 7.81 (s, 1H), 7.28 (dd, J_1 = 11.2 Hz, J_1 = 8.8 Hz, 1H),

7.17 (d, J = 8.8 Hz, 2H), 7.13 (d, J = 7.6 Hz, 1H), 6.91-6.93 (m, 1H), 6.67 (d, J = 9.2 Hz, 1H), 3.86 (s, 3H), 3.84 (s, 3H); HRMS (ESI): *m/z,* calcd. for $C_{23}H_{20}N_4O_7FS$ $[M+H]^+$: 515.1037, found 515.1025.

N-((4-Methoxyphenyl)sulfonyl)-7-nitro-4-((3,4,5-trimethoxyphenyl)amino)-1H-indole-2-carboxamide **(75):** red-brown solid; yield: 42%; mp: 268-270 °C; ^{1}H-NMR (400 MHz, DMSO-d_6) δ (ppm): 12.91 (brs, 1H), 11.88 (brs, 1H), 9.62 (s, 1H), 8.13 (d, J = 9.2 Hz, 1H), 7.98 (d, J = 8.4 Hz, 2H), 7.83 (s, 1H), 7.17 (d, J = 8.4 Hz, 2H), 6.75 (d, J = 9.2 Hz, 1H), 6.66 (s, 2H), 3.86 (s, 3H), 3.78 (s, 6H), 3.68 (s, 3H); ^{13}C-NMR (125 MHz, DMSO-d_6): δ (ppm): 163.26, 157.26, 153.35, 147.60, 134.83, 134.80, 132.03, 130.24, 127.45, 123.75, 116.36, 114.34, 110.45, 102.24, 101.12, 60.16, 55.93, 55.82. HRMS (ESI): *m/z,* calcd. for $C_{25}H_{25}N_4O_9S$ $[M+H]^+$: 557.1325, found 557.1337.

5-Fluoro-4-((3-methoxyphenyl)amino)-N-((4-methoxyphenyl)sulfonyl)-7-nitro-1H-indole-2-carboxamide **(76):** orange-red solid; yield: 82%; mp: 128-130 °C; ^{1}H-NMR (400 MHz, DMSO-d_6) δ (ppm): 12.92 (brs, 1H), 11.80 (brs, 1H), 9.49 (s, 1H), 8.17 (d, J = 12.8 Hz, 1H), 7.93 (d, J = 8.8 Hz, 2H), 7.27 (t, J = 8.0 Hz, 1H), 7.14 (d, J = 8.8 Hz, 2H), 7.10 (s, 1H), 6.77 (d, J = 8.4 Hz, 1H), 6.72 (s, 2H), 3.84 (s, 3H), 3.73 (s, 3H); ^{13}C-NMR (150 MHz, DMSO-d_6): δ (ppm): 163.25, 159.73, 157.08, 143.87 (J_{CF} = 234.5 Hz), 141.35, 134.83 (J_{CF} = 12.2 Hz), 130.45, 130.19, 129.68, 129.60, 129.46, 122.40 (J_{CF} = 9.0 Hz), 117.85 (J_{CF} = 4.5 Hz), 114.42, 114.29, 112.56 (J_{CF} = 26.4 Hz), 110.77, 110.05, 107.89, 59.72, 55.77; HRMS (ESI): *m/z,* calcd. for $C_{23}H_{20}N_4O_7FS$ $[M+H]^+$: 515.1031, found 515.1018.

5-Chloro-4-((3-methoxyphenyl)amino)-N-((4-methoxyphenyl)sulfonyl)-7-nitro-1H-indole-2-carboxamide **(77):** yellow solid; yield: 93%; mp: 216-218 °C; ^{1}H-NMR (400 MHz, DMSO-d_6) δ (ppm): 12.90 (brs, 1H), 11.82 (brs, 1H), 9.15 (s, 1H), 8.29 (s, 1H), 7.89 (d, J = 8.4 Hz, 2H), 7.28 (t, J = 8.0 Hz, 1H), 7.12 (d, J = 8.4 Hz, 2H), 6.83 (d, J = 8.0 Hz, 1H), 6.78 (s, 1H), 6.73 (d, J = 8.0 Hz, 1H), 6.56 (brs, 1H), 3.84 (s, 3H), 3.72 (s, 3H); ^{13}C-NMR (125 MHz, DMSO-d_6): δ (ppm): 163.25, 159.90, 143.29, 141.51, 131.19, 130.24, 129.91, 125.46, 124.40, 117.21, 115.86, 114.31, 111.01, 110.88, 109.39, 55.80, 55.21. HRMS (ESI): *m/z,* calcd. for $C_{23}H_{20}N_4O_7ClS$ $[M+H]^+$: 531.0741, found 531.0729.

4-((3-Methoxyphenyl)amino)-N-((4-methoxyphenyl)sulfonyl)-5-methyl-7-nitro-1H-indole-2-carboxamide **(78):** yellow solid; yield: 91%; mp: 215-217 °C; ^{1}H-NMR (400 MHz, DMSO-d_6) δ (ppm): 12.83 (brs, 1H), 11.64 (brs, 1H), 8.76 (s, 1H), 8.15 (s, 1H), 7.90 (d, J = 8.4 Hz, 2H), 7.24 (t, J = 8.0 Hz, 1H), 7.13 (d, J = 8.4 Hz, 2H), 6.72-6.75 (m, 2H), 6.65 (s, 1H), 6.62 (d, J = 8.0 Hz, 1H), 3.84 (s, 3H), 3.71 (s, 3H), 2.30 (s, 3H); HRMS (ESI): *m/z,* calcd. for $C_{24}H_{23}N_4O_7S$ $[M+H]^+$: 511.1282, found 511.1267.

4-((3-Methoxyphenyl)amino)-N-((4-methoxyphenyl)sulfonyl)-1H-indole-2-carboxamide **(79):** brown solid; yield: 56%; mp: 159-160 °C; ^{1}H-NMR (400 MHz, DMSO-d_6) δ (ppm): 12.35 (brs, 1H), 11.64 (s, 1H), 8.22 (s, 1H), 7.94 (d, J = 8.8 Hz, 2H), 7.54 (s, 1H), 7.15 (d, J = 8.4 Hz, 2H), 7.10-7.13 (m, 2H), 6.95 (d, J = 8.4 Hz, 1H), 6.83 (d, J = 7.6 Hz, 1H), 6.69 (d, J = 8.4 Hz, 1H), 6.65 (s, 1H), 6.41 (d, J = 8.0 Hz, 1H), 3.85 (s, 3H), 3.70 (s, 3H); ^{13}C-NMR (125 MHz, DMSO-d_6) δ (ppm): 163.10, 160.10, 159.23, 145.19, 138.93, 137.21, 131.12, 130.06, 129.75, 126.79, 126.09, 119.87, 114.21, 109.42, 106.79, 106.64, 105.20, 105.04, 102.49, 55.79, 54.79. HRMS (ESI): *m/z,*

calcd. for $C_{23}H_{22}N_3O_5S$ $[M+H]^+$: 452.1280, found 452.1264.

6-Fluoro-4-((3-methoxyphenyl)amino)-N-((4-methoxyphenyl)sulfonyl)-1H-indole-2-carboxamide **(80):** brown solid; yield: 47%; mp: 235-237 °C; ^{1}H-NMR (400 MHz, DMSO-d_6) δ (ppm): 12.35 (s, 1H), 11.70 (s, 1H), 8.49 (s, 1H), 7.94 (d, J = 8.4 Hz, 2H), 7.57 (s, 1H), 7.20 (t, J = 8.0 Hz, 1H), 7.15 (d, J = 8.4 Hz, 2H), 6.79 (d, J = 8.0 Hz, 1H), 6.74 (s, 1H), 6.60 (s, 1H), 6.57 (d, J = 4.4 Hz, 1H), 6.53 (d, J = 8.0 Hz, 1H), 3.85 (s, 3H), 3.73 (s, 3H); ^{13}C-NMR (125 MHz, DMSO-d_6) δ (ppm): 163.08, 161.84 (J_{CF} = 235.6 Hz), 160.13, 158.99, 143.69, 139.17 (J_{CF} = 13.6 Hz), 138.38 (J_{CF} = 15.8 Hz), 131.17, 130.04, 129.98, 127.14, 115.59, 114.20, 110.87, 107.07, 106.61, 104.21, 93.73 (J_{CF} = 29.1 Hz), 89.54 (J_{CF} = 26.3 Hz), 55.79, 54.92; HRMS (ESI): *m/z,* calcd. for $C_{23}H_{21}N_3O_5FS$ $[M+H]^+$: 470.1186, found 470.1170.

6-Chloro-4-((3-methoxyphenyl)amino)-N-((4-methoxyphenyl)sulfonyl)-1H-indole-2-carboxamide **(81):** brown solid; yield: 56%; mp: 253-255 °C; ^{1}H-NMR (300 MHz, acetone-d_6) δ (ppm): 10.94 (brs, 1H), 10.88 (s, 1H), 8.03 (d, J = 9.0 Hz, 2H), 7.70 (s, 1H), 7.49 (s, 1H), 7.22 (t, J = 7.8 Hz, 1H), 7.12 (d, J = 9.0 Hz, 2H), 7.07 (s, 1H), 6.86 (s, 1H), 6.76-6.80 (m, 2H), 6.58 (dd, J_1 = 8.4 Hz, J_2 = 1.8 Hz, 1H), 3.91 (s, 3H), 3.77 (s, 3H); ^{13}C-NMR (125 MHz, DMSO-d_6) δ (ppm): 163.12, 160.12, 159.06, 143.75, 138.98, 138.72, 131.06, 130.53, 130.07, 130.00, 127.43, 117.62, 114.22, 110.89, 106.84, 106.55, 105.05, 104.25, 103.70, 55.80, 54.91; HRMS (ESI): *m/z,* calcd. for $C_{23}H_{21}N_3O_5ClS$ $[M+H]^+$: 486.0890, found 486.0877.

4-((3-Methoxyphenyl)amino)-N-((4-methoxyphenyl)sulfonyl)-6-methyl-1H-indole-2-carboxamide **(82):** light-yellow solid; yield: 33%; mp: 223-225 °C; ^{1}H-NMR (400 MHz,

DMSO-d_6) δ (ppm): 12.27 (s, 1H), 11.48 (s, 1H), 8.16 (s, 1H), 7.93 (d, J = 8.8 Hz, 2H), 7.47 (s, 1H), 7.13 (t, J = 9.2 Hz, 3H), 6.74 (s, 1H), 6.67 (t, J = 8.0 Hz, 3H), 6.41 (d, J = 8.0 Hz, 1H), 3.84 (s, 3H), 3.70 (s, 3H), 2.31 (s, 3H); HRMS (ESI): *m/z,* calcd. for $C_{24}H_{24}N_3O_5S$ $[M+H]^+$: 466.1437, found 466.1425.

7-Fluoro-4-((3-methoxyphenyl)amino)-N-((4-methoxyphenyl)sulfonyl)-1H-indole-2-carboxamide **(83):** light-yellow solid; yield: 27%; mp: 151-152 °C; ^{1}H-NMR (400 MHz, DMSO-d_6) δ (ppm): 12.39 (s, 1H), 12.09 (s, 1H), 8.14 (s, 1H), 7.94 (d, J = 8.4 Hz, 2H), 7.55 (s, 1H), 7.16 (d, J = 8.8 Hz, 2H), 7.10 (t, J = 8.0 Hz, 1H), 6.98 (t, J = 8.8 Hz, 1H), 6.75 (dd, J_1 = 8.0 Hz, J_2 = 2.8 Hz, 1H), 6.60 (d, J = 8.0 Hz, 1H), 6.56 (s, 1H), 6.38 (d, J = 8.4 Hz, 1H), 3.85 (s, 3H), 3.69 (s, 3H); ^{13}C-NMR (125 MHz, DMSO-d_6) δ (ppm): 163.17, 160.15, 158.74, 145.75, 144.40 (J_{CF} = 238.4 Hz), 133.16, 130.94, 130.13, 129.79, 128.42, 126.28 (J_{CF} = 15.1 Hz), 123.37 (J_{CF} = 4.9 Hz), 114.26, 110.01 (J_{CF} = 16.4 Hz), 108.72, 107.76, 107.41 (J_{CF} = 5.0 Hz), 104.69, 101.81, 55.81, 54.78. HRMS (ESI): *m/z,* calcd. for $C_{23}H_{21}N_3O_5FS$ $[M+H]^+$: 470.1186, found 470.1175.

7-Chloro-4-((3-methoxyphenyl)amino)-N-((4-methoxyphenyl)sulfonyl)-1H-indole-2-carboxamide **(84):** light-yellow solid; yeild: 27%; mp: 124-125 °C; ^{1}H-NMR (400 MHz, DMSO-d_6) δ (ppm): 12.34 (brs, 1H), 11.68 (s, 1H), 8.35 (s, 1H), 7.96 (d, J = 8.8 Hz, 2H), 7.59 (s, 1H), 7.15-7.20 (m, 4H), 6.83 (d, J = 8.4 Hz, 1H), 6.73 (d, J = 8.0 Hz, 1H), 6.69 (s, 1H), 6.47 (d, J = 8.0 Hz, 1H), 3.85 (s, 3H), 3.71 (s, 3H); ^{13}C-NMR (125 MHz, DMSO-d_6) δ (ppm): 163.21, 160.10, 158.21, 144.23, 136.67, 135.39, 130.82, 130.19, 129.88, 128.04, 125.51, 120.38, 114.28, 110.27, 108.82, 107.19, 106.00, 105.97, 103.51, 55.82, 54.86. HRMS (ESI): *m/z,* calcd. for $C_{23}H_{21}N_3O_5ClS$

[M+H]$^+$: 486.0890, found 486.0877.

7-Cyano-4-((3-methoxyphenyl)amino)-N-((4-methoxyphenyl)sulfonyl)-1H-indole-2-carboxamide **(85):** light-yellow solid; yield: 34%; mp: 236-238 °C; ^{1}H-NMR (400 MHz, DMSO-d_6) δ (ppm): 12.28 (brs, 1H), 12.16 (s, 1H), 8.99 (s, 1H), 7.97 (d, J = 8.8 Hz, 2H), 7.69 (s, 1H), 7.56 (d, J = 8.0 Hz, 1H), 7.28 (t, J = 8.0 Hz, 1H), 7.17 (d, J = 8.4 Hz, 2H), 6.88 (d, J = 8.0 Hz, 1H), 6.83 (s, 1H), 6.81 (d, J = 8.8 Hz, 1H), 6.67 (d, J = 8.0 Hz, 1H), 3.86 (s, 3H), 3.75 (s, 3H); HRMS (ESI): *m/z,* calcd. for $C_{24}H_{21}N_4O_5S$ [M+H]$^+$: 477.1227, found 477.1210.

4-((3-Methoxyphenyl)amino)-N-((4-methoxyphenyl)sulfonyl)-7-(trifluoromethyl)-1H-indole-2-carboxamide **(86):** light-yellow solid; yield: 34%; mp: 119-120 °C; ^{1}H-NMR (400 MHz, DMSO-d_6) δ (ppm): 12.46 (brs, 1H), 11.47 (s, 1H), 8.75 (s, 1H), 7.97 (d, J = 8.8 Hz, 2H), 7.72 (s, 1H), 7.46 (d, J = 8.4 Hz, 1H), 7.25 (t, J = 8.0 Hz, 1H), 7.16 (d, J = 8.4 Hz, 2H), 6.87 (d, J = 8.0 Hz, 2H), 6.83 (s, 1H), 6.61 (d, J = 8.0 Hz, 1H), 3.86 (s, 3H), 3.74 (s, 3H); HRMS (ESI): *m/z,* calcd. for $C_{24}H_{21}N_3O_5F_3S$ [M+H]$^+$: 520.1148, found 520.1135.

4-((3-Methoxyphenyl)amino)-N-((4-methoxyphenyl)sulfonyl)-1-methyl-7-nitro-1H-indole-2-carboxamide **(87):** yellow solid; yield: 50%; mp: 252-254 °C; ^{1}H-NMR (400 MHz, DMSO-d_6) δ (ppm): 12.65 (brs, 1H), 9.39 (s, 1H), 7.99 (d, J = 10.0 Hz, 1H), 7.96 (d, J = 9.2 Hz, 2H), 7.89 (s, 1H), 7.33 (t, J = 8.4 Hz, 1H), 7.18 (d, J = 8.8 Hz, 2H), 6.94 (d, J = 8.0 Hz, 1H), 6.89 (s, 1H), 6.82 (d, J = 8.8 Hz, 1H), 6.75 (d, J = 8.0 Hz, 1H), 3.87 (s, 3H), 3.78 (s, 3H), 3.62 (s, 3H); ^{13}C-NMR (125 MHz, DMSO-d_6) δ (ppm): 163.19, 160.14, 159.20, 145.52, 141.06, 133.82, 130.93, 130.31, 130.05,

128.43, 127.63, 117.27, 114.34, 113.87, 110.42, 109.55, 107.37, 101.87, 55.81, 55.13, 36.56. HRMS (ESI): *m/z,* calcd. for $C_{24}H_{23}N_4O_7S$ $[M+H]^+$: 511.1282, found 511.1274.

1-Ethyl-4-((3-methoxyphenyl)amino)-N-((4-methoxyphenyl)sulfonyl)-7-nitro-1H-indole-2-carboxamide **(88):** yellow solid; yield: 51%; mp: 241-242 °C; ^{1}H-NMR (400 MHz, DMSO-d_6) δ (ppm): 12.70 (brs, 1H), 9.40 (s, 1H), 7.94-8.00 (m, 4H), 7.34 (t, J = 8.0 Hz, 1H), 7.19 (d, J = 8.4 Hz, 2H), 6.95 (d, J = 8.0 Hz, 1H), 6.90 (s, 1H), 6.82 (d, J = 8.8 Hz, 1H), 6.76 (d, J = 8.0 Hz, 1H), 4.38-4.39 (m, 2H), 3.87 (s, 3H), 3.78 (s, 3H), 0.91 (t, J = 6.8 Hz, 3H); ^{13}C-NMR (150 MHz, DMSO-d_6): δ (ppm): 163.14, 160.11, 159.60, 145.50, 140.97, 131.62, 130.88, 130.25, 129.95, 128.43, 128.08, 117.66, 114.29, 114.01, 111.09, 109.64, 107.51, 101.70, 55.78, 55.11, 41.81, 15.30; HRMS (ESI): *m/z,* calcd. for $C_{25}H_{25}N_4O_7S$ $[M+H]^+$: 525.1438, found 525.1423.

1-Isobutyl-4-((3-methoxyphenyl)amino)-N-((4-methoxyphenyl)sulfonyl)-7-nitro-1H-indole-2-carboxamide **(89):** yellow solid; yield: 16%; mp: 195-196 °C; ^{1}H-NMR (400 MHz, DMSO-d_6) δ (ppm): 12.68 (brs, 1H), 9.38 (s, 1H), 7.93-7.98 (m, 3H), 7.88 (s, 1H), 7.34 (t, J = 8.0 Hz, 1H), 7.18 (d, J = 8.8 Hz, 2H), 6.95 (d, J = 8.0 Hz, 1H), 6.90 (s, 1H), 6.82 (d, J = 8.8 Hz, 1H), 6.76 (d, J = 8.4 Hz, 1H), 4.20 (d, J = 6.4 Hz, 2H), 3.86 (s, 3H), 3.78 (s, 3H), 1.24-1.29 (m, 1H), 0.36 (d, J = 6.4 Hz, 6H); HRMS (ESI): *m/z,* calcd. for $C_{27}H_{29}N_4O_7S$ $[M+H]^+$: 553.1751, found 553.1736.

N-((4-methoxyphenyl)sulfonyl)-1-methyl-7-nitro-4-(m-tolylamino)-1H-indole-2-carboxamide **(90):** yellow solid; yield; 91%; mp: 255-257 °C; ^{1}H-NMR (400 MHz, DMSO-d_6) δ (ppm): 12.63 (brs, 1H), 9.37 (s, 1H), 7.95-7.99 (m, 3H), 7.89 (s, 1H),

7.32 (t, *J* = 7.6 Hz, 1H), 7.13-7.19 (m, 4H), 7.00 (d, *J* = 7.6 Hz, 1H), 6.73 (d, *J* = 8.8 Hz, 1H), 3.87 (s, 3H), 3.68 (s, 3H), 2.34 (s, 3H); HRMS (ESI): *m/z,* calcd. for $C_{24}H_{23}N_4O_6S$ $[M+H]^+$: 495.1338, found 495.1323.

4-((3-Ethoxyphenyl)amino)-N-((4-methoxyphenyl)sulfonyl)-1-methyl-7-nitro-1H-indole-2-carboxamide **(91):** yellow solid; yield: 85%; mp: 243-245 °C; ^{1}H-NMR (400 MHz, DMSO-d_6) δ (ppm): 12.63 (brs, 1H), 9.37 (s, 1H), 7.99 (d, *J* = 8.8 Hz, 1H), 7.96 (d, *J* = 8.8 Hz, 2H), 7.88 (s, 1H), 7.32 (t, *J* = 8.0 Hz, 1H), 7.18 (d, *J* = 8.8 Hz, 2H), 6.91 (d, *J* = 7.6 Hz, 1H), 6.86 (s, 1H), 6.80 (d, *J* = 8.8 Hz, 1H), 6.73 (d, *J* = 8.4 Hz, 1H), 4.04 (q, *J* = 7.2 Hz, 2H), 3.87 (s, 3H), 3.62 (s, 3H), 1.34 (t, *J* = 7.2 Hz, 3H); HRMS (ESI): *m/z,* calcd. for $C_{25}H_{25}N_4O_7S$ $[M+H]^+$: 525.1438, found 525.1421.

4-((3-Acetamidophenyl)amino)-N-((4-methoxyphenyl)sulfonyl)-1-methyl-7-nitro-1H-indole-2-carboxamide **(92):** yellow solid; yield: 82%; mp: >250 °C; ^{1}H-NMR (400 MHz, DMSO-d_6) δ (ppm): 12.62 (brs, 1H), 10.02 (s, 1H), 9.44 (s, 1H), 7.98 (d, *J* = 8.4 Hz, 1H), 7.96 (d, *J* = 8.0 Hz, 2H), 7.91 (s, 1H), 7.78 (s, 1H), 7.33 (t, *J* = 8.0 Hz, 1H), 7.26 (d, *J* = 8.0 Hz, 1H), 7.19 (d, *J* = 8.4 Hz, 2H), 7.01 (d, *J* = 7.6 Hz, 1H), 6.77 (d, *J* = 8.8 Hz, 1H), 3.87 (s, 3H), 3.62 (s, 3H), 2.05 (s, 3H); HRMS (ESI): *m/z,* calcd. for $C_{25}H_{24}N_5O_7S$ $[M+H]^+$: 538.1396, found 538.1384.

4-((3,5-Dimethoxyphenyl)amino)-N-((4-methoxyphenyl)sulfonyl)-1-methyl-7-nitro-1H-indole-2-carboxamide **(93):** yellow solid; yield: 91%; mp: 255-257 °C; ^{1}H-NMR (400 MHz, DMSO-d_6) δ (ppm): 12.63 (brs, 1H), 9.34 (s, 1H), 7.99 (d, *J* = 8.8 Hz, 1H), 7.95 (d, *J* = 8.8 Hz, 2H), 7.88 (s, 1H), 7.18 (d, *J* = 8.8 Hz, 2H), 6.87 (d, *J* = 8.8 Hz, 1H), 6.50 (s, 2H), 6.31 (s, 1H), 3.86 (s, 3H), 3.76 (s, 6H), 3.62 (s, 3H); ^{13}C-NMR

(125 MHz, DMSO-d_6) δ (ppm): 163.15, 161.08, 159.27, 145.24, 141.67, 133.75, 131.03, 130.03, 128.32, 127.75, 117.44, 114.32, 110.33, 102.37, 99.64, 95.84, 55.80, 55.24, 36.54. HRMS (ESI): *m/z,* calcd. for $C_{25}H_{25}N_4O_8S$ $[M+H]^+$: 541.1393, found 541.1379.

N-((4-Methoxyphenyl)sulfonyl)-1-methyl-7-nitro-4-((3,4,5-trimethoxyphenyl)amino)-1H-indole-2-carboxamide **(94):** yellow solid; yield: 73%; mp: 268-272 °C; ^{1}H-NMR (400 MHz, DMSO-d_6) δ (ppm): 12.64 (brs, 1H), 9.36 (s, 1H), 7.96-7.99 (m, 3H), 7.88 (s, 1H), 7.19 (d, J = 8.8 Hz, 2H), 6.80 (d, J = 8.8 Hz, 1H), 6.63 (s, 2H), 3.87 (s, 3H), 3.78 (s, 6H), 3.68 (s, 3H), 3.62 (s, 3H); ^{13}C-NMR (150 MHz, DMSO-d_6): δ (ppm): 163.06, 159.33, 153.32, 145.97, 135.53, 134.25, 133.83, 131.13, 129.95, 128.51, 127.21, 116.86, 114.25, 110.20, 101.70, 99.99, 60.13, 55.87, 36.53; HRMS (ESI): *m/z,* calcd. for $C_{26}H_{27}N_4O_9S$ $[M+H]^+$: 571.1493, found 571.1471.

4-((4-Chloro-3-methoxyphenyl)amino)-N-((4-methoxyphenyl)sulfonyl)-1-methyl-7-nitro-1H-indole-2-carboxamide **(95):** yellow solid; yield: 70%; mp: 248-250 °C; ^{1}H-NMR (400 MHz, DMSO-d_6) δ (ppm): 12.66 (brs, 1H), 9.45 (s, 1H), 7.95-8.00 (m, 3H), 7.87 (s, 1H), 7.44 (d, J = 8.4 Hz, 1H), 7.18 (d, J = 8.8 Hz, 2H), 7.08 (s, 1H), 6.94 (d, J = 8.4 Hz, 1H), 6.88 (d, J = 8.8 Hz, 1H), 3.86 (s, 6H), 3.63 (s, 3H); HRMS (ESI): *m/z,* calcd. for $C_{24}H_{22}N_4O_7ClS$ $[M+H]^+$: 545.0898, found 545.0884.

7-Chloro-4-((3-methoxyphenyl)amino)-N-((4-methoxyphenyl)sulfonyl)-1-methyl-1H-indole-2-carboxamide **(96):** yellow solid; yield: 53%; mp: 182-183 °C; ^{1}H-NMR (600 MHz, DMSO-d_6) δ (ppm): 12.49 (brs, 1H), 8.36 (s, 1H), 7.95 (d, J = 9.0 Hz, 2H), 7.67 (s, 1H), 7.16-7.19 (m, 4H), 6.85 (d, J = 8.4 Hz, 1H), 6.76 (dd, J_1 = 7.8 Hz, J_1 = 2.4

Hz, 1H), 6.73 (t, J = 2.4 Hz, 1H), 6.48 (dd, J_1 = 7.8 Hz, J_1 = 2.4 Hz, 1H), 4.13 (s, 3H), 3.86 (s, 3H), 3.72 (s, 3H); ^{13}C-NMR (150 MHz, DMSO-d_6) δ (ppm): 162.97, 160.10, 159.91, 144.11, 136.94, 135.25, 131.36, 129.95, 129.87, 129.20, 127.23, 120.36, 114.18, 110.21, 109.24, 106.73, 106.03, 105.91, 103.53, 55.73, 54.85, 33.89; HRMS (ESI): *m/z,* calcd. for $C_{24}H_{23}N_3O_5ClS$ $[M+H]^+$: 500.1047, found 500.1036.

7-Chloro-4-((3-methoxyphenyl)amino)-1-methyl-N-(phenylsulfonyl)-1H-indole-2-carboxamide **(97):** light-yellow solid; yield: 89%; mp: 172-173 ℃; ^{1}H-NMR (400 MHz, DMSO-d_6) δ (ppm): 12.66 (brs, 1H), 8.38 (s, 1H), 8.02 (d, J = 7.6 Hz, 2H), 7.72-7.76 (m, 2H), 7.67 (t, J = 7.6 Hz, 2H), 7.16-7.20 (m, 2H), 6.86 (d, J = 8.0 Hz, 1H), 6.76 (d, J = 8.0 Hz, 1H), 6.73 (s, 1H), 6.50 (d, J = 8.0 Hz, 1H), 4.11 (s, 3H), 3.73 (s, 3H); HRMS (ESI): *m/z,* calcd. for $C_{23}H_{21}N_3O_4ClS$ $[M+H]^+$: 470.0936, found 470.0923.

7-Chloro-4-((3-methoxyphenyl)amino)-N-((3-methoxyphenyl)sulfonyl)-1-methyl-1H-indole-2-carboxamide **(98):** light-yellow solid; yield: 71%; mp: 145-146 ℃; ^{1}H-NMR (400 MHz, acetone-d_6) δ (ppm): 7.68 (d, J = 8.0 Hz, 1H), 7.64 (s, 1H), 7.59 (s, 1H), 7.56 (d, J = 8.0 Hz, 1H), 7.30 (d, J = 8.4 Hz, 1H), 7.21 (d, J = 8.4 Hz, 1H), 7.19 (t, J = 8.4 Hz, 1H), 6.93 (d, J = 8.0 Hz, 1H), 6.75-6.78 (m, 2H), 6.53 (d, J = 8.4 Hz, 1H), 4.25 (s, 3H), 3.91 (s, 3H), 3.76 (s, 3H); ^{13}C-NMR (100 MHz, DMSO-d_6) δ (ppm): 160.09, 159.67, 159.14, 144.02, 140.87, 137.03, 135.37, 130.43, 129.88, 128.66, 127.99, 120.27, 119.45, 119.23, 112.63, 110.28, 109.66, 106.67, 106.11, 105.87, 103.58, 55.65, 54.85, 33.91; HRMS (ESI): *m/z,* calcd. for $C_{24}H_{23}N_3O_5ClS$ $[M+H]^+$: 500.1041, found 500.1027.

7-Chloro-N-((2-fluorophenyl)sulfonyl)-4-((3-methoxyphenyl)amino)-1-methyl-1H-ind

ole-2-carboxamide **(99):** yellow-green solid; yield: 50%; mp: 105-107 °C; ^{1}H-NMR (400 MHz, DMSO-d_6) δ (ppm): 8.25 (s, 1H), 7.84 (t, J = 7.6 Hz, 1H), 7.42-7.47 (m, 1H), 7.31 (s, 1H), 7.22 (t, J = 7.2 Hz, 1H), 7.10-7.18 (m, 2H), 7.01 (d, J = 8.0 Hz, 1H), 6.78 (t, J = 8.4 Hz, 2H), 6.74 (s, 1H), 6.42 (d, J = 8.0 Hz, 1H), 4.28 (s, 3H), 3.71 (s, 3H); ^{13}C-NMR (150 MHz, DMSO-d_6): δ (ppm): 166.46, 160.52, 158.72 (J_{CF} = 249.6 Hz), 145.15, 137.78, 136.29, 134.50, 134.24, 132.56, 130.93, 130.14, 125.41, 123.82, 121.40, 116.49 (J_{CF} = 21.9 Hz), 110.32, 107.38, 106.09, 105.86 (J_{CF} = 17.9 Hz), 103.62, 55.28, 34.13; HRMS (ESI): *m/z,* calcd. for $C_{23}H_{20}N_3O_4ClFS$ $[M+H]^+$: 488.0842, found 488.0829.

7-Chloro-N-((3-fluorophenyl)sulfonyl)-4-((3-methoxyphenyl)amino)-1-methyl-1H-ind ole-2-carboxamide **(100):** yellow-green solid; yield: 56.2%; mp: 108-110 °C; ^{1}H-NMR (400 MHz, DMSO-d_6) δ (ppm): 8.22 (s, 1H), 7.65 (d, J = 5.2 Hz, 1H), 7.59 (d, J = 6.8 Hz, 1H), 7.47 (s, 1H), 7.26-7.31 (m, 2H), 7.13 (brs, 1H), 7.01 (d, J = 6.4 Hz, 1H), 6.73-6.80 (m, 3H), 6.42 (d, J = 5.2 Hz, 1H), 4.29 (s, 3H), 3.71 (s, 3H); HRMS (ESI): *m/z,* calcd. for $C_{23}H_{20}N_3O_4ClFS$ $[M+H]^+$: 488.0842, found 488.0832.

7-Chloro-N-((4-fluorophenyl)sulfonyl)-4-((3-methoxyphenyl)amino)-1-methyl-1H-ind ole-2-carboxamide **(101):** yellow-green solid; yield: 51.4%; mp: 115-117 °C; ^{1}H NMR (400 MHz, DMSO-d_6) δ (ppm): 8.22 (s, 1H), 7.88 (s, 2H), 7.28 (s, 1H), 7.22 (brs, 2H), 7.13 (brs, 1H), 7.00 (d, J = 6.8 Hz, 1H), 6.73-6.78 (m, 3H), 6.42 (d, J = 5.6 Hz, 1H), 4.29 (s, 3H), 3.71 (s, 3H); HRMS (ESI): *m/z,* calcd. for $C_{23}H_{20}N_3O_4ClFS$ $[M+H]^+$: 488.0842, found 488.0834.

N-((3-Bromophenyl)sulfonyl)-7-chloro-4-((3-methoxyphenyl)amino)-1-methyl-1H-ind

ole-2-carboxamide **(102):** light-yellow solid; yield: 45 mg; mp: 230-233 °C; ^{1}H NMR (400 MHz, acetone-d_6) δ (ppm): 8.13 (s, 1H), 7.96 (d, J = 7.6 Hz, 1H), 7.60 (t, J = 8.0 Hz, 2H), 7.38 (t, J = 8.0 Hz, 1H), 7.31 (s, 1H), 7.14 (t, J = 8.4 Hz, 1H), 7.03 (d, J = 8.4 Hz, 1H), 6.84-6.89 (m, 3H), 6.46 (d, J = 8.0 Hz, 1H), 4.37 (s, 3H), 3.75 (s, 3H); HRMS (ESI): *m/z*, calcd for $C_{23}H_{20}N_3O_4BrClS$ [M+H$^+$]: 550.0026, found 550.0004.

7-Chloro-4-((3-methoxyphenyl)amino)-1-methyl-N-tosyl-1H-indole-2-carboxamide **(103):** yellow-green solid; yield: 64.1%; mp: 75-76 °C; ^{1}H-NMR (400 MHz, DMSO-d_6) δ (ppm): 12.50 (brs, 1H), 8.36 (s, 1H), 7.88 (d, J = 8.0 Hz, 2H), 7.66 (s, 1H), 7.44 (d, J = 7.6 Hz, 2H), 7.17 (t, J = 8.0 Hz, 2H), 6.85 (d, J = 8.4 Hz, 1H), 6.77(d, J = 8.0 Hz, 1H), 6.73 (s, 1H), 6.48 (d, J = 8.0 Hz, 1H), 4.13 (s, 3H), 3.72 (s, 3H), 2.41 (s, 3H); ^{13}C-NMR (150 MHz, DMSO-d_6): δ (ppm): 160.10, 159.85, 144.08, 136.97, 135.28, 129.88, 129.50, 128.98, 127.82, 127.59, 120.32, 110.24, 109.40, 106.70, 106.06, 105.91, 103.54, 54.85, 33.89, 21.07; HRMS (ESI): *m/z,* calcd. for $C_{24}H_{23}N_3O_4ClS$ [M+H]$^+$: 484.1092, found 484.1082.

7-Chloro-4-((3-methoxyphenyl)amino)-1-methyl-N-((2-(trifluoromethoxy)phenyl)sulfonyl)-1H-indole-2-carboxamide **(104):** yellow-green solid; yield: 50.8%; mp: 136-138 °C; ^{1}H-NMR (400 MHz, DMSO-d_6) δ (ppm): 8.28 (s, 1H), 8.04 (s, 1H), 7.60 (s, 1H), 7.39-7.47 (m, 3H), 7.14 (t, J = 8.0 Hz, 1H), 7.05 (s, 1H), 6.72-6.82 (m, 3H), 6.43 (d, J = 7.6 Hz, 1H), 4.23 (s, 3H), 3.71 (s, 3H); HRMS (ESI): *m/z,* calcd. for $C_{24}H_{20}N_3O_5ClF_3S$ [M+H]$^+$: 554.0759, found 554.0752.

7-Chloro-4-((3-methoxyphenyl)amino)-1-methyl-N-((3-(trifluoromethoxy)phenyl)sulfo

nyl)-1H-indole-2-carboxamide **(105):** yellow-green solid; yield: 50.7%; mp: 75-77 ℃; ^{1}H-NMR (400 MHz, DMSO-d_6) δ (ppm): 8.39 (s, 1H), 8.04 (d, J = 7.6 Hz, 1H), 7.93 (s, 1H), 7.83 (t, J = 8.0 Hz, 1H), 7.78 (d, J = 8.0 Hz, 1H), 7.72 (s, 1H), 7.16-7.20 (m, 2H), 6.86 (d, J = 8.4 Hz, 1H), 6.77 (d, J = 8.0 Hz, 1H), 6.73 (s, 1H), 6.50 (d, J = 8.0 Hz, 1H), 4.13 (s, 3H), 3.73 (s, 3H); HRMS (ESI): *m/z,* calcd. for $C_{24}H_{20}N_3O_5ClF_3S$ $[M+H]^+$: 554.0759, found 554.0752.

7-Chloro-4-((3-methoxyphenyl)amino)-1-methyl-N-((4-(trifluoromethoxy)phenyl)sulfonyl)-1H-indole-2-carboxamide **(106):** yellow-green solid; yield: 52.0%; mp: 96-98 ℃; ^{1}H-NMR (400 MHz, DMSO-d_6) δ (ppm): 12.79 (s, 1H), 8.38 (s, 1H), 8.13 (d, J = 8.4 Hz, 2H), 7.70 (s, 1H), 7.65 (d, J = 8.4 Hz, 2H), 7.18 (t, J = 8.0 Hz, 2H), 6.86 (d, J = 8.4 Hz, 1H), 6.78 (d, J = 8.0 Hz, 1H), 6.74 (s, 1H), 6.49 (d, J = 8.0 Hz, 1H), 4.14 (s, 3H), 3.73 (s, 3H); ^{13}C-NMR (150 MHz, DMSO-d_6): δ (ppm): 160.40, 160.09, 151.32, 144.07, 139.08, 136.96, 135.32, 130.24, 129.88, 127.81, 121.15, 120.32, 119.83 (J_{CF} =256.7 Hz), 110.25, 109.53, 106.68, 106.07, 105.80, 103.57, 54.85, 33.92; HRMS (ESI): *m/z,* calcd. for $C_{24}H_{20}N_3O_5ClF_3S$ $[M+H]^+$: 554.0759, found 554.0756.

7-Chloro-N-((3-cyanophenyl)sulfonyl)-4-((3-methoxyphenyl)amino)-1-methyl-1H-indole-2-carboxamide **(107):** yellow-green solid; yield: 55.1%; mp: 80-82 ℃; ^{1}H-NMR (400 MHz, DMSO-d_6) δ (ppm): 8.36-8.38 (m, 2H), 8.29 (d, J = 6.8 Hz, 1H), 8.19 (d, J = 5.6 Hz, 1H), 7.87 (t, J = 6.4 Hz, 1H), 7.70 (s, 1H), 7.16-7.18 (m, 2H), 6.85 (d, J = 7.6 Hz, 1H), 7.77 (d, J = 6.8 Hz, 1H), 6.74 (s, 1H), 6.49 (d, J = 6.8 Hz, 1H), 4.14 (s, 3H), 3.73 (s, 3H); ^{13}C-NMR (150 MHz, DMSO-d_6): δ (ppm): 160.72, 160.09, 144.06, 141.62, 136.95, 136.75, 135.31, 131.95, 131.05, 130.56, 129.87, 127.79, 120.31, 117.51, 112.51, 110.27, 109.57, 106.65, 106.08, 105.73, 103.59, 54.85, 33.94; HRMS

(ESI): *m/z,* calcd. for $C_{24}H_{20}N_4O_4ClS$ $[M+H]^+$: 495.0888, found 495.0878.

7-Chloro-N-((3-isobutylphenyl)sulfonyl)-4-((3-methoxyphenyl)amino)-1-methyl-1H-indole-2-carboxamide **(108):** light-yellow solid; yield: 55 mg; mp: 178-179 ℃；^{1}H-NMR (400 MHz, acetone-d_6) δ (ppm): 7.93-7.94 (m, 2H), 7.56-7.57 (m, 3H), 7.16-7.21 (m, 2H), 6.93 (d, J = 8.0 Hz, 1H), 6.76-6.78 (m, 2H), 6.53 (d, J = 8.0 Hz, 1H), 4.23 (s, 3H), 3.76 (s, 3H), 2.63 (d, J = 7.2 Hz, 2H), 1.89-1.98 (m, 1H), 0.92 (d, J = 6.4 Hz, 6H); HRMS (ESI): *m/z*, calcd for $C_{27}H_{29}N_3O_4ClS$ $[M+H^+]$: 526.1567, found 526.1553.

7-Chloro-4-((3-methoxyphenyl)amino)-1-methyl-N-(pyridin-3-ylsulfonyl)-1H-indole-2-carboxamide **(109):** light-green solid; yield; 55%; mp: 218-220 ℃; ^{1}H-NMR (400 MHz, DMSO-d_6) δ (ppm)： 8.99 (s, 1H), 8.65 (s, 1H), 8.26 (s, 1H), 8.21 (d, J = 7.2 Hz, 1H), 7.50 (s, 1H), 7.39 (s, 1H), 7.14 (t, J = 8.0 Hz, 1H), 7.04 (d, J = 8.0 Hz, 1H), 6.74-6.81 (m, 3H), 6.43 (d, J = 7.6 Hz, 1H), 4.25 (s, 3H), 3.71 (s, 3H); ^{13}C-NMR (150 MHz, DMSO-d_6): δ (ppm): 164.98, 160.03, 151.06, 147.83, 144.48, 140.73, 136.05, 134.95, 134.31, 129.70, 125.57, 123.19, 120.71, 109.93, 106.79, 106.58, 105.59, 105.30, 103.23, 54.80, 33.83; HRMS (ESI): *m/z,* calcd. for $C_{22}H_{20}N_4O_4ClS$ $[M+H]^+$: 471.0888, found 471.0881.

7-Chloro-N-((5-isobutylthiophen-2-yl)sulfonyl)-4-((3-methoxyphenyl)amino)-1-methyl-1H-indole-2-carboxamide **(110):** yellow-green solid; yield: 58.8%; mp: 212-215 ℃; ^{1}H NMR (400 MHz, DMSO-d_6) δ (ppm)： 12.75 (s, 1H), 8.37 (s, 1H), 7.70 (d, J = 2.8 Hz, 1H), 7.67 (s, 1H), 7.17 (t, J = 8.0 Hz, 2H), 6.97 (s, 1H), 6.86 (d, J = 8.4 Hz, 1H), 6.76 (d, J = 8.0 Hz, 1H), 6.72 (s, 1H), 6.48 (d, J = 8.0 Hz, 1H), 4.17 (s, 3H), 3.72 (s,

3H), 2.74 (d, J = 6.8 Hz, 2H), 1.84-1.91 (m, 1H), 0.91 (d, J = 6.4 Hz, 6H); ^{13}C-NMR (150 MHz, DMSO-d_6): δ (ppm): 160.09, 159.75, 152.99, 144.04, 137.03, 136.68, 135.36, 134.37, 129.88, 128.84, 127.93, 125.87, 120.29, 110.27, 109.53, 106.69, 106.10, 105.88, 103.58, 54.85, 38.33, 33.93, 30.06, 21.86; HRMS (ESI): *m/z,* calcd. for $C_{25}H_{27}N_3O_4ClS_2$ $[M+H]^+$: 532.1126, found 532.1115.

7-Chloro-4-((3-methoxyphenyl)amino)-1-methyl-N-((1-methylindolin-5-yl)sulfonyl)-1 H-indole-2-carboxamide **(111):** light-yellow solid; yield: 36%; mp: 210-212 °C; ^{1}H-NMR (400 MHz, DMSO-d_6) δ (ppm): 12.22 (s, 1H), 8.34 (s, 1H), 7.67 (d, J = 8.4 Hz, 1H), 7.61 (s, 1H), 7.53 (s, 1H), 7.17 (t, J = 7.6 Hz, 2H), 6.85 (d, J = 8.0 Hz, 1H), 6.76 (d, J = 8.0 Hz, 1H), 6.72 (s, 1H), 6.54 (d, J = 8.4 Hz, 1H), 6.48 (d, J = 8.0 Hz, 1H), 4.14 (s, 3H), 3.72 (s, 3H), 3.48 (t, J = 8.4 Hz, 2H), 2.99 (t, J = 8.0 Hz, 2H), 2.81 (s, 3H); ^{13}C-NMR (150 MHz, DMSO-d_6): δ (ppm): 160.10, 156.80, 144.16, 136.88, 135.15, 129.88, 129.69, 127.60, 123.35, 120.40, 110.16, 108.89, 106.77, 106.00, 104.22, 103.46, 54.85, 54.44, 33.92, 33.88, 27.10; HRMS (ESI): *m/z,* calcd. for $C_{26}H_{26}N_4O_4ClS$ $[M+H]^+$: 525.1358, found 525.1353.

7-Chloro-4-((3-methoxyphenyl)amino)-1-methyl-N-((1-methyl-1,2,3,4-tetrahydroquin olin-6-yl)sulfonyl)-1H-indole-2-carboxamide **(112):** yellow-solid; yield: 40%; mp: 222-224 °C; ^{1}H-NMR (400 MHz, DMSO-d_6) δ (ppm): 12.19 (s, 1H), 8.34 (s, 1H), 7.62 (s, 2H), 7.44 (s, 1H), 7.17 (t, J = 7.6 Hz, 2H), 6.85 (d, J = 8.0 Hz, 1H), 6.76 (d, J = 8.0 Hz, 1H), 6.72 (s, 1H), 6.65 (d, J = 8.8 Hz, 1H), 6.48 (d, J = 8.0 Hz, 1H), 4.14 (s, 3H), 3.72 (s, 3H), 3.31-3.24 (m, 2H), 2.94 (s, 3H), 2.73 (brs, 2H), 1.87 (brs, 2H); HRMS (ESI): *m/z,* calcd. for $C_{27}H_{28}N_4O_4ClS$ $[M+H]^+$: 539.1514, found 539.1505.

7-Chloro-4-((3-methoxyphenyl)amino)-1-methyl-N-((1-methyl-1,2,3,4-tetrahydroquinolin-7-yl)sulfonyl)-1H-indole-2-carboxamide **(113):** light-yellow solid; yield: 33%; mp: 209-211 °C; ^{1}H-NMR (400 MHz, $CDCl_3$) δ (ppm): 9.41 (brs, 1H), 7.91 (d, J = 8.4 Hz, 1H), 7.31 (s, 1H), 7.20 (t, J = 8.0 Hz,1H), 7.14 (t, J = 7.6 Hz, 2H), 6.86 (d, J = 8.4 Hz, 1H), 6.67-6.70 (m, 2H), 6.55 (d, J = 8.0 Hz, 1H), 6.06 (s, 1H), 4.28 (s, 3H), 3.81 (s, 3H), 3.11 (s, 2H), 2.84 (s, 5H), 1.85 (s, 2H); HRMS (ESI): *m/z,* calcd. for $C_{27}H_{28}N_4O_4ClS$ $[M+H]^+$: 539.1514, found 539.1502.

4-Chloro-7-((3-methoxyphenyl)amino)-N-((4-methoxyphenyl)sulfonyl)-1H-indole-2-carboxamide **(114):** light-yellow solid; yield: 10%; mp: 169-170 ℃; ^{1}H-NMR (400 MHz, acetone-d_6) δ (ppm): 11.01 (brs, 1H), 10.89 (brs, 1H), 8.06 (d, J = 8.8 Hz, 2H), 7.55 (s, 1H), 7.46 (s, 1H), 7.06-7.20 (m, 5H), 6.68-6.71 (m, 2H), 6.49 (d, J = 8.4 Hz, 1H), 3.91 (s, 3H), 3.75 (s, 3H).

4-Chloro-7-((3-methoxyphenyl)amino)-N-((4-methoxyphenyl)sulfonyl)-1-methyl-1H-indole-2-carboxamide **(115):** yellow solid; yield: 60%; mp: 180-182 °C; ^{1}H-NMR (400 MHz, DMSO-d_6) δ (ppm): 12.50 (brs, 1H), 7.94 (d, J = 8.4 Hz, 2H), 7.86 (s, 1H), 7.57 (brs, 1H), 7.14-7.18 (m, 3H), 7.05 (d, J = 8.4 Hz, 1H), 7.00 (d, J = 8.4 Hz, 1H), 6.29 (d, J = 8.0 Hz, 1H), 6.10-6.14 (m, 2H), 3.91 (s, 3H), 3.84 (s, 3H), 3.63 (s, 3H); ^{13}C-NMR (150 MHz, DMSO-d_6): δ (ppm): 163.11, 160.31, 159.34, 148.70, 135.60, 130.84, 130.15, 130.03, 127.74, 125.90, 123.54, 122.39, 120.70, 114.28, 108.13, 106.83, 103.60, 100.15, 55.73, 54.69, 33.14; HRMS (ESI): *m/z,* calcd. for $C_{24}H_{23}N_3O_5ClS$ $[M+H]^+$: 500.1041, found 500.1032.

7-Chloro-4-((3-methoxyphenyl)amino)-N-((4-methoxyphenyl)sulfonyl)-1-methyl-1H-b

enzo[d]imidazole-2-carboxamide **(116):** light yellow solid; yield: 64%; mp: 206-207 ℃; ^{1}H-NMR (500 MHz, DMSO-d_6) δ (ppm): 8.31 (s, 1H), 7.99 (d, J = 7.5 Hz, 2H), 7.24 (d, J = 8.5 Hz, 1H), 7.22 (d, J = 7.5 Hz, 1H), 7.18 (d, J = 7.5 Hz, 2H), 7.06 (d, J = 7.5 Hz, 1H), 6.90 (d, J = 7.5 Hz, 1H), 6.87 (s, 1H), 6.55 (d, J = 7.0 Hz, 1H), 4.24 (s, 3H), 3.86 (s, 3H), 3.75 (s, 3H); ^{13}C-NMR (150 MHz, DMSO-d_6): δ (ppm): 163.30, 160.13, 157.46, 142.85, 140.71, 135.31, 132.85, 132.48, 130.57, 130.19, 129.97, 127.64, 114.33, 110.87, 106.93, 106.13, 105.13, 104.38, 55.80, 54.95, 33.71; HRMS (ESI): *m/z,* calcd. for $C_{23}H_{22}N_4O_5ClS$ $[M+H]^+$: 501.0993, found 501.0974.

4-((3-Methoxyphenyl)amino)-N-((4-methoxyphenyl)sulfonyl)-1H-pyrrolo[2,3-b]pyridine-2-carboxamide **(117):** light-yellow solid; yield: 19%; mp: >250 ℃; ^{1}H-NMR (400 MHz, DMSO-d_6) δ (ppm): 9.32 (brs, 1H), 7.97-7.87 (m, 2H), 7.33 (s, 2H), 7.04-6.73 (m, 7H), 3.81 (s, 3H), 3.77 (s, 3H); HRMS (ESI): *m/z,* calcd. for $C_{22}H_{21}N_4O_5S$ $[M+H]^+$: 453.1227, found 453.1216.

Sodium (7-chloro-4-((3-methoxyphenyl)amino)-1-methyl-1H-indole-2-carbonyl)((4-methoxyphenyl)sulfonyl)amide **(118)**. To a solution of compound **96** (8 g, 16.03 mmol) in H_2O (25 mL), NaOH (770 mg, 19.24 mmol, 4 M aqueous solution) was added at room temperature and then stirred at 80 ℃ for 4 h. Then the mixture was cooled to room temperature and then filtered. The solid was washed with water and purified by recrystallization (EtOH/H_2O = 1:1) to give the title compound (7 g, 83.8 %) as a light-yellow solid; mp:>250 ℃; ^{1}H-NMR (400 MHz, DMSO-d_6) δ (ppm): 8.21 (s, 1H), 7.78 (d, J = 8.8 Hz, 2H), 7.26 (s, 1H), 7.12 (t, J = 8.0 Hz, 1H), 7.09 (d, J = 8.4 Hz, 1H), 6.93 (d, J = 8.8 Hz, 2H), 6.79 (d, J = 8.0 Hz, 1H), 6.72-6.77 (m, 2H), 6.41

(dd, J_1 = 8.0 Hz, J_2 = 2.0 Hz,1H), 4.29 (s, 3H), 3.78 (s, 1H), 3.71 (s, 3H). ^{13}C-NMR (150 MHz, DMSO-d_6): δ (ppm):165.93, 160.34, 160.03, 144.69, 138.29, 137.68, 135.70, 133.95, 129.66, 128.62, 124.78, 120.95, 112.72, 109.78, 106.92, 105.37, 105.32, 103.07, 55.27, 54.79, 33.87.

In Vitro Biological Assays. *Human Liver FBPase Inhibition Assay*. The pET-28a expression vector containing the human liver FBPase gene was cloned by Hanbio (Shanghai, China). The enzyme was expressed in Escherichia coli BL21 (DE3) and purified to homogeneity as described. [35] FBPase activity was measured spectrophotometrically by employing the coupling enzymes phosphoglucose isomerase (PGI) and glucose-6-phosphate dehydrogenase (G6PDH). The reduction of $NADP^+$ to NADPH was monitored directly at 340 nm. Specifically, Tris buffer (pH 7.5), 10 μM of a compound and 0.72 units of FBPase, were mixed in a cuvette and equilibrated at 37° C. 0.2 mM of $NADP^+$, 0.01 units of PGI and 0.01 units of G6PDH, and FBP were then added to initiate the reaction. Inhibitory effect of each compound at 10 μM was evaluated initially. Reactions were performed in triplicate. Those compounds with FBPase inhibitory activity more than 60%, compared to the total enzyme and substrate reaction mix, were selected to conduct inhibition curves and calculate IC_{50} values. Inhibition curves and IC_{50} values were obtained for each compound by plotting the relative activity versus concentration. Compounds at each concentration were set up in triplicate. AMP and MB05032 were used as positive controls in this assay system.

Hepatic FBPase Activity Assay. Liver tissues were collected after overnight fasting (12 h) and sonicated to prepare tissue homogenate with 2% (w/v) in the Tris buffer (pH 7.5). FBPase activity was measured spectrophotometrically by employing the coupling enzymes as described before.

Selectivity Evaluation of Cpd 118. AMP deaminase (mouse hemolysates) was purified and assayed by the precice AMPD assay kit (NovoCIB SAS, K0709-05-2, France). Glycogen phosphorylase (mouse liver) was assayed by the GP assay kit (HEPENG Biological, HPBIO-JM6398, China), phosphofructokinase (rat liver) was assayed by the PFK assay kit (Solarbio, BC0535, China), adenosine kinase (Human recombinant) was assayed by the precice ADK assay kit (NovoCIB SAS, K0507-01, France) and adenylate kinase was assayed by the AK activity assay kit (colorimetric, BioVision Inc, K350-100, USA). Kinetic parameters were calculated using four-parameter logistics regression with the use of GraphPad Prism 6. The evaluation of AMPK activity was conducted by using ^{33}P-ATP filter assay at Eurofins Cerep SA platform, the catalog number ITEM 14-840KP10. In this assay, **Cpd118** had no effect on AMPK activity at a concentration of 10 μM against human AMPKα1β1γ1.

Glucose Production in the HepG2 Cell Line. HepG2 cells were seeded in a 48-well plate and treated with **Cpd118** for 20 h at the indicated concentrations (2.5 μM, 5 μM and 10 μM). Cells were washed in a pre-warmed PBS twice and replaced with 200 μl of glucose production buffer consisting of glucose-free DMEM without Phenol Red,

supplemented with 30 mM sodium lactate, 3 mM sodium pyruvate, and 1mM glucose, in the presence of **Cpd118**. After 4 h of incubation, 100 μl glucose production buffer was collected and the glucose concentration was assayed using a glucose oxidase kit (Sigma).

In Vivo Biological Methods. *Animal Care.* All animal experiments protocol were performed strictly in compliance with Chinese guidelines, including the Standards for Laboratory Animals (GB14925-2001) and the Guideline on the Humane Treatment of Laboratory Animals (MOST 2006a), and all animal procedures, and approved by Beijing Administration Office for Laboratory Animals (approval number: SCXK-Beijing-2014-0004). 8 weeks old female KKAy mice (n=30) and gender-matched C57BL/6J mice (n=10, NOR) were obtained from the Experimental Animal Center, Chinese Academy of Medical Science (Beijing, China) and housed at constant room temperature (22 ± 3℃) in a 12 h light/dark cycle. The KKAy mice were fed ad libitum with a high-fat diet (ResearchDiets12451, 45% of calories from fat) for 3 weeks to accelerate the development of diabetes (DM). 11 weeks old male ZDF obese rats (n=20) and lean rats (n=8, NOR) were also housed under standard vivarium conditions with free access to Purina 5008 for 3 weeks.

Animal Grouping. Twenty KKAy mice with DM were enrolled for this study, with the criteria consistent with the standards require as fasting blood glucose (FBG) over 266 mg/dL, postprandial blood glucose (PBG) over 500 mg/dL and initial body weight over 50 g. Those diabetic mice were then divided into two groups

(n=10/group) and then administered by oral gavage of 0.5% CMC-Na (the DM group), **Cpd118** (200 mg/kg) for 38 days. Additionally, gender-matched C57BL/6J mice (n=10) were administered by oral gavage of 0.5% CMC-Na as the NOR group. Also, sixteen ZDF obese rats with DM were enrolled for this study, with the criteria consistent with the standards require as fasting blood glucose (FBG) over 270 mg/dL, postprandial blood glucose (PBG) over 320 mg/dL and initial body weight over 390 g. Those diabetic ZDF rats were then divided into two groups (n=8/group) and then administered by oral gavage of 0.5% CMC-Na (the DM group), Cpd 118 (50 mg/kg) for 39 days. Additionally, lean rats (n=8) were administered by oral gavage of 0.5% CMC-Na as the NOR group.

Long-term Antidiabetic Effects in KKAy Mice and ZDF Rats. During the treatment of the KKAy mice, postprandial blood glucose (PBG) and fasting blood glucose (FBG) were determined after 26-days treatment. HbA1c was detected after 30-days treatment. Oral pyruvate tolerance test (OPTT) was conducted to evaluate the gluconeogenesis in vivo after 34 days of treatment, overnight fasted animals were challenged by 2 g/kg pyruvate. Blood glucose was estimated at 0 min (before pyruvate challenge) and 30 min after pyruvate challenge. After 38-days of treatment, Liver tissue samples were collected after overnight fasting (12 h) for FBPase activity measurement. For the ZDF rats, postprandial blood glucose (PBG) and fasting blood glucose (FBG) were determined after 29-days treatment. HbA1c was detected after 32-days of treatment. Oral pyruvate tolerance test (OPTT) was conducted after

24-days treatment. After 39-days of treatment, Blood samples and liver tissues were collected after overnight fasting (12 h) for biochemical assay, FBPase activity measurement, and hepatic energy metabolomics assay. Blood glucose levels were determined with the glucose oxidase method (Biosino Bio-Technology & Science Inc., Beijing, China). The HbA1c level was measured with a commercial kit (Homa Biological, Beijing, China). The lactate level was detected with a commercial kit (Nanjing Jiancheng Bioengineering Institute, China).

Hepatic Targeted Energy Metabolomics Assay. Take 100 mg liver tissue sample, add 1 mL of cold methanol/acetonitrile/H_2O（2:2:1,v/v/v）and adequately vortexed. The lysate was homogenized by MP homogenizer (24×2, 6.0 M/S, 60 s, twice). The homogenate was sonicated at low temperature (30 min/each, twice). The mixture was centrifuged for 20 min (14000 g, 4℃). The supernatant was dried in a vacuum centrifuge. For LC-MS analysis, the samples were re-dissolved in 100 μL acetonitrile/water (1:1, v/v) and adequately vortexed, and then centrifuged (14000 rpm, 4onitrile/water (1:1, reanatants were collected for LC-MS/MS analysis. Analyses were performed using a UHPLC (1290 Infinity LC, Agilent Technologies) coupled to a QTRAP (AB Sciex 5500).

Western Blot. Liver tissues and HepG2 cell lysate were lysed in RIPA buffer, and protein concentration was quantified with a BCA protein quantitation kit (Applygen Technologies Inc, China). Lysate samples were fractionated by sodium dodecyl

sulfate-polyacrylamide gels and transferred to polyvinylidene difluoride membranes, blocked with 5% fat-free milk for 1.5 h at room temperature, and incubated with primary antibodies overnight at 4℃. Appropriate horseradish peroxidase-conjugated secondary antibodies were applied for 1 h at room temperature, before detection with an enhanced chemiluminescence kit. Polyclonal antibodies to anti-FBP1 were obtained from Proteintech technology (USA). The amount of protein expression was normalized to those of β-actin. Data represented the mean of at least three independent experiments.

Statistical Analysis. Statistical analyses were conducted using Graphpad Prism 6.0 software. All results are presented as mean ± SD. Data were analyzed by one-way ANOVA, with Bonferroni's correction or Student's t-test. P values <0.05 were taken to indicate statistical significance.

Protein Production and Crystallization. Human liver FBPase (UniprotKB entry P09467) was expressed in *E. coli* BL21 (DE3) and purified according to a modified protocol as described in literature. [42] In general, the isopropyl β-D-1-thiogalactopyranoside (IPTG) induced culture resuspension was lysed with ultrasonication and the cell lysis was centrifugated at 12000 rpm for 1 h. Then, supernatant was incubated at 58 ℃ for 3 min following a 20 min centrifugation. After the above preprocessing procedure, the crude protein was purified with ion-exchange column (Hitrap Q HP, GE healthcare) and gel-filtration chromatography (Superdex

G200 and G75, GE healthcare) sequentially. The purified protein with a concentration of about 1.2 mg/mL in stock buffer (20 mM KH_2PO_3-KOH, 20% v/v glycerol, 1 mM di-threitol, 0.1 mM EDTA, pH 7.5) was stored at -80 ℃.

Cpd118 was dissolved in DMSO at 100 mM and then diluted to 1 mM with stock buffer containing 2 mM fructose-1,6-diphosphate. Stock buffer containing FBPase (1.2 mg/mL) and stock buffer containing **Cpd118** (1 mM) and fructose-1,6-diphosphate (2 mM) were mixed in a 1:1 ratio, and then incubated on ice for 1 h. Protein concentration of the mixed solution was then adjusted to 25 mg/mL using an Amicon Ultra-4 10K Centrifugal Filter Device (Millipore). FBPase was crystallized at 18 ℃ by hanging drop vapor diffusion method with 2 uL mixed protein solution and 1 uL precipitant solution (200 mM ammonium acetate, 20% w/v polyethylenglycol 3350, 100 mM HEPES, pH 7.0), which was similar to the reported procedure.[42]

The Crystal Data Collection and Analysis. The harvested crystal was quickly soaked in 2 uL of cryo protectant consisting of 70% (v/v) reservoir solution and 30% (v/v) glycerol for 5 s and then flash frozen in liquid nitrogen. Diffraction images were collected at Shanghai Synchrotron Research Facility (SSRF) using the beam-line BL17U. Raw data were processed with XDS (Kabsch),[43] and the primary protein structure was built by molecular replacement with 2FIE as a search model. After refining by Refmac 5, Coot and Phenix with ligand restrains, the final coordinate of

the structure was deposited to Protein Data Bank with pdb code 6LW2, and the ligand was assigned code EW0.

In Vivo Pharmacokinetic Study. Male Sprague-Dawley rats (purchased from Beijing Vital River Laboratory Animal Technology Co., Ltd) were fasted for 12 h for oral administration before receiving **Cpd118**. The SD rats for intravenous injection were not fasted. The dosing solutions used for the animal studies were prepared by dissolving the required amounts of **Cpd118** in 0.5% hydroxypropyl methylcellulose for oral administration and in 20% hydroxypropyl-beta-cyclodextrin for intravenous injection. After oral or intravenous administration of **Cpd118** at a dose of 50 mg/kg or 3 mg/kg to rats, blood samples (~0.2 mL) were collected in heparinized 1.5 mL polythene tubes by orbital bleeding via capillary tubes at 0.03, 0.08, 0.25, 0.5, 1, 2, 4, 6, 8, 12, 24, 36, 48 and 72 h after dosing. The blood samples were immediately centrifuged at 8000 rpm for 5 min and the plasma was separated. Each plasma sample (50 μL) was spiked with acetonitrile (100 μL), and then vortexed and centrifuged at 14,000 rpm for 5 min to precipitate protein. The supernatant (5 μL) were used for analysis. **Cpd118** was determined with a liquid chromatography–MS/MS system consisted of a Surveyor Series high performance liquid chromatography, fitted with a ZorbaxSB-C18 column (3.5 μm, 2.1 mm x100 mm, Agilent, Santa Clara, USA) and a TSQ Quantum Access™ triple quadrupole mass spectrometer (Thermo Finigan, USA). The mobile phase consisted of solvent A (0.1% formic acid in water) and solvent B (0.1% formic acid in methanol).The analytes were eluted, at a flow rate of

0.25 mL/min, with the following gradient elution: from 0 to 1.0 min, 85% B; linear increase to 95% B in 0.2 min; 95% B during 3 min, decrease to 85% B in 0.2 min; and stabilization at initial conditions for 3 min. The mass spectrometer was set for multiple-reaction monitoring and was operated in a negative-ion mode with ESI source. The spray voltage was set at -4000V, and the sheath gas and auxiliary gas at 30 and 15psi. The capillary temperature was set at 350°C. The transition ion pairs were at m/z 498.1→285.0 for **Cpd118**. The pharmacokinetic parameter estimates were carried out using WinNonLin Software (Version 6.1, Pharsight Corporation).

■ ASSOCIATED CONTENT

Supporting Information Available: The preparation and spectra data of intermediate compounds, the synthesis procedure of some of aryl sulfonamide reagents, the ^{1}H NMR and ^{13}C NMR spectra of target compounds, and the PAINs assay (PDF). The HPLC profiles for target compounds (PDF). The table for data collection and structure refinement statistics and the PDB coordinates of the co-crystal structure (PDF). Molecular formular strings (CSV).

This material is available free of charge via the Internet at http://pubs.acs.org.

■ AUTHOR INFORMATION

Corresponding Authors

*S.L.: phone, +8610-63165194; e-mail, liusn@imm.ac.cn.

*Z.S.: phone, +8610-83172669; e-mail, shenzhf@imm.ac.cn.

*B.X.: phone, +8610-63166764; e-mail, xubl@imm.ac.cn.

ORCID

Bailing Xu: 0000-0003-2633-0887

Author Contributions

[I]J.Z., J.B., and X.W. contributed equally to this work.

Notes

The authors declare no competing financial interest.

■ ACKNOWLEDGMENTS

Financial support from National Science & Technology Major Project Key New Drug Creation and Manufacturing Program, China (2018ZX09711002-003-012, 2018ZX09711001-003-011), CAMS Initiative for Innovative Medicine (CAMS-I2M-2-004, 2017-I2M-1-010), National Natural Science Foundation of China (81502933, 81973379) and Natural Science Foundation of Beijing Municipality (7132138, 7202137) is gratefully acknowledged. We also appreciate the X-ray crystallography facility platform at the National Protein Research Facility Base (Tsinghua) and Shanghai Synchrotron Radiation Facility for the support in the protein crystallographic experiment.

■ ABBREVIATIONS

FBPase, fructose-1,6-biphosphatase; Cpd118, compound 118; T1DM, insulin-dependent diabetes mellitus; T2DM, non-insulin-dependent diabetes mellitus; EGP, endogenous glucose production; PEPCK, phosphoenopyruvatecarboxykinase; G-6-Pase, glucose-6-phosphatase; F6P,

fructose-6-phosphate; $Pd_2(dba)_3$, Tris(dibenzylideneacetone)dipalladium; DavePhos, 2-Dicyclohexylphosphino-2'-(N,N-dimethylamino)biphenyl; $Pd(dppf)Cl_2$, [1,1'-Bis(diphenylphosphino)ferrocene]dichloropalladium(II); MW, microwave; HATU, 2-(7-Azabenzotriazol-1-yl)-N,N,N',N'-tetramethyluronium hexafluorophosphate; ICR mice, institute of cancer research mice; ZDF rats, zucker diabetic fatty rats; DM, diabetic model; HbA1c, Glycated hemoglobin concentration; OPTT, oral pyruvate tolerance test; PGI, phosphoglucose isomerase; G6PDH, glucose-6-phosphate dehydrogenase; DMEM, dulbecco's modified eagle medium; FBG, fasting blood glucose; PBG, postprandial blood glucose; IPTG, isopropyl β-D-1-thiogalactopyranoside; SSRF, shanghai synchrotron research facility.

■ REFERENCES

(1) IDF DIABETES ATLAS 9 the edition 2019, https://diabetesatlas.org/en/ (accessed Nov 15, 2019).

(2) Bonadonna, R. C.; Cucinotta, D.; Fedele, D.; Riccardi, G.; Tiengo, A. The Metabolic Syndrome Is a Risk Indicator of Microvascular and Macrovascular Complications in Diabetes: Results from Meta-screen, a Multi-center Diabetes Clinic-Based Survey. *Diabetes Care* **2006**, *29*, 2701–2707.

(3) Ghanchi, F.; Bailey, C.; Chakravarthy, U.; Cohen, S.; Dodson, P.; Gibson, J.; Menon, G.; Muqit, M.; Pilling, R.; Olson, J.; Prasad, S.; Scanlon, P.; Stanga, P.; Vafidis, G.; Wright, A.; Wykes, W. The Royal College of Ophthalmologists' Clinical Guidelines for Diabetic Retinopathy: A Summary. *Eye* **2013**, *27*, 285–287.

(4) Ma, Z. J.; Chen, R.; Ren, H. Z.; Guo, X.; Chen, J. G.; Chen, L. M. Endothelial Nitric Oxide Synthase (ENOS) 4b/a Polymorphism and the Risk of Diabetic Nephropathy in Type 2 Diabetes Mellitus: A Meta-Analysis. *Meta Gene* **2014**, *2*, 50–62.

(5) Tracy, J. A.; Dyck, P. J. B. The Spectrum of Diabetic Neuropathies. *Phys. Med. Rehabil. Clin. N Am.* **2008**, *19*, 1–26.

(6) Shah, A. D.; Langenberg, C.; Rapsomaniki, E.; Denaxas, S.; Pujades-Rodriguez, M.; Gale, C. P.; Deanfield, J.; Smeeth, L.; Timmis, A.; Hemingway, H. Type 2 Diabetes and Incidence of Cardiovascular Diseases: A Cohort Study in 1·9 Million People. *Lancet Diabetes Endocrinol.* **2015**, *3*, 105–113.

(7) Porte, D.; Kahn, S. E. Mechanisms for Hyperglycemia in Type II Diabetes Mellitus: Therapeutic Implications for Sulfonylurea Treatment-an Update. *Am. J. Med.* **1991**, *90*, S8–S14.

(8) Voet, D.; Voet, J.G. Metabolism, Other Pathways of Carbohydrate Metabolism, In Biochemistry, fourth ed.; Pace, K., Recta P., Kalkut, J., Zolotorevskaya, Y., White, P., Ruff, K., Sinclair, D., Dumas, S., Lesure, M., Melhorn, A., Kulesa, T., Wedzecki, M., Newman, H., Rieder, E., Eds.; John Wiley & Sons, Inc.: New Jersey, **2011**; pp 871–900.

(9) Landau, B. R.; Wahren, J.; Chandramouli, V.; Schumann, W. C.; Ekberg, K.; Kalhan, S. C. Contributions of Gluconeogenesis to Glucose Production in the

Fasted State. *J. Clin. Invest.* **1996**, *98*, 378–385.

(10) Magnusson, I.; Rothman, D. L.; Katz, L. D.; Shulman, R. G.; Shulman, G. I. Increased Rate of Gluconeogenesis in Type II Diabetes Mellitus. A 13C Nuclear Magnetic Resonance Study. *J. Clin. Invest.* **1992**, *90*, 1323–1327.

(11) Tillmann, H.; Bernhard, D.; Eschrich, K. Fructose-1,6-Bisphosphatase Genes in Animals. *Gene* **2002**, *291*, 57–66.

(12) Barciszewski, J.; Wisniewski, J.; Kolodziejczyk, R.; Jaskolski, M.; Rakus, D.; Dzugaj A. T-to-R switch of muscle FBPase involves fundamental changes of secondary and quaternary structure. *Acta Cryst. D Struct. Biol.* 2016, 72, 536–550.

(13) Gizak, A.; Duda, P.; Wisniewski, J.; Rakus, D. Fructose-1,6-Bisphosphatase: From a Glucose Metabolism Enzyme to Multifaceted Regulator of a Cell Fate. *Adv. Biol. Regul.* **2019**, *72*, 41–50.

(14) Proenca, C.; Oliveira, A.; Freitas, M.; Ribeiro, D.; Sousa, J. L. C.; Ramos, M. J.; Silva, A. M. S.; Fernandes, P. A.; Fernandes, E. Structural Specificity of Flavonoids in the Inhibition of Human Fructose 1,6-Bisphosphatase. *J. Nat. Prod.* **2020**, *83*, 1541–1552.

(15) Sugiyama, Y.; Shimura, Y.; Ikeda, H. Pathogenesis of Hyperglycemia in Genetically Obese Hyperglycemic Rats, Wistar Fatty: Presence of Hepatic Insulin Resistance. *Endocrinol. Japon.* **1989**, *36*, 65–73.

(16) Ke, H.; Zhang, Y.; Lipscomb, W. N. Crystal Structure of

Fructose-1,6-Bisphosphatase Complexed with Fructose 6-Phosphate, AMP, and Magnesium. *Proc. Natl. Acad. Sci. U. S. A.* **1990**, *87*, 5243–5247.

(17) Ke, H.; Liang, J. Y.; Zhang, Y.; Lipscomb, W. N. Conformational Transition of Fructose-1,6-Bisphosphatase: Structure Comparison between the AMP Complex (T Form) and the Fructose 6-Phosphate Complex (R Form). *Biochemistry* **1991**, *30*, 4412–4420.

(18) Wright, S. W.; Carlo, A. A.; Danley, D. E.; Hageman, D. L.; Karam, G. A.; Mansour, M. N.; McClure, L. D.; Pandit, J.; Schulte, G. K.; Treadway, J. L.; Wang, I. K.; Bauer, P. H. 3-(2-Carboxy-ethyl)-4,6-Dichloro-1*H*-Indole-2-Carboxylic Acid: An Allosteric Inhibitor of Fructose-1,6-Bisphosphatase at the AMP Site. *Bioorganic Med. Chem. Lett.* **2003**, *13*, 2055–2058.

(19) Bie, J.; Liu, S.; Li, Z.; Mu, Y.; Xu, B.; Shen, Z. Discovery of Novel Indole Derivatives as Allosteric Inhibitors of Fructose-1,6-Bisphosphatase. *Eur. J. Med. Chem.* **2015**, *90*, 394–405.

(20) Von Geldern, T. W.; Lai, C.; Gum, R. J.; Daly, M.; Sun, C.; Fry, E. H.; Abad-Zapatero, C. Benzoxazole Benzenesulfonamides Are Novel Allosteric Inhibitors of Fructose-1,6-Bisphosphatase with a Distinct Binding Mode. *Bioorganic Med. Chem. Lett.* **2006**, *16*, 1811–1815.

(21) Lai, C.; Gum, R. J.; Daly, M.; Fry, E. H.; Hutchins, C.; Abad-Zapatero, C.; Von Geldern, T. W. Benzoxazole Benzenesulfonamides as Allosteric Inhibitors

of Fructose-1,6-Bisphosphatase. *Bioorganic Med. Chem. Lett.* **2006**, *16*, 1807–1810.

(22) Hebeisen, P.; Kuhn, B.; Kohler, P.; Gubler, M.; Huber, W.; Kitas, E.; Schott, B.; Benz, J.; Joseph, C.; Ruf, A. Allosteric FBPase Inhibitors Gain 105 Times in Potency When Simultaneously Binding Two Neighboring AMP Sites. *Bioorganic Med. Chem. Lett.* **2008**, *18*, 4708–4712.

(23) Heng, S.; Gryncel, K. R.; Kantrowitz, E. R. A Library of Novel Allosteric Inhibitors against Fructose 1,6-Bisphosphatase. *Bioorganic Med. Chem.* **2009**, *17*, 3916–3922.

(24) He, H. B.; Gao, L. X.; Zhou, Y. Y.; Liu, T.; Tang, J.; Gong, X. P.; Qiu, W. W.; Li, J. Y.; Li, J.; Yang, F. Design, Synthesis and Biological Activity Evaluation of 2,5-Diphenyl-1,3,4-Oxadiazole Derivatives as Novel Inhibitors of Fructose-1,6-Bisphosphatase. *Heterocycles* **2012**, *85*, 2693–2712.

(25) Liao, B. R.; He, H. B.; Yang, L. L.; Gao, L. X.; Chang, L.; Tang, J.; Li, J. Y.; Li, J.; Yang, F. Synthesis and Structure-Activity Relationship of Non-Phosphorus-Based Fructose-1,6-Bisphosphatase Inhibitors: 2,5-Diphenyl-1,3,4-Oxadiazoles. *Eur. J. Med. Chem.* **2014**, *83*, 15–25.

(26) Huang, Y.; Chi, B.; Xu, Y.; Song, R.; Wei, L.; Rao, L.; Feng, L.; Ren, Y.; Wan, J. In Silico Screening of a Novel Scaffold for Fructose-1,6-Bisphosatase (FBPase) Inhibitors. *J. Mol. Graph. Model.* **2019**, *86*, 142–148.

(27) Kaur, R.; Dahiya, L.; Kumar, M. Fructose-1,6-Bisphosphatase Inhibitors: A

New Valid Approach for Management of Type 2 Diabetes Mellitus. *Eur. J. Med. Chem.* **2017**, *141*, 473–505.

(28) Li, Z. M.; Bie, J. B.; Song, H. R.; Xu, B. L. Recent Advance in the Discovery of Allosteric Inhibitors Binding to the AMP Site of Fructose-1,6-Bisphosphatase. *Acta Pharm. Sin.* **2011**, *46*, 1291–1300.

(29) Kerru, N.; Singh-Pillay, A.; Awolade, P.; Singh, P. Current Anti-Diabetic Agents and Their Molecular Targets: A Review. *Eur. J. Med. Chem.* **2018**, *152*, 436–488.

(30) Kitas, E.; Mohr, P.; Kuhn, B.; Hebeisen, P.; Wessel, H. P.; Haap, W.; Ruf, A.; Benz, J.; Joseph, C.; Huber, W.; Sanchez, R. A.; Paehler, A.; Benardeau, A.; Gubler, M.; Schott, B.; Tozzo, E. Sulfonylureido Thiazoles as Fructose-1,6-Bisphosphatase Inhibitors for the Treatment of Type-2 Diabetes. *Bioorganic Med. Chem. Lett.* **2010**, *20*, 594–599.

(31) Hebeisen, P.; Haap, W.; Kuhn, B.; Mohr, P.; Wessel, H. P.; Zutter, U.; Kirchner, S.; Ruf, A.; Benz, J.; Joseph, C.; Sanchez, R. A.; Gubler, M.; Schott, B.; Benardeau, A.; Tozzo, E.; Kitas, E. Orally Active Aminopyridines as Inhibitors of Tetrameric Fructose-1,6-Bisphosphatase. *Bioorganic Med. Chem. Lett.* **2011**, *21*, 3237–3242.

(32) van Poelje, P. D.; Dang, Q.; Erion, M. D. Fructose-1,6-Bisphosphatase as a Therapeutic Target for Type 2 Diabetes. *Drug Discov. Today Ther. Strateg.* **2007**, *4*, 103–109.

(33) https://www.clinicaltrials.gov/ (accessed Jun 6, 2020).

(34) Dang, Q.; Van Poelje, P. D.; Erion, M. D. The Discovery and Development of MB07803, a Second Generation Fructose-1,6-bisphosphatase Inhibitor with Improved Pharmacokinetic Properties, as a Potential Treatment of Type 2 Diabetes. *RCS Drug Discovery Series, New Therapeutic Strategies For Type 2 Diabetes: Small Molecule Approaches* **2012**, *27*, 306–322.

(35) Bie, J.; Liu, S.; Zhou, J.; Xu, B.; Shen, Z. Design, Synthesis and Biological Evaluation of 7-Nitro-1*H*-Indole-2- Carboxylic Acid Derivatives as Allosteric Inhibitors of Fructose-1,6- Bisphosphatase. *Bioorganic Med. Chem.* **2014**, *22*, 1850–1862.

(36) Gidh-Jain, M.; Zhang, Y.; Van Poelje, P. D.; Liang, J. Y.; Huang, S.; Kim, J.; Elliott, J. T.; Erion, M. D.; Pilkis, S. J.; El-Maghrabi, M. R.; Lipscomb, W. N. The Allosteric Site of Human Liver Fructose-1,6-Bisphosphatase. Analysis of Six AMP Site Mutants Based on the Crystal Structure. *J. Biol. Chem.* **1994**, *269*, 27732–27738.

(37) Dang, Q.; Liu, Y.; Cashion, D. K.; Kasibhatla, S. R.; Jiang, T.; Taplin, F.; Jacintho, J. D.; Li, H.; Sun, Z.; Fan, Y.; Dare, J.; Tian, F.; Li, W.; Gibson, T.; Lemus, R.; Van Poelje, P. D.; Potter, S. C.; Erion, M. D. Discovery of a Series of Phosphonic Acid-Containing Thiazoles and Orally Bioavailable Diamide Prodrugs That Lower Glucose in Diabetic Animals through Inhibition of Fructose-1,6-Bisphosphatase. *J. Med. Chem.* **2011**, *54*, 153–165.

(38) Dang, Q.; Kasibhatla, S. R.; Xiao, W.; Liu, Y.; DaRe, J.; Taplin, F.; Reddy, K. R.; Scarlato, G. R.; Gibson, T.; Van Poelje, P. D.; Potter, S. C.; Erion, M. D. Fructose-1,6-Bisphosphatase Inhibitors. 2. Design, Synthesis, and Structure-Activity Relationship of a Series of Phosphonic Acid Containing Benzimidazoles That Function as 5′-Adenosinemonophosphate (AMP) Mimics. *J. Med. Chem.* **2010**, *53*, 441–451.

(39) Dang, Q.; Brown, B. S.; Liu, Y.; Rydzewski, R. M.; Robinson, E. D.; Van Poelje, P. D.; Reddy, M. R.; Erion, M. D. Fructose-1,6-Bisphosphatase Inhibitors. 1. Purine Phosphonic Acids as Novel AMP Mimics. *J. Med. Chem.* **2009**, *52*, 2880–2898.

(40) Riou, J. P.; Claus, T. H.; Flockhart, D. A.; Corbin, J. D.; Pilkis, S. J. In Vivo and in Vitro Phosphorylation of Rat Liver Fructose-1,6-Bisphosphatase. *Proc. Natl. Acad. Sci. U. S. A.* **1977**, *74*, 4615–4619.

(41) DeLano L, W. PyMOL: An Open-Source Molecular Graphics Tool. *Ccp4 Newsl. Protein Crystallogr.* **2002**, *40*, 82–92.

(42) El-Maghrabi, M. R.; Gidh-Jain, M.; Austin, L. R.; Pilkis, S. J. Isolation of a Human Liver Fructose-1,6-Biphosphatase cDNA and Expression of the Protein in Escherichia Coli. Role of Asp-118 and Asp-121 in Catalysis. *J. Biol. Chem.* **1993**, *268*, 9466–9472.

(43) Kabsch, W. XDS. *Acta Crystallogr. Sect. D Biol. Crystallogr.* **2010**, *66*, 125–132.

Table of Contents graphic

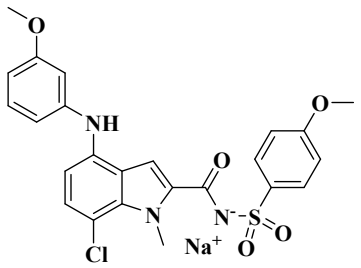

FBPase: IC_{50} = 0.029±0.006 μM

$t_{1/2}$ = 5.32 h

F% = 99.1